Aalto University
School of Chemical
Engineering

**Sonja Päärnilä**

# Lignin films – production and characterization

Master´s Programme in Chemical, Biochemical and Materials Engineering
Major in Fibre and Polymer Engineering

Master's thesis for the degree of Master of Science in Technology
submitted for inspection, Espoo, 26th June, 2018.

Supervisor Professor Orlando Rojas

Instructor D. Sc. Anna-Stiina Jääskeläinen

Aalto University
School of Chemical
Engineering

Aalto University, P.O. BOX 11000, 00076 AALTO
www.aalto.fi

**Abstract of master's thesis**

**Author** Sonja Päärnilä

**Title of thesis** Lignin films – production and characterization

**Degree Programme** Chemical, Biochemical and Materials Engineering

**Major** Fibre and Polymer Engineering

**Thesis supervisor** Professor Orlando Rojas

**Thesis advisor(s) / Thesis examiner(s)** D. Sc. Anna-Stiina Jääskeläinen

**Date** 26.06.2018 **Number of pages** 81+4 **Language** English

**Abstract**

Due to the increased awareness of the negative effects of petroleum-based products, biobased alternatives have been considered for their suitability and environmental friendliness. Among these, lignin macromolecules have several interesting properties, related to their role in mass transport (barrier), as well as antioxidative, antimicrobial and UV-blocking activity. Moreover, lignin is less hydrophilic compared to most biobased polymers. However, to facilitate lignin`s use in applications, its chemical heterogeneity should be reduced, which can be accomplished via fractionation. Thus, the aim of this thesis was to study the relationship between the structure and properties of lignin by preparing supported films from kraft lignin and its fractions. Further, to provide preliminary information about which fractions would function better in given applications, particularly in food packaging and edible films, was targeted.

The physicochemical properties of the lignins were studied by using spin-coated films. Atomic force microscopy, contact angle measurement and X-ray photoelectron spectroscopy were used to investigate the topography, wettability and surface chemical composition of the films. More heterogeneous, globular structured films were obtained from the unfractionated kraft lignin and its soluble fractions when polystyrene was used as a prime layer on the silica wafer substrates. The critical surface energy was quantified based on results from contact angle measurements with different liquids. Small differences in surface energy were determined. The higher critical surface tension obtained for unfractionated kraft lignin was partly related to its larger carbohydrate content.

Heat treatments applied on the films showed that their hydrophobicity increased to the same level regardless of the differences in the lignin structures between the fractions. Moreover, the polystyrene pre-layer had an increasing effect on the hydrophobicity which was attributed to lignin and polystyrene fusing together during the thermal treatment. XPS measurement revealed that during heating the oxygen content increased. Hence, the degradation of carbohydrates was responsible for the increased hydrophobicity.

No significant differences between lignin fractions in wetting or hydrophobicity after heating were observed. Thus, based on this study, all the fractions have similar potential for utilization that require given surface chemical behaviours, such as in food products. Basic research on the film properties, such as water interaction and viscoelasticity, should be carried out next in order to gain more knowledge on lignin`s behaviour.

**Keywords** Kraft lignin, fractionation, film, morphology, contact angle, critical surface tension, heat treatment

Aalto-yliopisto
Kemian tekniikan korkeakoulu

Aalto-yliopisto, PL 11000, 00076 AALTO
www.aalto.fi

**Diplomityön tiivistelmä**

**Tekijä** Sonja Päärnilä

**Työn nimi** Ligniini filmit – valmistus ja karakterisointi

**Koulutusohjelma** Chemical, Biochemical and Materials Engineering

**Pääaine** Fibre and Polymer Engineering

**Työn valvoja** Professori Orlando Rojas

**Työn ohjaaja(t)/Työn tarkastaja(t)** TkT Anna-Stiina Jääskeläinen

**Päivämäärä** 26.06.2018 **Sivumäärä** 81+4 **Kieli** englanti

**Tiivistelmä**

Kasvava tietoisuus öljypohjaisten tuotteiden negatiivisista vaikutuksista on lisännyt biopolymeerien kiinnostavuutta ympäristöystävällisempinä vaihtoehtoina erilaisissa tuotteissa. Ligniinillä on useita kiinnostavia ominaisuuksia liittyen esimerkiksi sen rooliin aineen kulkeutumisessa, sekä sen antioksidatiiviseen ja antimikrobiseen aktiivisuuteen. Jotta näitä ominaisuuksia voitaisiin hyödyntää sovelluksissa, ligniinin kemiallisen rakenteen monimutkaisuutta pitää vähentää. Tämä voidaan saavuttaa ligniinin fraktioinnilla. Täten tämän diplomityön tarkoituksena oli tutkia ligniinin rakenteen ja ominaisuuksien välistä suhdetta valmistamalla ligniinifilmejä sulfaattiligniinistä ja sen fraktioista. Lisäksi tarkoituksena oli saada käsitys siitä, mihin sovelluksiin tietyt fraktiot sopisivat paremmin kuin toiset, erityisesti elintarvikepakkauksissa ja syötävissä filmeissä.

Ligniinin fysikaaliskemiallisia ominaisuuksia tutkittiin käyttämällä spin-päällystettyjä filmejä. Atomivoimamikroskopiaa (AFM), kontaktikulmamittausta ja röntgenfotoelektronispektroskopiaa (XPS) käytettiin filmien topografian, kosteusalttiuden ja pinnan kemiallisen koostumuksen tutkimiseen. Tasaisempia, pallomaisista rakenteista koostuvia filmejä saatiin valmistettua sulfaattiligniinistä ja sen liukenevista fraktioista polystyreenipäällysteiselle piipinnalle. Kriittinen pintajännitys määritettiin mittaamalla kontaktikulma erilaisilla nesteillä. Eri fraktioiden välillä ei havaittu suuria eroja. Fraktioimattoman sulfaattiligniinin korkeampi kriittinen pintajännitys yhdistettiin osittain korkeaan hiilihydraattipitoisuuteen.

Ligniinifilmien lämpökäsittely osoitti, että hydrofobisuus nousi samalle tasolle riippumatta eri ligniinirakenteista. Lisäksi polystyreenikerros nosti hydrofobisuutta, johtuen sen sekoittumisesta ligniinin kanssa lämpökäsittelyn aikana. XPS mittaus osoitti, että hapen osuus filmeissä kasvoi käsittelyn aikana. Täten hiilihydraattien hajoaminen aiheutti hydrofobisuuden kasvun.

Kosteusalttiudessa ja hydrofobisuudessa ei havaittu suuria eroja ligniinin eri fraktioiden välillä. Siksi tämän tutkimuksen perusteella kaikilla käytetyillä fraktioilla on yhtä suuri potentiaali elintarviketuotteissa, joissa vaaditaan tiettyjä pintakemiallisia ominaisuuksia. Ligniinifilmien perustutkimusta, liittyen esimerkiksi vesivuorovaikutuksiin tai viskoelastisuuteen, tulisi jatkaa, jotta tietämys ligniinin käyttäytymisestä voi kasvaa.

**Avainsanat** Sulfaattiligniini, fraktiointi, filmi, morfologia, kontaktikulma, kriittinen pintajännitys, lämpökäsittely

# Preface

The research for this Master`s thesis was done at VTT Technical Research Centre of Finland in Espoo, from November 2017 until May 2018.

I would like to thank my supervisor Professor Orlando Rojas for his advice and opinions, as well as the discussion that helped me to deepen my understanding. I want to also thank my advisor Anna-Stiina Jääskeläinen for her guidance and enthusiastic attitude. Thank you for encouraging and helpful discussions.

Moreover, I want to thank everyone at VTT who I had the pleasure to meet and who have in any way helped me. Special thanks to Päivi Matikainen and Ville Rissanen.

Thank you Joseph Campbell for the XPS measurement.

Lastly, I want to thank my friends at university and my family for their support during my studies. Especially my parents, who always remind me that I myself know best what is best for me.

Espoo, June 26th, 2018
Sonja Päärnilä

# Table of Contents

# List of abbreviations

| | |
|---|---|
| AFM | Atomic force microscopy |
| DHP | Dehydrogenation polymer |
| DMA | N,N-dimethylacetamide |
| DMF | Dimethylformamide |
| DPPH• | 2,2-diphenyl-1-picrylhydrazyl |
| KL | Kraft lignin |
| LB | Langmuir-Blodgett |
| LbL | Layer-by-Layer |
| LS | Lignosulfonate |
| MWL | Milled wood lignin |
| $NH_4OH$ | Ammonium hydroxide |
| OP | Oxygen permeability |
| OTR | Oxygen transmission rate |
| PDDA | Poly (diallyldimethylammomium chloride) |
| PLA | Polylactic acid |
| PVD | Physical vapor deposition |
| QCM-D | Quartz crystal microbalance with dissipation monitoring |
| RH | Relative humidity |
| RMS | Root-mean-square |
| SEM | Scanning electron microscopy |
| THF | Tetrahydrofuran |
| TOFA | Tall oil fatty acids |
| WCA | Water contact angle |
| WVP | Water vapor permeability |
| WVTR | Water vapor transmission rate |
| XPS | X-ray photoelectron spectroscopy |

# 1 Introduction

Today, people recognize the effect of production and usage of petroleum based products on the environment more clearly than ever before. Therefore, industries and researchers are forced to focus on finding more environmentally friendly resources for products and energy production. Biorenewable polymers have been attracting the attention of the research community because of their several advantages, such as biocompatibility, biodegradability, low cost, low density and minimized environmental effect. (Figueiredo et al., 2018.)

Currently, one of the most interesting biorenewable polymers is lignin. Lignin is an aromatic, branched macromolecule that is structured from three different phenylpropane units. (Hatakeyama and Hatakeyama, 2010, pp. 1-20.) It is the second most abundant biopolymer on earth, right after cellulose. Annually, over 70 million tons of lignin is produced, mainly by the paper and pulp industry from wood biomass, of which approximately 5 % is used for different applications, such as dispersant agents, phenolic resins, precursors for chemicals and additives, while rest is burned as energy. (Laurichesse and Avérous 2016.) One reason for the poor utilization is the complex structure that depends on the extraction source and method, as well as wide molecular weight distribution, which leads to poor solubility and difficulty to modify the structure. However, because of its wide range of interesting properties, lignin has a massive potential to be utilized effectively in value-added applications. Thus, this kind of research has been growing steadily over the past few decades. (Stewart 2008.)

Food waste is a globally serious issue. According to Food and Agriculture Organization of the United Nations (FAO) one third of the food produced for human goes to waste every year (Anon. A). One way to contribute in decreasing the wastage is to develop food packaging with enhanced barrier properties. At the same time, the petrochemical-based plastic packaging materials have caused environmental waste concerns. (De Vlieger, 2003, pp. 519-520.) Lignin has many properties that could be beneficial in packaging materials to help in preserving food: it is antioxidant, antimicrobial, UV-absorbent and less hydrophilic than for example cellulose (Figueiredo et al., 2018). Moreover, replacing the non-biodegradable, non-renewable plastics with lignin would be of interest as well. In addition to packaging applications, one interesting aspect is the possibility for edible lignin films. These kinds of films would preserve the food without creating

any waste since the film could be eaten alongside the food. (Dawson et al., 2008, pp. 504-507.) Lignin is a natural component in human diet since for example cereal husks, which are dietary fibers, consist mostly of lignin and carbohydrates (Anon. C). In addition, lignin may even have beneficial health implications: lignin is known to adsorb bile acids, which could further lead to lowered cholesterol levels (Eastwood and Girdwood, 1968). Thus eating lignin also in the form of a film, if extracted from a suitable source with a suitable method, is possible.

Regardless of the great potential of lignin utilization in food film products, this research area has not been covered much yet. One great reason for this is the poor film forming property of lignin compared to polysaccharides (Thiebaud et al., 1997). Thus, the aim of this thesis is to study the possibility to produce lignin films, as well as examine their properties while keeping in mind the final application target, food industry. One important objective is to evaluate how lignin fractionation affects the film formation and the features. This is because fractionation makes the properties of lignin, such as molar mass, more homogeneous which further should facilitate the usage and possibly provide new application routes for lignin (Lovell and Hibbert, 1941; Mörck et al., 1988). These kind of studies do not exist much yet. The thesis will start with a literature review, where the methods used to prepare lignin films so far are presented. Moreover, the properties studied for these films are discussed as well. However, since limited research is published on pure or chemically modified lignin films, properties of some lignin composite films are discussed, too, in order to gain an understanding of the effects that lignin has in films. After the literature review, follows the experimental part where lignin films are produced by spin-coating first from unfractionated kraft lignin, in order to optimize the film formation process. Then, films are formed from the different fractions. Morphology, wetting, surface energy and chemical composition are analyzed with different methods. Finally, heat treatments are applied to evaluate their effect, especially on wetting.

# 2 Preparation methods of supported lignin films

Some studies in the research area of lignin film preparation exist. However, compared to for example cellulose, the number of publications is lower (Kontturi et al., 2006). One main reason for this is the poor film forming property of lignin. In a few studies, this ability has been tried to be enhanced by chemical modifications, for example esterification (Hult and Koivu et al., 2013, Hult and

Ropponen et al., 2013, Gordobil et al., 2017). In the existing studies, lignin films have been prepared mainly as model films on different substrates in order to model the plant cell wall and to understand its interactions with other wood components, water and enzymes. Several lignin raw materials extracted with different methods have been used, such as kraft, milled wood and organosolv lignin. The film forming methods utilized have been mainly spin-coating (Cai et al., 2017; Hambardzumyan et al., 2011; Kent et al., 2015; Meincken and Evans 2010; Norgren et al., 2006; Notley and Norgren 2006, 2008 and 2010; Pereira et al., 2017; Tammelin et al., 2006), Langmuir-Blodgett (Aguié-Béghin et al., 2002; Barros et al., 1999; Constantino et al., 1996; Pasquini et al., 2005; Pereira et al., 2007), Layer-by-layer deposition (Liu et al., 2009; Maximova et al., 2004; Pillai et al., 2014) and some other rarer methods (Dallmeyer et al., 2013; Gordobil et al., 2017; Hult and Koivu et al., 2013; Hult and Ropponen et al., 2013; Volpati et al., 2011; Wang et al., 2015). In this chapter, the different methods are introduced.

## 2.1 Spin-coating

Spin-coating is a robust method when smooth and uniform films are wanted on flat surfaces. In spin-coating, an excess amount of a polymer solution is placed on top of a substrate. Next, the substrate is rotated at a high speed so that the solution spreads due to the centrifugal force. A film forms on top of the substrate when the rotation is continued and the fluid is being spun of the edges. Moreover, the solvent used is usually volatile, so that a simultaneous evaporation takes place. (Birnie, 2004, pp. 49-55.) The spin-coating set-up is illustrated in Figure 1.

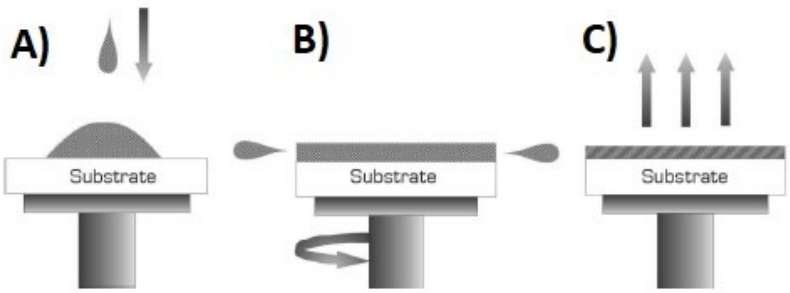


Figure 1. Spin-coating set-up. In image A), the polymer solution is deposited on top of the substrate. In B), the substrate is rotated and the solution spreads. In C), the solvent is spun over the edges of the substrate while the rotation is continued. (Szindler, 2012.)

Many factors need to be considered in order to achieve a successful spin-coating result. Quality of the solvent is one important factor: wetting and spreading

characteristics, evaporation rate, as well as the ability to dissolve or disperse the polymer should be considered. Moreover, viscosity of the polymer solution has a significant effect on spin-coating. (Klein, 1991, pp. 511-512.) In addition, the film thickness, roughness and reproducibility can be controlled and adjusted with several parameters, such as solution concentration, solvent properties, spinning speed, acceleration and spinning time (Meyerhofer 1978; Sukanek 1991; Bornside et al., 1993).

Tammelin et al. (2006) used milled wood lignin (MWL) isolated from spruce to spin-coat films. The substrate used was a hydrophobic polystyrene-coated QCM-D (quartz crystal microbalance with dissipation monitoring) crystal. The crystal was pre-coated with polystyrene in order to increase the adhesion between the surface and the lignin. Spin-coating was used as a method because of the poor solubility of MWL, which complicates the utilization of for example the Langmuir-Blodgett technique. The chosen solvent for lignin was 1,4-dioxane and the sample was dissolved for two days. Pereira et al. (2017) used a very similar procedure. They extracted lignins from Eucalyptus globulus wood, wheat straw and spruce wood by the MWL method, dissolved them to 1,4-dioxane and spin-coated on polystyrene pre-coated substrates. The substrates were silica for atomic force microscopy (AFM) analysis, gold-coated quartz for QCM and surface plasmon resonance (SPR) analysis and silicon for AFM and contact angle analysis.

Norgren et al. (2006) dissolved kraft lignin in several different solvents, followed by spin-coating the solutions on silica wafers. The best film formation occurred when aqueous ammonium hydroxide ($NH_4OH$) was used as the solvent and silica as a substrate. Thus, films spun from aqueous $NH_4OH$ solutions were chosen for further characterization. Notley and Norgren (2006) used this same method to spin-coat kraft lignin from softwood (*Picea abies*), while Rahikainen et al. (2013) utilized it for enzymatic mild acidolysis lignins isolated from wheat straw and spruce.

Later, Notley and Norgren prepared lignin thin films by the same spin-coating method as before. In 2008, they used again softwood kraft lignin and in 2010 three different lignins: a kraft lignin from softwood (*Picea abies*), a MWL from softwood (*Radiata Pine*) and hardwood (*Eucalyptus Regnans*). The kraft lignin

was dissolved in $NH_4OH$, like before, and the hardwood and softwood MWL were dissolved in a 9:1 mixture of acetone and water.

Lignin model compounds, dehydrogenation polymers (DHP), have also been used for film production. They can be synthesized by polymerization of the lignin precursors while using hydrogen peroxide and peroxidase as oxidizing agents (Sarkanen, 1971, pp. 95). These model compounds are closer to the native form of lignin than the isolated lignins (Brunow et al., 1999, pp. 77-124). Hambardzumyan et al. (2011) used this DHP to prepared cellulose nanocrystal/lignin multilayered films by alternatively depositing cellulose and lignin layers by spin-coating. The model compound was synthesized by a slow and continuous addition of coniferyl alcohol (4-hydroxy-3-methoxy-cinnamyl alcohol) and hydrogen peroxide to a solution of peroxidase. After drying, the lignin was dissolved to dioxane/water mixture (9:1, by volume). The multilayered structure was assembled on quartz slides and $BaF_2$.

Other studies where spin-coating has been used are for example Kent et al. (2015). They used organosolv lignin to spin-coat on aminopropyltriethoxysilane (APS) pre-coated silicon substrate. The lignin was dissolved at 2% or 3% in 1,4-dioxane prior to spin coating. Furthermore, Meincken and Evans (2010) prepared lignin films of technical lignin from Sigma Aldrich on glass slide and Cai et al. (2017) used the method of Norgren et al. (2006).

Like the earlier studies show, technical lignins, such as kraft lignin, dissolve in alkali. Since the common alkali NaOH cannot be evaporated, other solvents, such as $NH_4OH$, must be considered if spin-coated is used as the film preparation method. Although lignin films have been prepared by spin-coating, a systematic study on their properties and characteristics is lacking.

## 2.2 Langmuir-Blodgett

Another method to produce thin films is the Langmuir-Blodgett (LB) technique. In this method, a substrate is dipped into a liquid, which is often water. Next, a monolayer of the polymer dissolved in a volatile solvent is deposited and spread on top of the water surface. After this, the substrate is withdrawn from the water and the polymer monolayer is transferred on its surface. An appropriate, constant surface pressure has to be applied continuously from the sides while the substrate is being withdrawn in order to achieve compact, well-formed, uniform films. After the substrate has been removed, the volatile solvent evaporates from

the surface and only the polymer film stays. LB technique is applied to a large number of different substances, for example polymers, proteins and organic dyes. High-quality, ordered monomolecular layers or multilayers can be prepared. (George, 1992, pp. 335-338). However, because of the sensitivity towards pressure, LB is slightly more challenging method to be applied than spin-coating. In Figure 2, the principle of the preparation of Langmuir-Blodgett films is presented.

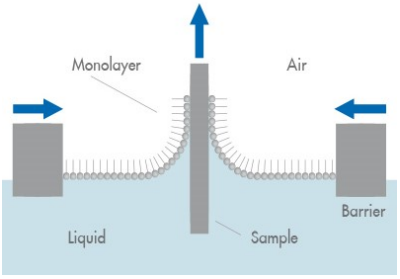


Figure 2. The principle of Langmuir-Blodgett films. Water surface is deposited with a substance layer and a substrate is dipped into it. By applying a constant pressure while withdrawing the substrate, a thin film can be formed on top. (Wagner)

Constantino et al. (1996) extracted lignins from softwood (*Pinus caribaea hondurensis*) and sugar cane bagasse in order to prepare LB films from them. The bagasse lignin was fractionated with gel permeation chromatography (GPC) before film formation in order to obtain less polydisperse films. The films were done by dissolving the softwood and bagasse lignins in tetrahydrofuran (THF) and stable Langmuir monolayers were formed on ultrapure water. Next, the layers were transferred onto glass substrates in the form of LB films. It was noticed that it was easier to form films from bagasse lignin because it was less polydisperse. Moreover, it was discovered that the formation of multilayer stacks was more likely than that of true monomolecular films. This was probably due to the poor interaction with the water subphase, as well as the poor stabilizing interactions between the lignin molecules. This could be associated with the non-amphiphilic nature of lignin.

Barros et al. (1999) made Langmuir monolayers from lignins isolated with different methods: kraft, acetone-oxygen-organosolv, acetic acid-organosolv and

acetone-organosolv. The lignin raw materials used were, respectively, *Eucalyptus globulus*, *Populus tremula* and sugar cane bagasse for the last two methods. The lignins were dissolved in a mixture of N,N-dimethylacetamide (DMA) and chloroform (20:80 by volume), which provided complete lignin dissolution and stable spreading solutions. Barros et al. (1999) studied the pressure-area isotherms and the molecular organization at the interface. Also Aguié-Béghin et al. (2002) studied the formation of lignin layer at air-water interface. The lignins they used were extracted from wheat straw and wild cherry wood, and dissolved in a deuterium oxide/dioxane mixture (1:9, by volume). Both the films by Barros et al. (1999) and by Aguié-Béghin et al. (2002) were metastable.

Pasquini et al. (2005) continued on the same path as Barros et al. (1999) earlier. However, they concentrated more on the effects of the extraction process by using only lignin from sugar cane bagasse and extracting it with different organosolv methods: acetone–oxygen, soda, ethanol–water and acetone/water/sulfuric acid. In order to reduce the polydispersity of the lignins, solvent fractionation was performed using dichloromethane and acetone in succession. Like Barros et al. (1999), the pressure-area isotherm and the molecular organization and re-arrangement with time were studied. In addition, unlike Barros et al. (1999), Pasquini et al. (2005) transferred the monolayers on mica, quartz and zinc selenide substrates as LB films.

Pereira et al. (2007) used lignin extracted from sugar cane bagasse with organosolv-$CO_2$ supercritical pulping process, by using four different alcohols: methanol, ethanol, n-propanol, and 1-butanol. They dissolved the lignins in THF and then dropped carefully on top of the water subphase. They noticed that the layer formed from 1-butanol was the most stable, which was attributed with carbonyl groups promoting a better interaction between lignin and the water surface. Homogeneous LB films could be produced from 1-butanol on quartz and ZnSe substrates.

## 2.3 Layer-by-Layer

In Layer-by-layer (LbL) deposition technique, a layered structure is formed by immersing the substrate alternately to selected solutions, for example polymer or polyelectrolyte solutions. The multilayered structure is usually formed based on electrostatic interactions but also other forces, for example hydrogen bonding, can foster the assembly. (Niepel et al., 2015, pp. 3-5) One example of this

method is the study by Pillai et al. (2014). They prepared multilayered nanocomposite films with this method by adding lignin and oxidized nanofibril cellulose alternately on top of each other. The structure was built on top of mica or silicon wafer and poly(diallyldimethylammomium chloride) (PDDA) was used as a linking layer between lignin and cellulose. Two different lignins were produced with different extraction techniques: a technical lignin from the organosolv pulping process, and a lignin isolated from ball-milling with less modification during isolation.

First, a PDDA layer was deposited on the mica by dipping the substrate in to the aqueous solution of PDDA. Next, the substrate was immersed in the aqueous, alkaline lignin solution, followed by immersing again in PDDA and after that to the nanocellulose solution. Furthermore, free-standing LBL films were created on top of cellulose acetate. A number of 250 deposition cycles with each cycle containing two PDDA, one lignin, and one nanocellulose layer, were deposited. The film was obtained when cellulose acetate was dissolved in acetone.

Liu et al. (2009) deposited lignosulfonates (LS) on mica by LbL, using $Cu^{2+}$ as a binding agent. The layers were created by immersing the mica plates in the Na-LS solution for 10 min and then immersing to $CuSO_4$ (10 mM) solution. In addition, Maximova et al. (2004) applied a version of LbL by absorbing only one layer of kraft lignin from aqueous NaOH-solution on the surfaces of mica and cellulose fibres. The cellulose fibers were formed to sheets after. The mica plates were immersed to the lignin solution and the cellulose fibers were mixed with the lignin solution. Two cationic polyelectrolytes, cationic starch and poly diallyldimethylammonium chloride (PDADMAC), were added to enable the adsorption between lignin and the substrates.

## 2.4 Other methods

While the methods mentioned above, especially spin-coating, have been relatively popular in preparing model lignin surfaces and films, some other methods have been utilized in smaller scale as well. In this section, a few examples of these methods are introduced.

Vacuum thermal evaporation technique, also known as physical vapor deposition (PVD) was exploited by Volpati et al. (2011). In PDV, the materials are first vaporized from solid state, followed by transportation under vacuum and low pressure. The materials are solidified again when they come in contact with the

substrate. One advantage of this method is that it allows high deposition rates without causing damage to the substrate surface. (Mattox, 1998, pp. 288-295.) Volpati et al. (2011) prepared thin lignin films from lignin that was extracted from sugar cane bagasse with a modified organosolv process using solvent mixture of ethanol/water associated with supercritical $CO_2$. The substrates were quartz and gold. Moreover, the films were grown in steps, where each step corresponded to a mass of approximately 5.5 mg of lignin evaporated.

Press moulding technique was utilized by Gordobil et al. (2017) to prepare lignin coatings of esterified lignin on top of wood using a. The lignin was organosolv Spruce and Eucalyptus. The esterification was done by using a long aliphatic chain (12C) of dodecanoyl chloride as reagent. The esterification decreased the glass transition temperature, $T_g$, of lignin, which allowed the processing by press moulding. For Spruce lignin, $T_g$ reduced from 121 °C to 15.8 °C, and for eucalyptus lignin from 115 °C to 17.4 °C. The decrease was associated with the replacement of hydroxyl groups by ester substituent and thus with reduction in hydrogen bonding. In Figure 3, the change of $T_g$ for spruce lignin is presented.

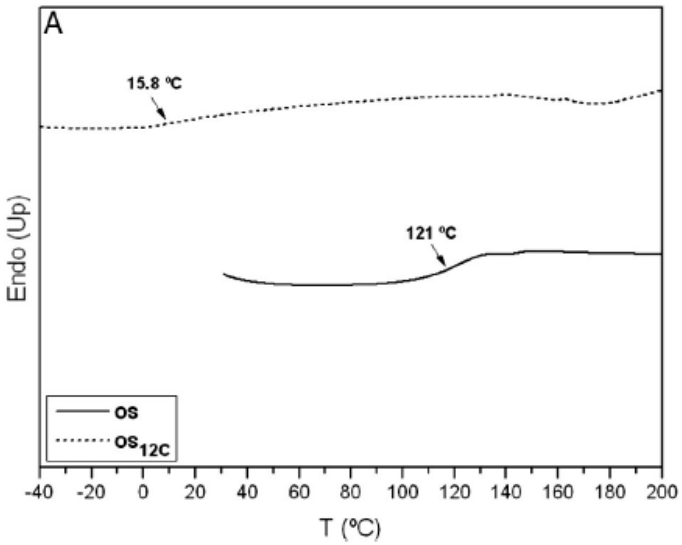


Figure 3. DSC (differential scanning calorimetry) curve for the Spruce lignin.

The esterified lignin coatings were applied on top of wood veneers by two different techniques. First, the veneer was coated by press molding in two different conditions, 90 °C/100 bar and 100 °C/200 bar. The amount of lignin and time of pressing was selected so that the product was coated to the substrate

without visual defects. In the other method, the veneers were impregnated to 0.5 wt % lignin/acetone solution.

In Solution casting, a film is formed for example on top of a Petri dish when a polymer solution is poured and the solvent is let to evaporate. An illustration of solution casting is shown in Figure 4. Wang et al. (2015) applied solution casting for ball-milled lignin, isolated from Jack pine (*Pinus banksiana*), and lignosulphonate, isolated from a solution of sulphite spent liquor produced primarily from Douglas fir wood. The two materials were methylated with dimethyl sulphate or with both dimethyl sulphate and diazomethane. Next, the ball-milled lignin or lignosulphonate were dissolved in dimethyl sulphoxide. After degassing, the lignins were solution casted in several different temperatures for different times. Fresh surfaces of the cast unmethylated and methylated lignosulphonate-based materials were created by ultramicrotome-cutting with a 45° glass blade.

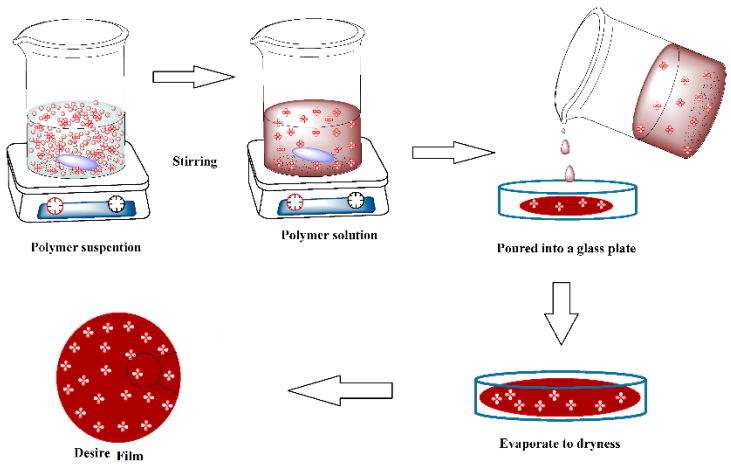


Figure 4. Illustration of solution casting. (Roy and Ranjan Singha 2017.)

An Erichsen bar coater was used by Hult and Ropponen et al. (2013) in order to form an even coating of esterified lignin on top of a paperboard substrate with. The softwood kraft lignin (Indulin AT) raw material was first esterified in order to improve the thermoplastic and thus also the film formation properties of lignin. The esterification was done to different degrees of substitution with tall oil fatty acids (TOFA) to produce TOFA lignin. The fatty acids of TOFA were covalently linked to the lignin in DMF solution at room temperature. Next, the TOFA lignin was dissolved in acetone. The novel thermoplastic lignin material was then applied on the paperboard and its barrier properties were studied.

In another study, Hult and Koivu et al. (2013) again esterified lignin, but now with palmitic and lauric acid chloride. In addition to softwood kraft lignin, also hardwood kraft was used as a raw material. After esterification, the lignins were dissolved in deuterated chloroform and applied on the paperboard by an Erichsen coater, like in the other study as well.

# 3 Preparation methods of self-standing lignin films

While for example spin-coating has been a feasible method for supported lignin model film production, only a few studies on its usage on composite or biocomponent film forming exist (Hoeger et al., 2012). Thus, in this section, casting, dip-coating and electrospinning, which lead to self-standing lignin composite films, are discussed as more popular lignin composite film preparation methods.

## 3.1 Casting

Casting is a very popular film forming method used in many studies. Espinoza-Acosta et al. (2015) prepared an aqueous dispersion of starch, followed by addition of glycerol (40 wt %, based on starch) and a lignin-methanol solution in ratios up to 20 % (wt %, based on starch content). The mixture was homogenized, methanol was evaporated and finally the films were casted by pouring the solution into a Petri dish. The solution was spread evenly, followed by drying and conditioning at 57% relative humidity (RH) for 72 h at room temperature.

Crouvisier-Urion et al. (2016) used the casting method as well by incorporating lignin to chitosan based films. They prepared a lactic acid aqueous solution of chitosan and an ethanol solution of lignin, followed by mixing of these two solutions. This final film forming solution was then poured in a polystyrene Petri dish and dried during 24 h at 25 °C and 40% RH.

In addition to these, lignin containing films from for example polylactic acid (PLA) (Gordobil et al., 2016), cellulose (Sadeghifar et al., 2016), agar (Shankar et al., 2015) and alginate (Aadil et al., 2016) have been prepared by casting method.

## 3.2 Dip-coating

Dip-coating technique was applied by Li et al. (2017) who prepared coatings of PLA blended with softwood kraft lignin on top of urea in order to produce

fertilizers with controlled nitrogen release. The lignin was pre-functionalized by esterification (with $Ac_2O$ or palmitic anhydride together with pyridine) to increase the hydrophobicity of the coating. PLA was dissolved in dichloromethane at a concentration of 60 wt %, and lignin was dissolved in dioxane at a concentration of 6 wt %. Then, these two solutions were mixed together in a volume ratio of 1:1. Dip-coating was performed by immersing urea pellets in the obtained PLA/lignin mixture solution for five minutes. Different thicknesses of the coating were obtained by repeating the dip-coating process different number of times. Lignin esterification with palmitic anhydride with pyridine resulted in less lignin aggregates and higher water contact angle (WCA) of the coating. Moreover, a good attachment of the coating layer on the surface of urea pellets was observed, as well as a compact, rather homogeneous and well distributed coating layer. A schematic illustration of dip-coating procedure is shown in Figure 5.

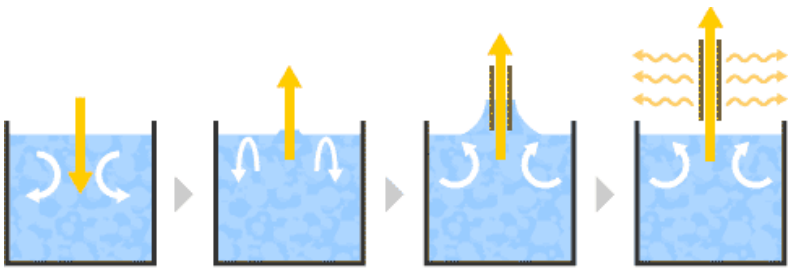

Figure 5. Illustration of dip-coating. (Anon. B) The substrate is immersed into the solution and a film is formed on top when the substrate is withdrawn. Finally, the solvent evaporates from the film surface.

## 3.3 Electrospinning

Electrospinning has also been used to prepare lignin films. Electrospinning is an electrohydrodynamical method where a continuous fiber is formed from a polymer solution. The diameter of the fiber can be in micro or nanometer scale. A large variety of polymers can be applied to electrospinning and the produced fibers can have very interesting properties. (Ramakrishna, 2005, pp. 90-96) In Figure 6, a schematic illustration of electrospinning is shown.

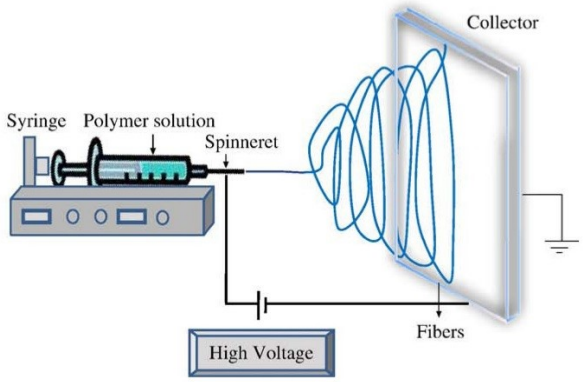


Figure 6. Illustration of electrospinning. (Zhu and Chen 2013.)

Dallmeyer et al. (2013) used electrospinning to produce moisture-responsive kraft lignin (Indulin AT) based films. As a material, different mixtures of different kraft lignin fractions were applied. As already mentioned, fractionation reduces the heterogeneity of lignin. Lignin has a great variability in molecular weight, thermal properties, polydispersity, and chemical structure, which makes its utilization in applications challenging. Thus, solvent extraction method was used to generate lignin fractions with different physical and chemical properties. The lignin fractions were dissolved in a dilute poly(ethylene oxide) (PEO) (0.2 wt %) in dimethylformamide (DMF) solution, followed by electrospinning. Next, the electrospun “fabrics” were treated with oxidative thermostabilization, clamped between glass plates and finally heated. By varying the amount of different lignin fractions, the total lignin concentration and the heating rate, films with different morphologies could be obtained. (Dallmeyer et al., 2013.)

# 4 Properties of the lignin films

The properties studied for pure lignin films are limited. Mainly morphology, thickness, water stability and water adsorption have been of interest so far. Moreover, films of modified lignin have also been explored only a little. Wider variety of properties has been studied for lignin composite films, such as barrier, mechanical, thermal and antioxidant properties. Thus, in the following section, in addition to pure and modified lignin films, also the properties of composite films are introduced.

## 4.1 Pure and chemically modified lignin films

### 4.1.1 Morphology

Morphology studies of films are important in the sense that they reveal the surface roughness, as well as if the produced films are continuous and fully covering. In food application products, these issues have an effect on the efficiency to protect and preserve food. Atomic force microscopy (AFM) is one of the most popular techniques used for morphology studies. In AFM, a sharp tip is integrated with a flexible microcantilever. The probe interacts with a selected substrate when it is moved across the substrate surface. At the same time, one or more interactions are monitored between the probe and the surface, which can further be employed to unveil for example the surface morphology or organization. On advantage of AFM is that it is very sensitive and can give information already from a few nanometers depth on the surface. Moreover, in addition to hard materials, also soft materials can be scanned without damaging them, because of the gentler tapping-mode. (Tsukruk and Singamaneni, 2012, pp. 3-10) In Table 1, the root-mean-square (RMS) roughness measured by AFM in the different studies are shown.

Table 1. Root-mean-square (RMS) roughness of different lignin films.

| Lignin type/solvent in coating | Method | RMS (nm) | Reference |
|---|---|---|---|
| MWL/1,4-dioxane | Spin-coating | 0.4 | Tammelin et al., 2006 |
| Kraft/$NH_4OH$ | Spin-coating | 1.1 | Norgren et al., 2006 |
| Kraft/ $NH_4OH$ | Spin-coating | 0.93 | Notley and Norgren 2010 |
| Hardwood MWL/acetone-$H_2O$, 9:1 | Spin-coating | 1.38 | |
| Softwood MWL/ acetone-$H_2O$, 9:1 | Spin-coating | 1.31 | |
| Model compound DHP/dioxane-$H_2O$, 9:1 | Spin-coating | 3.7-5.4 | Hambardzumyan et al., 2011 |
| MWL (Spruce)/1,4-dioxane | Spin-coating | 5.41 | Pereira et al., 2017 |
| MWL (Wheat straw) /1,4-dioxane | Spin-coating | 4.15 | |
| MWL (Eucalyptus) /1,4-dioxane | Spin-coating | 2.14 | |
| Ethanol–water /DMA-chloroform, 20:80 | LB | 0.24 | Pasquini et al., 2005 |
| acetone–oxygen /DMA-chloroform, 20:80 | LB | 0.30 | |
| Soda /DMA-chloroform, 20:80 | LB | 1.25 | |
| acetone–water–sulfuric acid /DMA-chloroform, 20:80 | LB | 3.80 | |
| Hardwood MWL/NaOH (aq) | LbL | 1.6 | Pillai et al., 2014 |
| Organosolv/ NaOH (aq) | LbL | 3.8 | |
| Lignosulfonate/aq | LbL | 1.13 | Liu et al., 2009 |
| Modified organosolv | PVD | 6.7 | Volpati et al., 2011 |

From Table 1, it can be seen that the lignin source and film preparation method affect the RMS of the films. Moreover, since the films were prepared by using different methods, also this most likely has an effect. However, the results between different studies using same film preparation methods vary a lot. Thus, it is difficult to say which method results in the best films. The smoothest films were obtained by Tammelin et al. (2006), who had rigid, evenly distributed films on the substrate.

The difference in the RMS roughness caused by the different extraction methods could be seen in the study by Notley and Norgren (2010). All the films were free from any cracks or large holes (Figure 7 A-C). However, the kraft lignin films showed much smaller aggregates on the surface and hence were smoother. This is most likely due to the difference in solubility of the kraft lignin in ammonium hydroxide compared to the MWL in the acetone-water mixture. Moreover, Pasquini et al. (2005) noticed that a much lower roughness was indicated for the lignins with higher contents of COOH groups. This is because the molecular arrangement in the films depends on the contents of these polar groups. Consequently, the extraction processes of acetone-oxygen and ethanol-water yielded lignins with smoother film formation capability.

The difference in the RMS roughness caused by lignin type was shown in the study by Pereira et al. (2017). While all the lignins covered the whole substrate surface, spruce and wheat straw films were slightly rougher compared to the films obtained from eucalyptus. This is possible due to the more significant presence of syringyl units in eucalyptus, which resulted in smoother films. In syringyl units, the methoxyl groups can block the 3 and 5 positions of the aromatic rings, which further results in more linear lignin structure. Moreover, the interactions between molecules are different. (Pereira et al. 2017.)

The films by Volpati et al. (2011) had small aggregates of lignin spread all over the substrate surface and they showed a homogeneous film when imaged in micrometer scale with optical microscopy. Complete coverage of the surface by lignin was also discovered in the LbL lignin/nanocellulose films by Pillai et al. (2014), in all deposition cycles. Moreover, pH had on effect on the lignosulfonate films by Liu et al. (2009). At pH 12, lignin particles in the monolayer were well attached and uniformly covered the mica surface (Figure 7E). In lower pH, the

lignin tended to aggregate. Moreover, the roughness increased to 5.33 when the number of layers increased from one to 18.

The multilayered cellulose nanocrystal/lignin films by Hambardzumyan et al. (2011) showed that lignin formed globular structures on the cellulose surface, thus improving the adhesion of cellulosic layers (Figure 7D). Furthermore, the bulk concentration of the lignin was noticed to affect the morphology. The surface roughness of the lignin layer on cellulose increased from 2.5 nm to 5.4 nm when the lignin bulk concentration increases from 0 to 1 g/L. Sarkanen et al. (1984) reported that lignin starts to aggregate in concentrations above 0.5 g/l in alkaline solution, which can explain the increased roughness detected by Hambardzumyan et al. (2011).

AFM was also applied in other studies where RMS roughness was not mentioned. Maximova et al. (2004), adsorbed lignin on both mica and cellulose substrates. As a substrate, mica is very similar to silica: smooth, nonporous and hydrophilic. Mica also has nearly perfect cleavage. It was noticed that on mica lignin adsorbed as granules or patches. On the other hand, on cellulose the lignin adsorbed as a thin film when lignin was mixed with cationic starch before mixing with the cellulose fibers. However, even if the concentration of lignin in the solution was increased to 0.2 g/l, the film did not cover the whole sample but rather formed larger aggregates with more scattered adsorption.

Gordobil et al., 2017 prepared lignin coatings on wood veneers by immersing and press molding. They noticed that the roughness depended on the coating method used. The roughness increased less than 12 % when immersing but over 60 % when coating method was applied. The roughness of films prepared by spin-coating by Meincken and Evans (2010) increased with radiation of UV, visible and IR light. The percentage roughness change of lignin films exposed to the total solar spectrum was much greater (161.2%) than that of films exposed to visible and IR radiation (86.7%) or only to IR radiation (94.3%). AFM images showed smooth surfaces of the unexposed and only IR exposed lignin films. Lignin films exposed to the full solar spectrum developed spherical structures with diameter of approximately 300 nm. When the lignin films were exposed to visible and IR light in the absence of UV radiation, fewer of these spherical structures were visible and they were also smaller, with a diameter of approximately 100 nm. The increase in roughness and the formation of the

spherical structures were related to the photodegradation, and further re-organization of lignin.

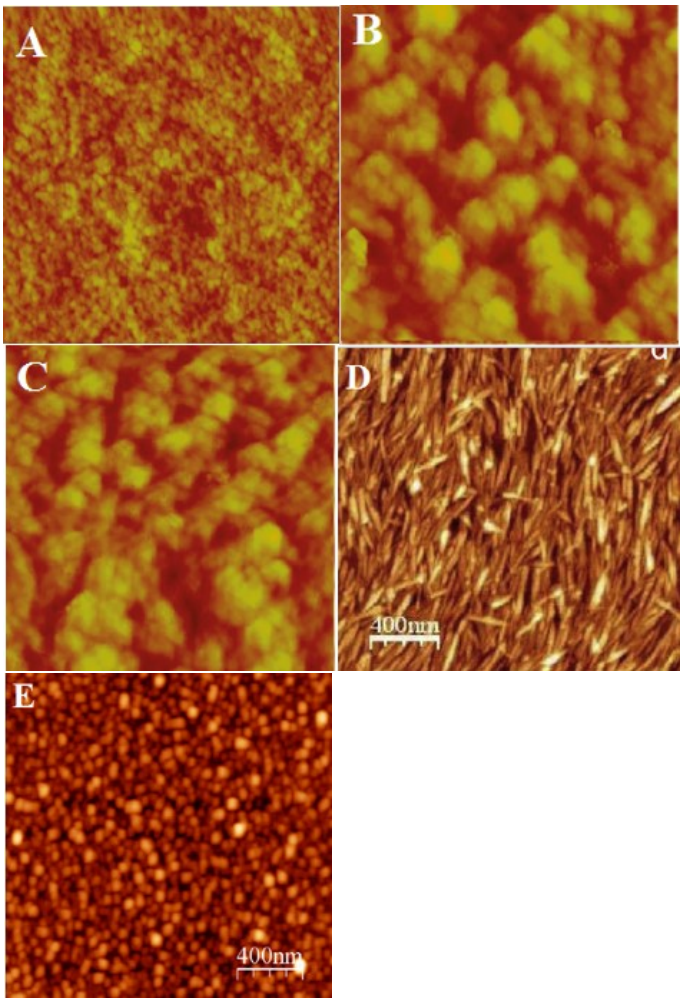


Figure 7. AFM and SEM images (1x1 $\mu m^2$, unless otherwise stated) of lignin films. A) Kraft lignin on silica, B) Hardwood MWL on silica and C) Softwood MWL on silica (Notley and Norgren 2010); D) DHP lignin model compound on cellulose nanocrystals (Hambardzumyan et al., 2011); E) Monolayer of lignosulfonate on mica (Liu et al., 2009).

### 4.1.2 Thickness

In addition to morphology and roughness, AFM is also one of the most used techniques to measure the film thickness. The films can be scratched or only partly spin-coated by covering half of the QCM-D crystal with tape. Then, the thickness can be measured based on the height differences on the substrate. The film thickness depends on various factors, including amount of lignin used and film forming method. The spin-coated films by Tammelin et al. (2006) were measured to have thicknesses of 200-300 nm. Meincken and Evans (2010), as

well as Pillai et al. (2014), obtained film thickness of approximately 1 µm and 17 nm, respectively. In the case of Pillai et al. (2014), the films were multilayered nanocomposites of lignin and nanofibrillar cellulose, where PDDA was used in between to increase the adhesion. Thus, the given thickness, 17 nm, is the thickness per one adsorption cycle of PDDA-lignin-PDDA-nanocellulose. Visualization of micro, nano and molecular scale structures is possible with AFM (Tsukruk and Singamaneni 2012, p. 28), which is supported by the film thickness results obtained in the studies listed above (Tammelin et al., 2006; Meincken and Evans 2010; Pillai et al., 2014).

Another widely utilized thickness measurement method is ellipsometry. In ellipsometry, a light beam is polarized and the polarization state is manipulate before it hits the sample. The sample produces a change in the polarization state, and this change is detected. (Humlíček, 2005, pp. 9-10) The film thickness can be determined by the interference between the light reflecting from the surface and the light travelling through the film. The maximum film thickness that can be measured has to be less than the coherence length of the light source. Film thickness can thus range from less than one nanometer to several micrometers. (Garcia-Caurel et al., 2013, pp. 32-62) In Figure 8, the set-up of ellipsometry is shown.

Norgren et al. (2006) measured the film thickness with a high-resolution phase modulated ellipsometer. The film thicknesses were between 20 and 140 nm, depending on the conditions, such as solution concentration and spinning rate. Notley and Norgren (2006) had films with thickness of 80-90 nm, while in 2008 and 2010, they determined the film thickness of kraft lignin films to be 60-75 nm and 50-60 nm, respectively.

Ellipsometry was also used by Pereira et al. (2017), Kent et al. (2015) and Constantino et al. (1996). The thicknesses of Pereira`s et al. (2017) lignin model surfaces were 14, 9, and 9 nm for spruce, wheat straw, and eucalyptus MWL, respectively. Kent et al. (2015) gained films with thicknesses of 560 Å and 950 Å for 2% and 3% lignin solutions, respectively. Constantino et al. (1996) obtained films with 60 Å thicknesses per deposited layer.

Hambardzumyan et al. (2011), who prepared cellulose nanocrystal/lignin films, measured the thickness of one lignin layer with ellipsometry. The thickness was about 7.5 -141 Å, after 6 hours of contact, depending on the bulk concentration of

the lignin model compound. After washing with water and drying with $N_2$, the layer collapsed and the thickness was decreased to 0.2-79.9 Å, for the same bulk concentration range.

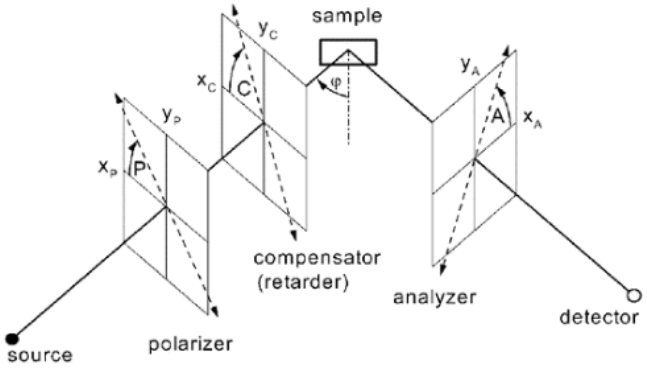


Figure 8. Set-up of ellipsometry. A light beam is polarized while it travels to the sample through a polarizer and a compensator. An analyzer and a detector detect the change in polarization caused by the sample. (Humlíček 2005, p. 10.)

Volpati et al. (2011) measured their film thickness in situ by quartz crystal microbalance and ex-situ by UV-visible absorption spectroscopy. The in situ measurement resulted in film thicknesses from 20 nm to 120 nm. The results obtained by the UV-visible absorption showed that since the deposition of lignin was done in steps, similar amount of lignin is deposited in each evaporation step, leading to an average thickness of approximately 20 nm for each 5.5 mg of lignin deposited.

One interesting method to be used for film thickness measurements is attenuated total reflection infrared (ATR-IR) spectroscopy, even though it has not been applied for lignin films yet. Kivioja et al. (2012) showed the possibilities of this method by measuring the thickness of thin polystyrene films on polypropylene substrate, based on the band intensities of polystyrene and polyethylene. From the ratio of these intensities, the films thickness could be calculated mathematically. The results were compared with the ones obtained from more conventional methods, ellipsometry and the spin-coating model. The obtained thickness ranged from 50 to 350 nm for the polystyrene and thus, thin films of lignin could possibly be measured with this technique as well.

### 4.1.3 Barrier against water and oxygen

Considering films for food applications, the most important function of them is to protect and preserve the food as well as possible. Especially important are the barrier properties against oxygen and water vapor because oxygen can penetrate from air, and foods and food packages are often exposed to RH of 50 % and above (Pike 1991, p. 37). Barrier against oxygen and water vapor can be studied, however, only for self-standing films and not for example silica-supported films. In addition to these properties, also water stability and wetting properties of lignin films have been studied (Tammelin et al., 2006; Norgren et al., 2006; Notley and Norgren 2006 and 2010; Liu et al., 2009; Gordobil et al 2017).

Hult and Ropponen et al. (2013) discovered that the water vapor transmission rate (WVTR) of the paperboard (840 g/m$^2$ × 24 h) could be reduced to 260 g/m$^2$ × 24 h with a TOFA lignin double coating of 3.9 g/m$^2$. Moreover, the gained value was in the similar range of magnitude as PLA. In addition, a decrease in oxygen transmission rate (OTR) was observed for the TOFA lignin coated paperboard. Moreover, a double coat layer resulted in even lower OTR values. However, even though a reduction in OTR was observed for the coating material, the values are not low enough compared, for example, to ethylene vinyl hydroxide (OTR = 0.01–0.1 cm$^3$ µm/m$^2$ day kPa). This was probably because fully homogeneous and continuous films were not obtained, even though in the high magnification (x 10 000) scanning electron microscopy (SEM) images in Figure 9 the film looks very smooth and homogeneous.

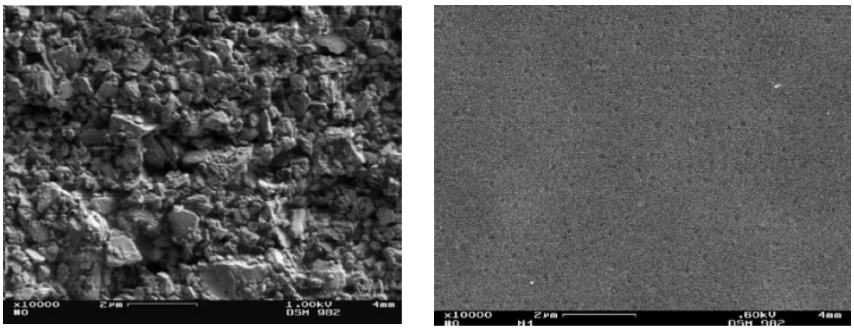

Figure 9. SEM images of uncoated paperboard (left) and TOFA-lignin coated paperboard with a coat weight of 3.9 g/m$^2$ (right). (Hult and Ropponen et al., 2013.)

Hult and Koivu et al. (2013) prepared films also from lignin esterified with palmitic and lauric acid chloride. Based on WVTR values, lignin palmitate coatings seem to provide better water vapor barrier compared to that of lignin laurate coatings.

This may be due to the different chain lengths of the fatty acids. The lowest WVTR value was reached with a double coating of lignin palmitate: 40 g/m$^2$ x 24 h. A paperboard sample coated with 10 g/m$^2$ PLA has a WVTR of 300 g/m$^2$ x 24 h and thus the WVTR of the TOFA lignin coated paperboards was lower than that of PLA. Considering the OTR, palmitate provides better barrier against oxygen than laurate. Since OTR is sensitive to defects on the coat layer, it is possible that lignin-palmitate can form more uniform films than lignin-laurate. However, the achieved OTR values are higher compared with synthetic films, such as ethylene vinyl alcohol, or polypropylene with OTR values of 0.01-0.1 and 494-987 cm$^3$ µm/m$^2$ day kPa, respectively.

In addition to water vapor, also the barrier against water and water stability has been studied a little. Water stability at different ionic strengths of the spin-coated films prepared by Tammelin et al. (2006) was studied with QCM-D. The addition of water/electrolyte solution on the substrate did not affect the dissipation change, showing that the lignin film did not swell. However, the vibration frequency decreased, indicating that some water penetrated into the lignin. The frequency and dissipation curves are presented in Figure 10.

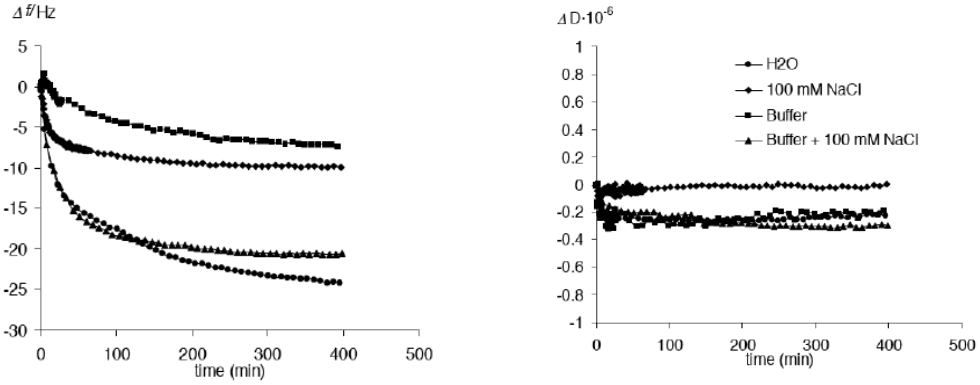


Figure 10. Changes in frequency (left) and in dissipation (right) with different solutions. Buffer is 10 mM sodium acetate/acetic acid solution. (Tammelin et al., 2006.)

Norgren et al. (2006) found that the stability of their lignin films in aqueous solutions was excellent. No changes in the thickness could be detected when the films were immersed in slightly alkaline NaOH solutions (pH 9.2) even for 5 hours. This was probably because of the hydrogen bonding between lignin and the silica substrate. A 10 percent reduction in the thickness of the lignin film was observed after 5 h of exposure to a solution containing 0.1 M NaCl. It is most probably due to an ion-exchange taking part at the outer layer of the film. Some

of the hydrogen ions are exchanged to sodium ions, which decreases the hydrogen bonding capacity and causes the lignin to dissolve.

Notley and Norgren (2006) tested their film stability against water at different pH (7, 8.5, 9 and 9.5) with QCM. It was noticed that up until pH of 9 very little changes occurred. At pH 9.5 a strong swelling of the film was observed. This swelling was attributed to physical cross-linking through hydrogen bonding between the available phenolic groups on the lignin structures. Also ionic strength was noticed to affect the stability. Dissociation of phenolic groups in the lignin film was approximately 0.5 % at pH 9.5 and at a background electrolyte concentration of 0.1 mM. When the electrolyte concentration was increased to 1 and 10 mM, the degree of phenolic dissociation was increased to 1.7 and 5.3 %, respectively. Thus, it was concluded that under these conditions the lignin film is close to instability.

A lignin coating on top of wood veneer (Gordobil et al., 2017) decreased the moisture content of all the treated veneers. Depending on the veneer type, the moisture content decreased from 6.47 ± 0.58 (beech) to 2.44 ± 0.18 for spruce lignin and to 2.19 ± 0.21 for eucalyptus lignin, when the coating method was applied. When immersion was used, the moisture content decreased to 2.82 ± 0.34 for spruce lignin and to 2.88 ± 0.48 for eucalyptus lignin.

Wetting properties have also been studied, by the contact angle measurement. WCA of the films by Norgren et al. (2006) decreased only a little, from 46° to 38°, during 20 minutes and thus it was concluded that the films did not swell a lot, but the decrease could be due to the water evaporation. In the case of Notley and Norgren (2010), water partially wet all of the lignin films. However, for example for the hardwood MWL films, the contact angle stayed quite stable, only decreasing a little over 10 minutes time. Hardwood MWL had the highest WCA, then the softwood MWL, and finally the kraft had the smallest: 55.5, 52.5 and 46, respectively. However, these kinds of WCAs show that the lignin did not manage to make the surfaces hydrophobic.

Gordobil et al. (2017) measured the wetting behavior of their esterified lignin coatings on wood veneers with water and ethylene glycol contact angle measurement. The original wooden veneers presented hydrophilic and oleophilic character, since their contact angles were unstable and decreased over time. However, the coated wood veneers had values between 90–120° for water and

70–100° for ethyleneglycol due to the high hydrophobicity of the esterified lignin. Water and ethylene glycol contact angles for the coated beech veneer are shown in Figure 11. In the case of impregnated wood veneers, the contact angles were higher and more stable than coated woods, remaining practically unchanged during the test period with 120–140° for water and between 110–130° for oil.

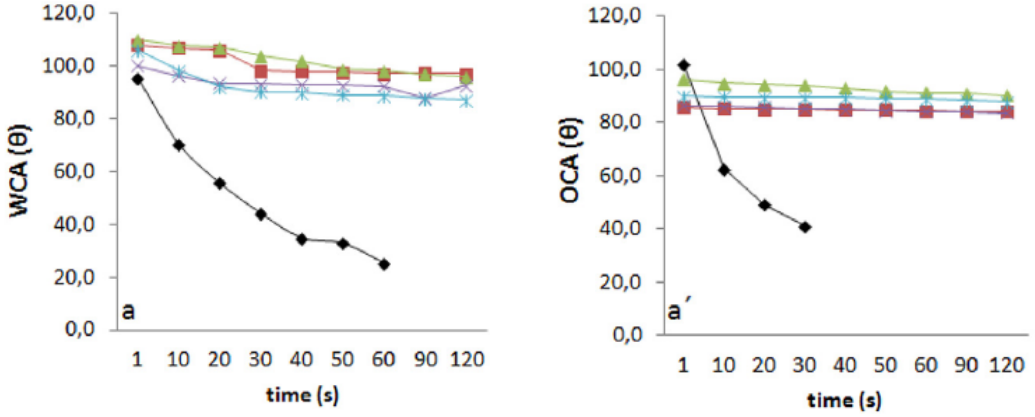


Figure 11. Water (WCA) and ethylene glycol (OCA) contact angles for beech veneer. Black line is the uncoated veneer and the colorful lines are veneers press molded in slightly different conditions (pressure and temperature). (Gordobil et al., 2017.)

Liu et al. (2009) noticed as well that the WCA increased from $6.5^0$ to $86^0$ after 18 layers of lignosulfonate had been deposited on the mica substrate. The increase in surface roughness of the multilayer contributes to the increase in surface hydrophobicity as evidenced by the contact angle measurements. Additionally, the presence of numerous nanopores can lower the surface contact area of water.

### 4.1.4 Mechanical

Mechanical properties of films are important to understand because they give information on how the film responds to stresses. Stress can have deleterious effects on films for example cracking and loss of the original molecular structure. This can further lead to loss of the original properties of the film. Typical mechanical properties measured for films and materials in general are tensile strength, elastic modulus and yield. Tensile strength tells the maximum stress that the material can withstand, while elastic modulus tells the stiffness of the material. On the other hand, yield stress is the point where the original properties of the material are lost and cannot be restored anymore. Moreover, elongation at break tells how much the material strains from the original before it breaks.

Finally, impact strength is an important characteristic of a film as well. (Ohring, 2002, pp. 711-716)

Mechanical tests by Wang et al. (2015) showed that the 100 % ball-milled and methylated lignin film, cast at 150 °C for a day and annealed at 180 °C for three hours, had a tensile strength of 43 MPa and a 5% elongation-at-break. This result compares favorably with polystyrene (46 MPa, 2.2% elongation-at-break). Lignosulphonate methylated with dimethyl sulphate alone had a 28 MPa tensile strength and a 5% elongation-at-break. This corresponds to polyethylene (30 MPa strength and 9% elongation-at-break). However, lignosulphonate methylated with both dimethyl sulphate and diazomethane, had an elongation-at-break of 11 %. The addition of other polymers, such as poly (ethylene glycol) or polycaprolactone caused improvement in tensile strength, elongation-at-break or in both. The un-methylated lignosulphonate had a tensile strength of approximately 22 MPa and 3.5% elongation-at-break, showing that the methylation had a large effect on the properties.

## 4.2 Lignin composite films

As already mentioned at the beginning of chapter 4, more studies exist on the properties of lignin composite films than pure or modified lignin films. To get a wider understanding on the features of lignin, examples of the properties of lignin composite films are also included in this thesis. The examples are selected in a way that the impact of lignin can evaluated relatively well.

### 4.2.1 Morphology

In many previous studies, the addition of lignin to a matrix has increased the surface roughness and formation of agglomerates, often shown with SEM. Agar-lignin films, with lignin contents of 3, 5 and 10 %, were prepared by Shankar et al. (2015). According to the SEM images, lignin particles were well dispersed into agar biopolymer but still more agglomerated when 10 wt % lignin was incorporation compared to 3 and 5 wt % incorporation. Bodirlau et al. (2013) added 4 wt % of lignin to corn-starch/starch microparticle matrix resulting in slightly increased surface roughness and some particle aggregation. Similar behavior was observed by De Miranda et al. (2015), who prepared films of cassava and corn starch combined with lignin and glycerol. Moreover, Espinoza-Acosta et al. (2015), who prepared composite films of durum wheat starch and

lignin, noticed that with incorporation of lignin at the high 20 wt % concentration, discontinuities were observed in the films. However, cavities, agglomerations or undissolved particles of lignin were not seen. In Figure 12, SEM images (x 500 magnification) of neat durum wheat starch film and 20 wt % lignin containing composite film, are presented.

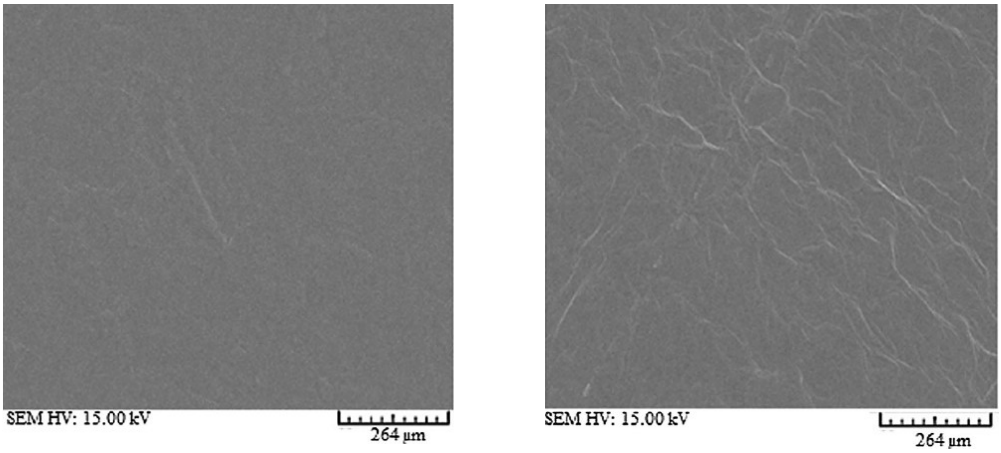


Figure 12. SEM images of neat durum wheat starch film (left) and lignin (20 wt %)-starch composite film. (Espinoza-Acosta et al., 2015.)

However, alginate-lignin films by Aadil et al. (2016) with lignin contents up to 30 wt % were homogeneous as well as stretchy and easily handled, which could be due to cross-linking between alginate and lignin. Moreover, sago-starch-lignin films by Bhat et al (2013) were smooth and uniform because the lignin (5 wt %) was found to be completely dispersed. Films were also flexible and the flexibility increased with addition of glycerol.

Sadeghifar et al. (2016) prepared cellulose-lignin films, where lignin and cellulose were introduced together by covalent bonding via click chemistry. Because the cellulose was modified with azide functional groups and the lignin contained propargyl groups, the formed composite films were homogeneous and lignin was distributed evenly.

Dallmeyer et al. (2013) prepared lignin films of different kraft lignin fractions and their blends by electrospinning. They noticed that smooth films could be obtained with higher thermostabilization heating rates (5 °C/min). This is because higher heating rate favors the relaxation over cross-linking and consequently higher flow forms fused fibers. Moreover, the films became smoother when the amount of low molecular weight lignin fractions was increased in the blend because these

fractions had a higher thermal mobility. Thus, films made of only the high molecular weight fraction lignin did not form smooth fibers but when mixed with low molecular weight fraction lignins, smooth films were formed even at very low, 0.5 °C/min, heating rates.

It was also discovered that chemical composition of lignin affects the morphology. Because the strength of hydrogen bonds depends on the type of hydroxyl group, the amount of aliphatic and phenolic OH groups is important. Since the high molecular weight fraction of lignin had higher content of aliphatic OH groups, which form stronger hydrogen bonds in comparison to phenolic, it further explains the low thermal mobility of this lignin fraction. It must also be pointed out that carbohydrates were removed with the insoluble, highest-molecular-weight lignins and thus they did not have an effect on the mobility of the used lignin fractions. (Dallmeyer et al., 2013.)

### 4.2.2 Thickness

The thicknesses of the lignin composite films have in general been larger than that of the pure lignin model films. Mostly hand-held micrometers, or in some cases ellipsometry have been used to measure the thicknesses. In Table 2, some examples of lignin composite films thicknesses from literature are listed.

Table 2. Thicknesses of lignin composite films.

| Film composition (maximum lignin wt %) | Thickness | Reference |
|---|---|---|
| Corn-starch/ starch microparticle–lignin (4) | 0.2 mm | Bodirlau et al., 2013 |
| Sago-starch–lignin (5) | 0.13–0.14 mm | Bhat et al., 2013 |
| Durum wheat starch–lignin (20) | 0.07–0.09 mm | Espinoza-Acosta et al., 2015 |
| Cellulose–lignin (16.7) | 30 ± 5 µm | Aguié-Béghin et al., 2015 |
| Chitosan–lignin (30) | 50–100 µm | Crouvisier-Urion et al., 2016 |
| Cellulose–lignin (2) | 50 µm | Sadeghifar et al., 2016 |
| Alginate–lignin (30) | 0.17–0.9 mm | Aadil et al., 2016 |

### 4.2.3 Barrier against water and oxygen

Water vapor permeability (WVP) and oxygen permeability (OP) values studied for different lignin composite films are shown in Table 3. In general, the WVP decreased or stayed almost the same with lignin addition. Shankar et al. (2015) and Bhat et al. (2013) attributed these kind of results with the strong intermolecular interaction between the matrix and lignin, which further leads to good compatibility and lower permeation of water molecules through the film. In

the study by Bhat et al. (2013), the WVP decreased almost linearly with increasing lignin addition and lowest WVP was obtained with 5 wt % lignin addition (0.011). However, it must be noted that the conditions have a significant effect on the WVP values. High temperature and high humidity promote the transferring of water vapor, thus leading to much higher WVT values. Therefore, the results between different studies cannot be compared blindly. (Gordobil et al., 2016.) Results obtained by Crouvisier-Urion et al. (2016) were not very promising, since WVP and OP increased with increasing lignin content (Table 3). This was explained with the morphology of the film: incorporation of lignin makes the film less dense and the polymer network less cohesive.

Table 3. Water vapor permeability (WVP) and oxygen permeability (OP) for different lignin composite films.

| Film composition (lignin wt %) | Matrix | | Composite | | Reference |
|---|---|---|---|---|---|
| | WVP ($\frac{g*m}{m^2*s*Pa}$) | OP | WVP ($\frac{g*m}{m^2*s*Pa}$) | OP | |
| PLA–lignin (25) | $1.89*10^{15}$ | - | $1.85*10^{15}$ | - | Gordobil et al., 2016 |
| Agar–lignin (10) | $2.11*10^{-9}$ | - | $1.53*10^{-9}$ | - | Shankar et al., 2015 |
| Sago-starch–lignin (3) | $4.72*10^{-12}$ | - | $4.17*10^{-12}$ | - | Bhat et al 2013 |
| Chitosan–lignin (30) | 3.3* | 12.2** | 3.7* | 13.8** | Crouvisier-Urion et al., 2016 |

* The unit for WPV is $10^{-10}$ g $*m^{-1} * s^{-1} * Pa^{-1}$

** The unit for OP is $10^{-18}$ mol $*m^{-1} * s^{-1} * Pa^{-1}$

Rojo et al. (2015) measured barrier properties against water vapor and oxygen for nanocellulose films containing residual lignin. At lower RH (50%), OP was reduced from 0.23 to 0.01 $\frac{ml*mm}{m^2\ day\ atm}$ when the films contained 14 wt % of lignin. However, in higher RH (80 %), OP was slightly increased. Improved oxygen barrier properties were associated with smaller pore structure when lignin was present. WVP depended more on the density of the film and not the amount of lignin.

In addition to water vapor permeability, also water stability and wetting properties of lignin composite films have been studied widely. In a few studies, water solubility of the film was noticed to increase with increasing lignin content, while in others it decreased. The increase was most probably due to the plasticizing effect of lignin, which facilitates the diffusion of permeable water molecules (Espinoza-Acosta et al., 2015), or to the dissolution of alkali lignin in the case of

Shankar et al. (2015). On the other hand, the decrease was attributed to the cross-linking and miscibility of phenolic compounds of lignin with a hydrophilic moiety of alginate (Aadil et al., 2016) or to the high hydrophobicity of the used lignin in the case of Bhat et al. (2013). In Table 4, the water solubility of different lignin composite films are presented.

Table 4. Water solubility of different lignin composites.

| Composite (wt % lignin) | Solubility (%) | Reference |
|---|---|---|
| Starch–lignin (5) | 7.82 | Espinoza-Acosta et al., 2015 |
| Starch–lignin (10) | 13.37 | Espinoza-Acosta et al., 2015 |
| Starch–lignin (15) | 20.96 | Espinoza-Acosta et al., 2015 |
| Agar–lignin (0) | 25.6 | Shankar et al., 2015 |
| Agar–lignin (10) | 34 | Shankar et al., 2015 |
| Alginate–lignin (0) | 74.50 | Aadil et al., 2016 |
| Alginate–lignin (30) | 26 | Aadil et al., 2016 |
| Sago-starch–lignin (0) | 60 | Bhat et al., 2013 |
| Sago-starch–lignin (4) | 40 | Bhat et al., 2013 |

Wetting properties are often evaluated by WCA measurement. In general, lignin increased the WCA because of its higher hydrophobicity compared to the matrix. For example, for nanocellulose films the increase was from 35 to 78° with 14 wt % of lignin addition (Rojo et al., 2015). However, for example the agar based films the WCA was reduced with lignin addition, possible because lignin is more hydrophilic than agar (Shankar et al., 2015). In addition, for chitosan films the decrease in contact angle can be seen in Figure 13 (Crouvisier-Urion et al., 2016).

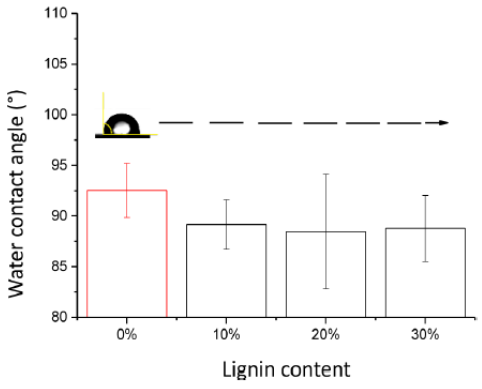


Figure 13. Water contact angle of lignin-chitosan composite films with different lignin amounts. (Crouvisier-Urion et al., 2016.)

Swelling of the films is not either very straightforward to explain. Alginate-lignin films experienced a higher swelling with increasing lignin addition, even though the solubility and water uptake decreased. This was explained by high degree of cross-linking between alginate and lignin molecules or that the carboxyl groups facilitated the swelling property of alginate. However, the swelling of corn-starch films (Bodirlau et al., 2013) and cellulose hydrogel films (Nakasone and Kobayashi 2016) was reduced upon lignin addition. In addition, water uptake was reduced in these cases, probably because of the interfere in cellulose-water interaction caused by lignin.

### 4.2.4 Antioxidant

Oxidation is often the primary factor limiting the shelf-life of food. During oxidation, substances, such as alkanes, alkenes, aldehydes and ketones, are produced, which cause bad smell and flavor to the food. Moreover, these compounds react with other functional groups, leading to damage of the texture of the food. Thus, preventing oxidation with packaging or addition of antioxidants is crucial. (Sun Lee, 2014, pp. 111-112) The structure of lignin contains aromatic rings with hydroxyl and methoxyl functional groups. Because of these groups, oxidation reactions can be terminated through hydrogen donation. (Lu et al., 1998.) Thus, lignins could act as an inexpensive and safe antioxidants in various food applications to replace for example E- and C-vitamins (Espinoza-Acosta et al., 2016).

The antioxidant property of a material can be evaluated with the ability to scavenge free radicals. A popular radical for this purpose has been 2,2-diphenyl-1-picrylhydrazyl (DPPH•). The radical scavenging ability of the starch–lignin films (Espinoza-Acosta et al., 2015) increased as the lignin content increased: lignin incorporation of 5, 10 and 20 wt % resulted in 12.33, 23.37 and 43.68 % inhibition of DPPH• respectively. With a 20 wt % addition of lignin in a chitosan matrix, a 60 % decrease of the free radical DPPH• was detected (Crouvisier-Urion et al., 2016). With 10 and 30 wt % of lignin, the decrease was lower. In the case of 30 wt % lignin, this can be due to a too high lignin concentration inducing lignin aggregates, which could further hide active groups. The antioxidant capacity of lignin was attributed to surface activity of lignin. This means that radical-scavenging activity was mainly present on the film surface instead of being based

on the migration of free active radical-scavengers, such as monomers, oligomers or other free phenols, to the food.

Aguié-Béghin et al. (2015) studied the antioxidant activity of lignins in multiphase systems mimicking the food and packaging matrices. The cellulose-lignin films, with 16.7 wt % of lignin, were immersed into an ethanol/DPPH• solution and the DPPH• reduction was followed until a steady state was reached. The total antiradical capacity of the film ranged between 18.9 and 40.7 µmol of reduced DPPHH• per mg film, depending on the lignin extraction process. Moreover, the radical scavenging capacity increased with decreasing molecular mass averages and increasing ethanol solubility of the lignin. In Figure 14, the DPPH• scavenging activity of cellulose films incorporated with lignin is illustrated. The black bar represents the activity of the lignin in the films and the hatched bar the lignin released in the ethanol medium.

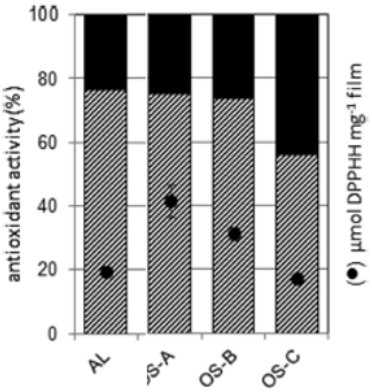


Figure 14. DPPH• scavenging activity of cellulose films incorporated with alkali (AL) and organosolv (OS) lignin. OS-A, OS-B and OS-C were extracted with different methods. (Aguié-Béghin et al., 2015.)

Oxygen-scavenging is an alternative way to evaluate the antioxidativity. It means the ability to remove oxygen from a medium. An oxygen-scavenger adsorbs oxygen and thus prevents it from reacting with the compounds of food. The scavengers can be in the form of sachets or part of the packaging structures. (Rooney, 2005, pp. 123-135) Johansson et al. (2012) studied oxygen-scavenging ability of films containing starch or latex incorporated with lignosulfonates and laccase as catalyst. Board was coated with the films and placed inside an airtight container. After three days of incubation at RH of 100 %, the coated board began to scavenge oxygen. After 6 days, the oxygen concentration had reduced to 0.3 % from the initial 1 %. Without laccase catalyst or at RH of 84 %, no reduction in

oxygen content was detected. In 2014, Johansson et al., prepared different lignin coatings on top of aluminum foil and board. Once again, the oxygen-scavenging ability was tested, this time by immersing the films on top of foil in an aqueous solution, as well as incubating the films on top of board in oxygen-containing gas chamber. In the solution, lignosulfonate lignin performed the best, the oxygen consumption being 1.1 µmol/min/g of film. In the gas environment, organosolv lignin performed the best by reducing the oxygen content of the board from 1.0 % to 0.4 % in seven days.

### 4.2.5 Antimicrobial

Different types of lignins poses antimicrobial properties, depending on their origin and processing method. Different microorganisms, such as *E. coli, S. cerevisiae, B. licheniformis, and A. niger,* as well as several yeasts, such as *Candida tropicalis, Trichosporon cutaneum, and Candida albicans,* have been inhibited successfully with different lignins. In general, the inhibitory effect is explained by the presence of methyl groups and C-C double bonds in the phenolic fragments. Moreover, different positions of these groups cause differences in the antimicrobial efficiency. (Espinoza-Acosta et al., 2016.) In food applications, lignin could thus act as an antimicrobial element.

One example of a lignin composite film that have been evaluated for its antimicrobial property is the alginate-lignin film by Aadil et al. (2016). While pure alginate film did not show any antimicrobial activity, alginate-lignin film with 30 wt % of lignin showed good activity against gram positive bacterial *Staphylococcus aureus*. This was studied by a plate containing the films. A zone of inhibition was discovered. However, no antimicrobial activity was observed against *E. coli* after 24 h of incubation. The origin and extraction procedure might influence the antimicrobial activity of lignins.

In addition to antimicrobial, lignin has also shown some antifungal activity as well (Doherty et al., 2011). This, however, need more research to be utilized properly.

### 4.2.6 UV-radiation

Due to its phenolic structure, lignin is an excellent UV-light absorber (190-400 nm) and thus can also absorb UV-B light at 280-320 nm. Accordingly, lignin could protect food against possible degradation caused by UV-light. (Duval and Lawoko 2014.) Sadeghifar et al. (2016) tested the UV protection of the cellulose-

lignin films that contained only small amount of lignin (0.5-2 %). The films containing 0.5 % lignin had a UV-B transmittance of 15−30 % which is equal to a sun protecting factor (SPF) of 15, used in sunscreens. With lignin addition of 2 %, the film absorbed around 100% of UV-B, which is equal to an SPF of about 100. Moreover, a strong UV irradiation using a UV xenon lamp or a thermal treatment at 120 °C did not have an effect on absorption ability.

Agar-lignin films prepared by Shankar et al. (2015) also showed reducing transmittance with the increasing amount of lignin. At 280 nm wavelength, the transmittance reduced from 51.9 to 4.7 % with the addition of 1 wt % of lignin. For alginate-lignin films (Aadil et al., 2016), the transmittance reduced from 21.31 to 0.01 when 30 wt % of lignin was incorporated to the matrix.

A small, 0.5 wt %, lignin addition improved the light barrier properties of PLA films produced by Xie et al. (2015). These PLA–lignin films blocked up to 80 % of UV-C (230–280 nm) and 40 % of UV-B light. In addition, 1 wt % of lignin in PLA resulted in nearly full blocking of the UV-C and UV-B, as well as 75–80 % of UV-A light.

### 4.2.7 Mechanical

In general, lignin addition has had both positive and negative effects on the mechanical properties of composite films, depending on the matrix used. Improvements in tensile strength, elastic modulus or both have probably been due to the small lignin additions, which enabled more uniform lignin dispersion in the matrix. Table 5 summarizes results from studies where enhanced mechanical properties have been detected.

Table 5. Mechanical properties of lignin composite films.

| Composite (lignin wt %) | Matrix | | | Composite | | | Reference |
|---|---|---|---|---|---|---|---|
| | Tensile strength (MPa) | Elastic modulus (MPa) | Elongation at break (%) | Tensile strength (MPa) | Elastic modulus (MPa) | Elongation at break (%) | |
| Agar–lignin (3) | 45.5 | 1070 | 26.7 | 52.1 | 1350 | 27.0 | Shankar et al., 2015 |
| Starch–lignin (4) | 12.8 | 1169 | 8.3 | 16.5 | 1084 | 5.3 | Bodirlau et al., 2013 |
| PVA–lignin (6) | 19.12 | 9.52 | 266.50 | 38.44 | 83.22 | 213.9 | Korbag and Saleh 2015 |
| Sago–starch-lignin (3) | 3 | 0.25 | 63 | 4.20 | 0.45 | 47 | Bhat et al., 2013 |
| Cassava-starch–lignin (29) | 21.600 | 2.144 | - | 930.100 | 20.153 | - | De Miranda et al., 2015 |
| Corn-starch–lignin (29) | 12.100 | 1.717 | - | 673.500 | 14.293 | - | De Miranda et al., 2015 |

An increase in tensile strength and elastic modulus were achieved in all of the studies listed in Table 5. This can be due to hydrogen bonding between the matrix and the lignin, which contributes to high level of interfacial adhesion and good dispersion of the lignin (Korbag and Saleh 2015, Bhat et al 2013). Moreover, lignin can act as a cross-linker and rigid structural component in the composite (Korbag and Saleh 2015). However, when the lignin content was increased, tensile strength decreased. This can be attributed to weakened interfacial adhesion (Shankar et al., 2015, Bhat et al 2013). Tensile modulus decreased too in some cases but in a few studies it increased with increasing lignin content (Shankar et al., 2015).

An exception is the study by De Miranda et al. (2015). Even with relatively high lignin contents, tensile strength remained high. Higher concentrations of lignin increased the ability of forming a rigid continuous network where for example hydrogen bonding is present. This increases the stiffness of the films due to the good interaction between starch, lignin and glycerol, which was added to the composite as well. In addition, elongation at break was reduced for all the composites in Table 5. This might also be due to the strong hydrogen bonding, or the low ductility of lignin (Bodirlau et al., 2013, Korbag and Saleh 2015).

On the other hand, in several studies the addition of lignin has decreased the tensile strength and elastic modulus, but increased the elongation at break

(Espinoza-Acosta et al., 2015; Gordobil et al., 2016). In Table 6, examples of these kinds of study results are shown.

Table 6. Mechanical properties of lignin composite films. (S) means spruce lignin and (E) means eucalyptus lignin.

| Composite (lignin wt %) | Matrix | | | Composite | | | Reference |
|---|---|---|---|---|---|---|---|
| | Tensile strength (MPa) | Elastic modulus (MPa) | Elongation at break (%) | Tensile strength (MPa) | Elastic modulus (MPa) | Elongation at break (%) | |
| Durum wheat starch–lignin (20) | 1.8 | 0.60 | 24.2 | 0.43 | 0.04 | 22.9 | Espinoza-Acosta et al., (2015) |
| PLA–lignin (25) | 38 | 2000 | 3 | 16 (S)<br>12 (E) | 1050 (S)<br>800 (E) | 27 (S)<br>15 (E) | Gordobil et al., (2016) |
| Chitosan–lignin (30) | 84.1 | 2540 | 7.1 | 29.8 | 2400 | 1.7 | Crouvisier-Urion et al., (2016) |
| Cellulose–lignin (2) | 118 | 3200 | 10 | 92 | - | 6 | Sadeghifar et al., (2016) |
| Alginate–lignin (20) | 0.562 | - | - | 0.146 | - | - | Aadil et al., (2016) |

The decrease in tensile strength and elastic modulus, and on the other hand the increase in elongation at break, were attributed to the plasticizing effect of lignin (Espinoza-Acosta et al., 2015, Gordobil et al., 2016, and Aadil et al., 2016). Moreover, the low compatibility between the matrix and lignin, lower crystallinity or lignin aggregation could also cause the reduction in the mechanical properties (Aadil et al., 2016, Sadeghifar et al., 2016, and Crouvisier-Urion et al., 2016). The difference between eucalyptus and spruce lignin in elongation at break could be due to the lower molecular weight of spruce (Crouvisier-Urion et al., 2016).

### 4.2.8 Thermal

The thermal stability of lignin composite films can be studied through weight loss and decomposition at different temperatures. In many cases, the maximum degradation temperature increased or stayed the same with lignin addition, which is attributed to good compatibility between lignin and the matrix. When 20 wt % of lignin was incorporated to starch matrix, the final degradation temperature increased from 480 °C to 700 °C (Espinoza-Acosta et al., 2015). Moreover, the addition of 25 wt % of spruce and eucalyptus lignin to PLA matrix increased the maximum degradation temperature from 331.6 °C to 357.1 °C and 339.1 °C, respectively, as it is shown in Figure 15 (Gordobil et al., 2016). For agar-lignin films, the presence of lignin did not have a significant effect (Shankar et al.,

2015), nor did it for PLA based lignin films containing up to 10 wt % of lignin (Xie et al., 2015).

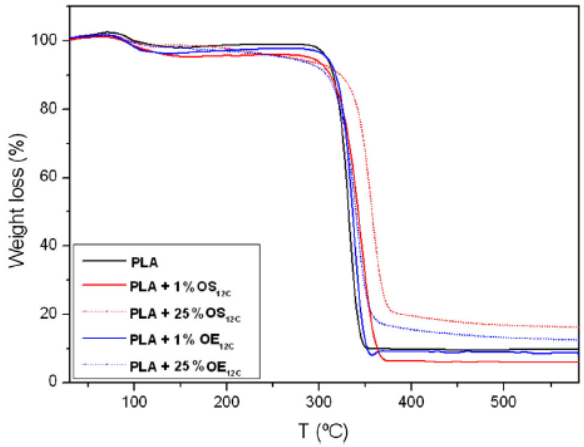


Figure 15. TGA (thermogravimetric analysis) curves of the PLA based films with 1 and 25 wt % of spruce (OS) and eucalyptus (OE) lignin, measured in nitrogen atmosphere. (Gordobil et al., 2016.)

However, the initial degradation temperature is often shifted towards lower temperatures. This temperature decreased to 270.7 °C for spruce lignin and to 266.7 °C for eucalyptus lignin when they were added 25 wt % to PLA matrix, the value being 309.7 °C for neat PLA (Gordobil et al., 2016). For agar-lignin films the decrease was from 220 °C to 218, 217 and 213 °C for 10, 20 and 30 wt %, respectively (Aadil et al., 2016). An overall, slight improvement in thermal stability was also observed along lignin addition for cassava and corn-starch (De Miranda et al., 2015), cellulose (Sadeghifar et al., 2016) and sago-starch (Bhat et al., 2013) based films.

## 5 Conclusions of the literature review

In several studies, lignin model films prepared with different methods on silica consisted of small, evenly distributed aggregates. The roughness depended on the lignin source and extraction method, as well as on the film preparation method, varying in the range of 0.4-6.7 nm. In addition, the films have shown great water stability in pH up to 9. On the other hand, according to WCA measurements the films are not hydrophobic but are still nonswelling and fully covering because of the relatively stable contact angles. Moreover, it has been shown that esterified lignin could enhance the barrier properties of paperboard

and that methylated lignosulphonates compared to polystyrene and polyethylene in their mechanical properties.

In composite films, lignin contents have been very low. Thus, only lignin has a minor effect on the film properties and factors, such as compatibility and cross-linking, have more significant impacts. When good compatibility between the matrix and lignin was achieved, the water vapor permeability decreased, while mechanical properties and thermal properties were enhanced. Good compatibility also enabled the formation of smooth and uniform films with smaller agglomerates. Water stability and wetting depended a lot on the plasticizing effect and hydrophobicity of lignin. Antioxidant and antimicrobial activity, as well as UV-light absorbance were all improved when lignin was added.

Based on the literature, it is possible to prepare homogeneous films of pure lignin without additives. The films are stable in water over wide pH and salt ranges. Lignin films can also act as a barrier against water vapor and UV-light, as well as prevent oxidation and microbial activity. To protect food from these kinds of threats is very important when longer shelf-lives and smaller food wastage are of interest. Thus, lignin films have a great potential to be utilized in food packaging. Moreover, since lignin is also a dietary fiber, edible lignin films can have health, as well as environmental benefits.

Because of its simplicity and repeatability, spin-coating was chosen as the film preparation method in this thesis. Moreover, the film roughness for kraft lignin, which was also the starting material in this thesis, has been relatively low (0.93-1.1) compared to other film formation techniques. Roughness, thickness and distribution of lignin, as well as chemical composition, wetting properties and surface energy were measured for the prepared films. Finally, heat treatments were applied on the films to evaluate their effect on wetting properties and chemical composition.

# 6 Materials and methods

In this part all the materials and methods used in the experimental work are introduced and described in detail.

## 6.1 Lignin raw materials

The starting kraft lignin (KL), obtained from industrial softwood kraft pulping process was provided by UPM, Helsinki, Finland. Solvent fractionation of the kraft

lignin was done at VTT earlier and a schematic illustration of the process diagram in shown in Figure 16 (Jääskeläinen et al., 2017). During the process, lignin was dissolved in 60 % (by volume) acetone. The insoluble fraction (INS) was collected first. Next, water was added as anti-solvent and thus, the lignin started to precipitate. The precipitate was collected, followed by addition of more water and hence allowing a new lignin precipitate to form. This was repeated until all of the acetone was replaced with water and the four precipitates, here referred to as PREC1, PREC2, PREC3 and PREC4, were obtained. The fractions differed in molar mass and in chemical composition. In Tables 7, 8, 9 and 10, results from molar mass and $^{31}$P NMR measurements, as well as from elemental analysis and carbohydrate content for all the fractions and the original unfractionated KL, are collected, respectively.

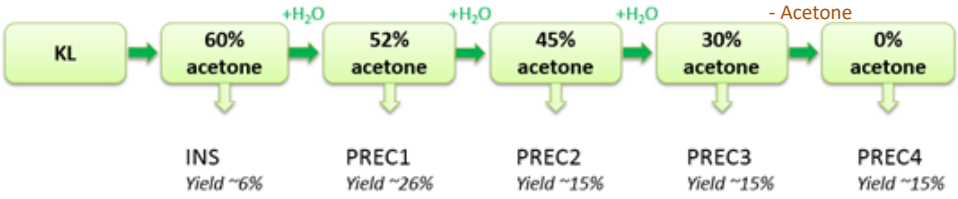


Figure 16. A schematic illustration of the solvent fractionation process using 60 % acetone (by volume) (Jääskeläinen et al. 2017).

Table 7. Molar masses and polydispersity of KL, INS, PREC1, PREC2, PREC3 and PREC4. Method according to Jääskeläinen et al., 2017.

| | Mn (Da) | Mw (Da) | PD |
|---|---|---|---|
| KL | 1384 | 3583 | 2.4 |
| INS | 1821 | 6850 | 3.8 |
| PREC1 | 2065 | 5833 | 2.8 |
| PREC2 | 1679 | 3383 | 2.0 |
| PREC3 | 1384 | 2498 | 1.8 |
| PREC4 | 960 | 1639 | 1.7 |

Table 8. Results from $^{31}$P NMR measurement (mmol/g of different OH groups in lignin) for KL, INS, PREC1, PREC2, PREC3 and PREC4. Method according to Granata and Argyropoulos, 1995.

| | Aliphatic OH | Carboxylic acid | Condensed + Syringyl | Guaiacyl | p-hydroxyphenyl | Phenolic OH | Total OH | Lignin purity |
|---|---|---|---|---|---|---|---|---|
| KL | 1.38 | 0.30 | 1.43 | 1.61 | 0.20 | 3.25 | 4.92 | 1 |
| INS | 1.65 | 0.27 | 1.57 | 1.56 | 0.21 | 3.34 | 5.27 | 1 |
| PREC1 | 1.76 | 0.32 | 1.74 | 1.62 | 0.26 | 3.63 | 5.71 | 1 |
| PREC2 | 1.69 | 0.40 | 1.85 | 1.86 | 0.27 | 3.98 | 6.07 | 1 |
| PREC3 | 1.41 | 0.41 | 1.84 | 2.12 | 0.30 | 4.25 | 6.08 | 1 |
| PREC4 | 1.74 | 0.52 | 1.82 | 2.74 | 0.32 | 4.88 | 7.14 | 1 |

Table 9. Results from elemental analysis (percentage of different elements in lignin) for KL, INS, PREC1, PREC2, PREC3 and PREC4.The standard deviation is presented in the parenthesis. Method according to Jääskeläinen et al., 2017.

| | C | H | N | S | O |
|---|---|---|---|---|---|
| KL | 64.26 (0.48) | 5.64 (0.03 | 0.04 (0.01) | 1.52 (0.05) | 28.88 (4.32) |
| INS | 64.48 (0.26) | 5.71 (0.02) | 0.08 (0.01) | 1.21 (0.01) | 28.18 (0.33) |
| PREC1 | 66.35 (0.09) | 5.72 (0.01) | 0.06 (0.02) | 1.23 (0.01) | 26.37 (0.11) |
| PREC2 | 65.68 (0.37) | 5.70 (0.00) | 0.06 (0.02) | 1.22 (0.01) | 25.63 (0.84) |
| PREC3 | 66.39 (0.14) | 5.76 (0.03) | 0.05 (0.00) | 1.17 (0.00) | 26.23 (0.05) |
| PREC4 | 65.38 (0.82) | 5.71 (0.04) | 0.03 (0.00) | 1.08 (0.05) | 26.89 (0.04) |

Table 10. Total monosaccharide content (mg/100 mg sample) of KL, INS, PREC1, PREC2, PREC3 and PREC4. Method according to Jääskeläinen et al., 2017.

| | Total monosaccharide content (mg/100 mg sample) |
|---|---|
| KL | 1.8 |
| INS | 7.6 |
| PREC1 | 0.2 |
| PREC2 | 0.3 |
| PREC3 | 0.7 |
| PREC4 | 1.5 |

## 6.2 Optimization of film preparation

Optimization of the film forming process was done with the unfractionated KL. An original 14.8 M aqueous ammonium hydroxide ($NH_4OH$, by Sigma-Aldrich) was first diluted to 1 M concentration, followed by dissolution of lignin in three different concentrations: 4, 5 and 8 g/l. The solutions were left to dissolve on a magnetic stirrer overnight, for at least 24 hours to ensure complete dissolution of lignin.

The lignin films were prepared by spin-coating. Prior to spin-coating, the silicon wafer substrates (1x1 $cm^2$, by Compugraphics, Jena, Germany) were cleaned by immersing them in 2.5 M sodium hydroxide (NaOH) for 15 minutes. The NaOH was washed away with tap water, followed by rinsing the substrates with milliQ-water and drying with nitrogen gas (approximately 0.2 bars pressure). Finally, the substrates were placed inside a UV-ozonizer (UV/Ozone ProCleaner by Bioforce Nanosciences, Ames, USA) for 15 minutes. Moreover, the extra silica substrates were stored in ethanol (Etax A by Altia Oyj).

The lignin/$NH_4OH$ solutions were spin-coated on top of the silica substrates using the following parameters: 2000 rpm speed, 2 minutes time and 2014 rpm/s

acceleration. The used spin-coater was Model WS-400 BZ-6NPP/LITE by Laurell Technologies Corporation (North Wales, USA). Prior to the lignin deposition, the silica substrates were rinsed with pure $NH_4OH$, using the same parameters as those for lignin. Moreover, the ability of polystyrene to increase the adhesion between silica and lignin was tested with the lignin concentration of 4 g/l. For this, polystyrene ($M_w \approx 192\,000$, by Sigma Aldrich) was dissolved in toluene (purity ≥ 99.9 %, Merck kGaA) in a 0.5 wt % concentration. Next, the silica substrates were wetted with pure toluene, followed by spin-coating the polystyrene/toluene (0.5 wt %) and finally the lignin/ $NH_4OH$ solution. Also here the same spinning conditions were applied as for lignin spin-coated on silica.

For each concentration, 1, 2 and 8 layers of lignin were deposited in order to evaluate the effect of the number of layers on the film formation. Once ready, the films were placed in oven (Heraeus), at 40 $^0$C temperature for 30 minutes to dry.

## 6.3 Film preparation from kraft lignin fractions

Films of the kraft lignin fractions PREC2, PREC3 and PREC4 were produced according to the obtained film forming protocol for unfractionated KL. The different fractions were dissolved in 4 g/l concentration in 1 M $NH_4OH$ for at least 24 hours. The lignin films were spin-coated on polystyrene pre-coated silica substrates, as described in section 6.2. Only one layer of lignin was deposited. The spinning parameters, as well as the film drying conditions used were the same as in section 6.2.

Films from the PREC1 and INS fractions were not obtained with the same method due to poor solubility of these fractions in $NH_4OH$. The ability of another solvent, 1,4-dioxane/water (9:1, by volume) mixture, to dissolve unfractionated KL was tested. Here, 1,4-dioxane (purity ≥ 99.5 %, Merck kGaA) was mixed with water in 9:1 ratio, followed by dissolving KL in 4 g/l concentration for 24 hours.

## 6.4 Atomic force microscopy

All the prepared lignin films were analyzed with atomic force microscopy (AFM) (Nano IR2 by Anasys Instruments) to evaluate the morphology, roughness and thickness of the films. Scanning was done in air using tapping mode. Auto-tune was applied to the silica cantilevers. The scan rate was 1 Hz. The areas scanned were 5x5 $\mu m^2$ and at least three different spots were imaged from each sample.

Moreover, 1x1 $\mu m^2$ areas were scanned for selected samples as well. No image processing except flattening was performed.

The film thickness was measured with scratch method. A step was created on the film by scratching it with a sharp scalpel. Film thickness was measured based on the height difference between the bottom of the step and the film surface. Two steps were scratched in each film and the height difference was obtained at least from two different spots from both scratches. Hence, the film thickness was calculated as an average of at least four different spots on the film. Film roughness was calculated by the AFM device as the root-mean-square roughness (RMS).

## 6.5 X-ray photoelectron spectroscopy

The XPS measurement was done for the KL, PREC2 and PREC4 films both before and after the heat treatments (Chapter 6.7). Films analyzed by XPS were produced on silica in order to avoid interference of the polystyrene on the measurement. The measurement was conducted at Aalto University in the Forest department according to the method by Johansson and Campbell (2004). An AXIS Ultra spectrometer with monochromatic Al Kα irradiation at 100 W was used under neutralization. Pure cellulose filter paper (Whatman) was measured with each film sample as an in-situ reference. The film samples were pre-evacuated overnight before the measurement. Wide scans (low resolution) and C 1s and O 1s high-resolution regions were acquired from 2-3 locations. The analysis area was approximately 1 $mm^2$ and the analysis depth 10 nm. CasaXPS software was utilized in data analysis: carbon and oxygen contents were determined from the wide scans, while chemical states of carbon were obtained from the high-resolution data.

## 6.6 Contact angle

Contact angle of several liquids of the KL, PREC2, PREC3 and PREC4 films was measured with sessile drop method with Attension Theta Optical Tensiometer (by Biolin Scientific, Espoo, Finland). The films were kept in a conditioned room (23 $^0$C, RH = 50 %) for at least 24 hours before the measurement. During the measurement, a water drop was let to fall on top of the lignin film from a dispenser tip. The size of the dispenser tip was 200 µl and the disp and fill rates were 20 µl/s. The liquid drop size was 4 µl and drop rate was 1 µl/s. The shape of

the drop was modelled by the computer program according to the Young-Laplace equation and the contact angle was obtained. The contact angle was recorded for total of 60 seconds. The saving was started when stroke was at the bottom. Light phase was air. Only one measurement was made on each sample because of the small size of the silica substrates. Thus, two parallel measurements were executed for all of the lignin fractions.

The used liquids for the contact angle measurement were water (milliQ) and three different dilute aqueous acetic acid solutions. The aqueous acetic acid solutions were prepared by adding acetic acid (100 % purity, Merck kGaA) to water in different mole fractions: 0.016, 0.032 and 0.05. Based on the contact angles, the critical surface tensions of the different lignin fractions were obtained by plotting the Zisman plots. The contact angles for the Zisman plots were calculated as an average of the two parallel measurements from the last five seconds of recording.

### 6.7 Heat treatment

Heat treatments of the lignin films were performed in air atmosphere with a chromatography oven (Agilent Technologies). Only films prepared from the KL, as well as from the PREC2 and PREC4 fractions, were heat treated. Films produced on both polystyrene and silica were heat treated in order to evaluate the possible effect of the presence of polystyrene. The lignin coated silica substrates were placed inside the oven on a glass petri dish. The films were heated from 30 ºC to 250 ºC with a heating rate of 10 ºC/min. Moreover, the films were kept at the end temperature of 250 ºC for 12 minutes. After this, the temperature was let to drop freely back to 30 ºC before the films were taken out of the oven.

## 7 Results and discussion

### 7.1 Optimization of film formation

In order to be able to produce homogeneous, fully covering films from the different lignin fractions, film formation optimization tests were first performed on KL. In this part, the results of the optimization are introduced. The effect of lignin concentration, the number of layers deposited and the presence of polystyrene pre-layer on the film forming is evaluated based on AMF images and WCA.

### 7.1.1 Atomic force microscopy

Based on earlier experience at VTT, the starting lignin concentration in $NH_4OH$ was chosen to be 4 g/l. Moreover, lignin starts to aggregate already at relatively low concentrations in alkaline solution: Sarkanen et al. (1984) reported kraft lignin aggregation when the lignin concentration was above 0.5 g/l, while Fritz et al. (2017) noticed aggregation in concentrations above 0.1 wt % for softwood kraft lignin. Also in previous lignin film preparation studies, the lignin concentrations have been relatively low, for example 0.5-3 wt % (Norgren et al., 2006) and 0.5 wt % (Tammelin et al., 2006; Pereira et al., 2017). $NH_4OH$ was chosen as the solvent because of its ability to evaporate and dissolve kraft lignin (Norgren et al., 2006). In Figure 17, the AFM height images (5x5 $\mu m^2$) of the films prepared with lignin concentration of 4 g/l on silica substrate are shown. Films with one, two and eight layers of lignin were created (17B, 17C and 17D, respectively). In addition, the image of the pure silica surface is included as well (17A).

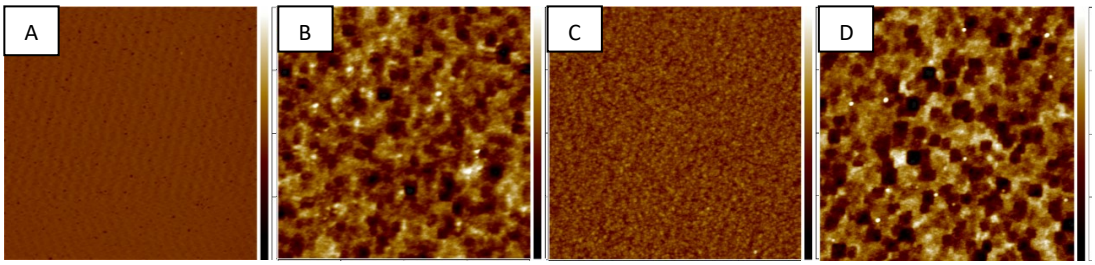


Figure 17. AFM height images (5x5 $\mu m^2$) of lignin films with the concentration of 4 g/l on silica substrate. A) Silica substrate, no lignin; B) One lignin layer, C) Two lignin layers, D) Eight lignin layers.

With one and eight layers of lignin, the films were not smooth and cavities can be detected in the structure (dark areas). With two layers of lignin, there were no cavities and the film was much smoother. However, since the thickness of this film was much smaller (6 nm) than that of one and eight layers (9 and 11 nm, respectively), the smoothness was most probably due to very low amounts of lignin adsorbed. The RMS roughnesses and thicknesses for all the films in Figure 17 are listed in Table 11.

The AFM height images (5x5 $\mu m^2$) of the films prepared with lignin concentration of 5 g/l are shown in Figure 18. It can be seen that the number of layers did not have an influence on the film structure. Regardless of the number of layers, it was not possible to prepare smooth films that fully covered the silica substrate but similar cavities as for 4 g/l films were formed. This also further proves that in the case of two-layered 4 g/l lignin film (Figure 17C), the achieved smoothness

was because of low adsorption. The RMS roughnesses and thicknesses for all the films in Figure 18 are listed in Table 11.

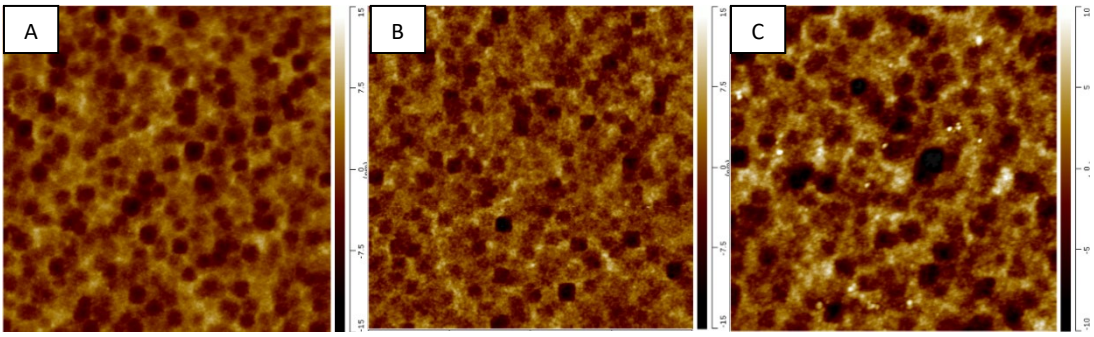


Figure 18. AFM height images (5x5 $\mu m^2$) of lignin films with the concentration of 5 g/l on silica substrate. A) One lignin layer, B) Two lignin layers, C) Eight lignin layers.

In literature, adding several layers has been done to ensure complete coverage of the film (Tammelin et al., 2006; Pereira et al., 2017). Thus, it was expected here that adding layers would reduce the cavities and make the films more even. However, based on Figures 17 and 18 it seems that when more layers are added, the new layer does not fill the lignin-free spots on the silica. One explanation for this could be that lignin rather gathers where lignin from previous layers is placed. This could be due to stronger internal cohesion of lignin compared to adhesion to the silica, resulting in lignin stacking with increasing number of lignin layers (Maximova et al., 2004). It is also possible that by adding layers, the previous lignin layer is partly dissolved by the new layer. Hence, the cavities are not filled. In addition, in spin-coating, many parameters have to be considered that can affect the structure of the resulting film. Spinning parameters, like speed and time, evaporation of the solvent, seasonal variation in laboratory humidity all affect the film formation. It also has to be remembered that different lignins can behave in very different ways. Thus, these factors can also contribute to the formation of cavities. (Meyerhofer, 1978; Klein, 1991, pp. 511-512; Sukanek, 1991; Bornside et al., 1993.)

Furthermore, according to spin-coating theory, layer addition should increase the thickness linearly (Lee et al., 2001; Lee et al., 2003). Also roughness is expected to increase with layer addition (Pasquini et al., 2005; Liu et al., 2009). However, Table 11 shows that neither follow such trend clearly, which is most probably due to the uneven films prepared. It is all so worth mentioning that the 4 g/l and 5 g/l films all had RMS roughness in the range of 2.6-3.1 nm (Table 11). These values are quite high compared to kraft lignin films prepared by spin-coating before, with

RMS of 0.4-1.1 nm (Tammelin et al., 2006; Norgren et al., 2006; Notley and Norgren 2010). The high roughness detected here is probably due to the cavities in the structure. On the other hand, the film thicknesses were lower than the ones reported in literature: 200-300 nm, 60-75 nm and 50-60 nm (Tammelin et al., 2006; Notley and Norgren 2008; Notley and Norgren 2010). However, the variation between different studies is significant due to different spinning conditions used (Norgren et al., 2006).

Table 11. Rms roughnesses and thicknesses of KL films on silica with different concentrations (4,5 and 8 g/l) and number of layers (1, 2 and 8).

| Concentration (g/l) | Number of layers | RMS (nm) | Thickness (nm) |
|---|---|---|---|
| 0 (pure silica plate) | - | 0.33 | - |
| 4 | 1 | 2.56 | 9 |
| | 2 | 0.99 | 6 |
| | 8 | 3.11 | 11 |
| 5 | 1 | 2.82 | 13 |
| | 2 | 3.01 | 11 |
| | 8 | 2.82 | Not determined |
| 8 | 1 | 1.31 | 10 |
| | 2 | 1.58 | 11 |
| | 8 | 3.33 | Not determined |

It has been shown with both lignin and cellulose that increasing the concentration can increase the coverage of a film (Maximova et al., 2004; Kontturi et al., 2003). On the other hand, it has been demonstrated that a rise in concentration can increase the roughness (Hambardzumyan et al., 2011). Thus, the effect of concentration was evaluated by increasing it more significantly, to 8 g/l. In Figure 19, the AFM height images (5x5 $\mu m^2$) of 8 g/l concentration films are shown. The RMS roughnesses and thicknesses for all the films in Figure 19 are listed in Table 11. The obtained films with one and two layers did not have cavities and were much smoother than with the concentration of 5 g/l, having RMS roughnesses of 1.31 nm and 1.58 nm. On the other hand, for the eight-layered film, the roughness is high, even 3.33 nm. Hence, the roughness increases with layer addition, like it has been claimed earlier (Pasquini et al., 2005; Liu et al., 2009). Based on the 8 g/l film results, it can be concluded that at least for the KL used, higher concentration enables formation of more uniform, smooth films. However, it must be noted that the repeatability of the 8 g/l films was not perfect because also films with some cavities (not shown here) were created. An

increase in concentration should also cause an increase in film thickness (Schubert, 1997) but due to the cavities in the structure of the lower concentration films, the comparison of thickness is difficult.

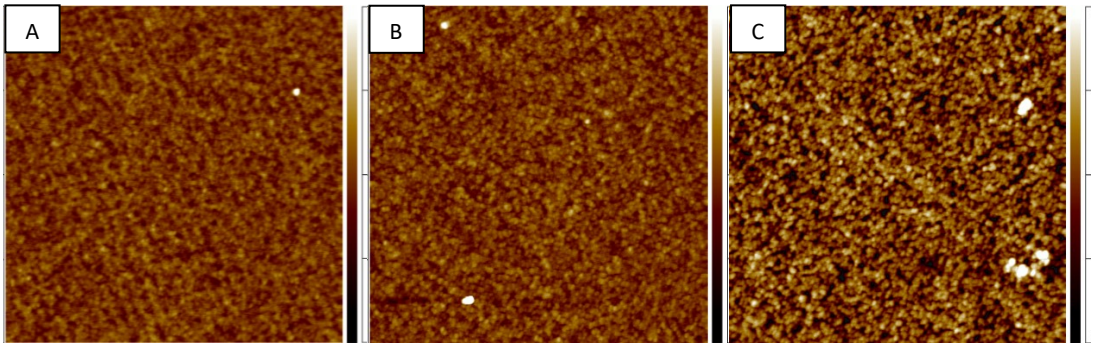


Figure 19. AFM height images (5x5 $\mu m^2$) of lignin films with the concentration of 8 g/l on silica substrate. A) One lignin layer, B) Two lignin layers, C) Eight lignin layers.

Lignin did not form smooth, fully covering films on top of silica in neither 4 g/l nor 5 g/l concentrations. Only in higher lignin concentration, 8 g/l, films without cavities were created but the repeatability was not perfect. Thus, the ability of a polystyrene layer to increase the adhesion between lignin (in low concentration) and the silica substrate and further to facilitate the film formation, was tested. This has been done earlier by Tammelin et al. (2006) and Pereira et al. (2017). The AFM images (5x5 $\mu m^2$), both height and phase, of the lignin films spin-coated on a polystyrene pre-coated silica substrate are shown in Figure 20. Moreover, an image of the pure polystyrene layer is included as well. In Table 12, the RMS roughnesses and thickness of all the films in Figure 20 are collected.

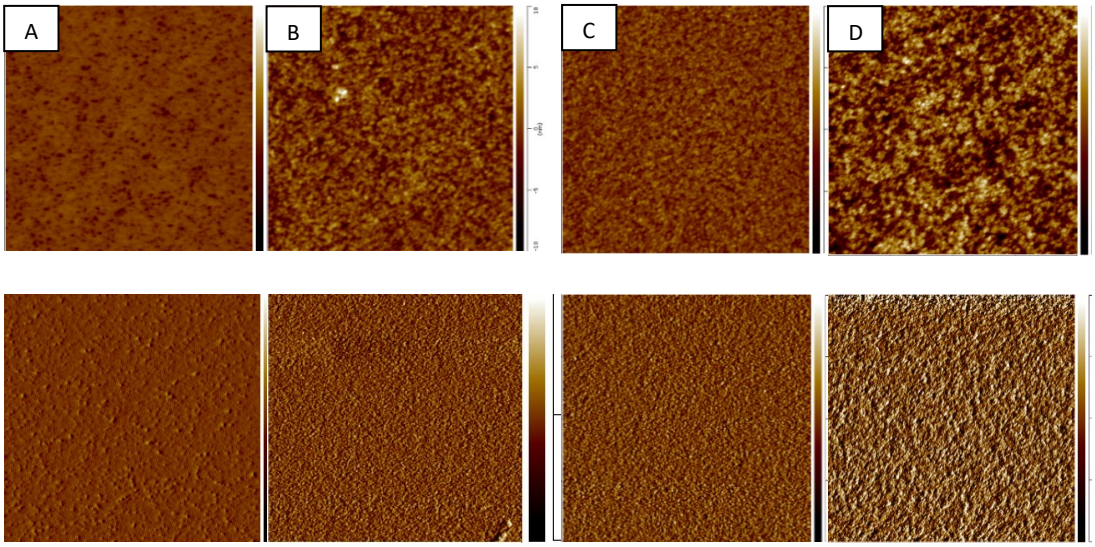


Figure 20. AFM height (upper row) and phase (lower row) images (5x5 $\mu m^2$) of lignin films with the concentration of 4 g/l on polystyrene pre-coated silica substrate. A) Polystyrene on silica, no lignin; B) One lignin layer, C) Two lignin layers, D) Eight lignin layers.

Table 12. Rms roughnesses and thicknesses of KL films on polystyrene with different number of layers (1, 2 and 8).

| Number of layers | RMS (nm) | Thickness (nm) |
|---|---|---|
| 0 (pure PS) | 0.69 | 2 |
| 1 | 1.7 | 10-12 |
| 2 | 1.1 | 14-16 |
| 8 | 2.73 | 18-20 |

The AFM height images (Figure 20) look quite similar to the ones for 8 g/l lignin concentration (Figure 19). One difference is, however, that the thicknesses of the films were slightly higher and increase more linearly when silica was pre-coated with polystyrene. Thus, it looks like polystyrene indeed increases the adhesion and acts as an anchoring layer between lignin and silica. In Figure 21, AFM height and phase images of the same films as in Figure 20, but in 1x1 $\mu m^2$ magnification, are shown. It can be seen very clearly that lignin formed granular structures, which has been reported before in literature (Liu et al., 2009; Norgren et al., 2006; Notley and Norgren 2010; Pereira et al., 2017; Tammelin et al., 2006). Thus, these images further prove that polystyrene helps to form uniform, smooth lignin layers.

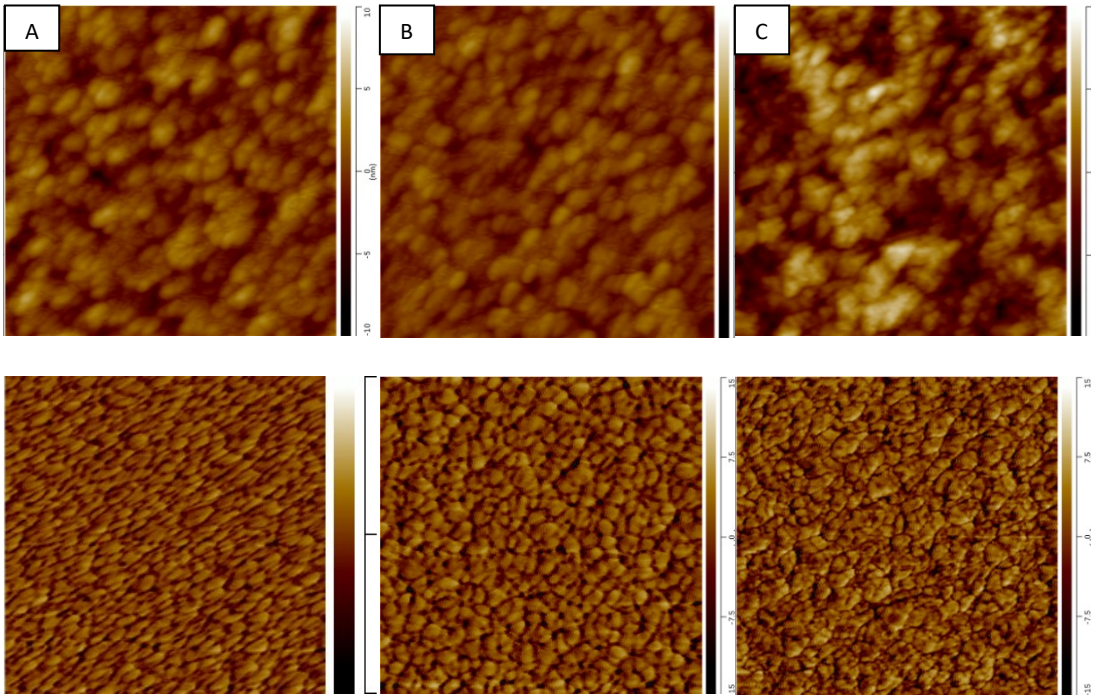


Figure 21. AFM height (upper row) and phase (lower row) images (1x1 $\mu^2$) of lignin films with the concentration of 4 g/l on polystyrene pre-coated silica substrate. A) One lignin layer, B) two lignin layers, C) eight lignin layers.

### 7.1.2 Water contact angle

The wetting properties of the KL films were analyzed with WCA measurement. Figure 22 illustrates the contact angles as a function of time for films with lignin concentrations of 4, 5 and 8 g/. Also, the contact angle for the pure silica substrate with no lignin, is included. Figure 22 shows a slight decrease in the WCA during the 60 seconds recording time, approximately 10-15$^0$, for all concentrations.

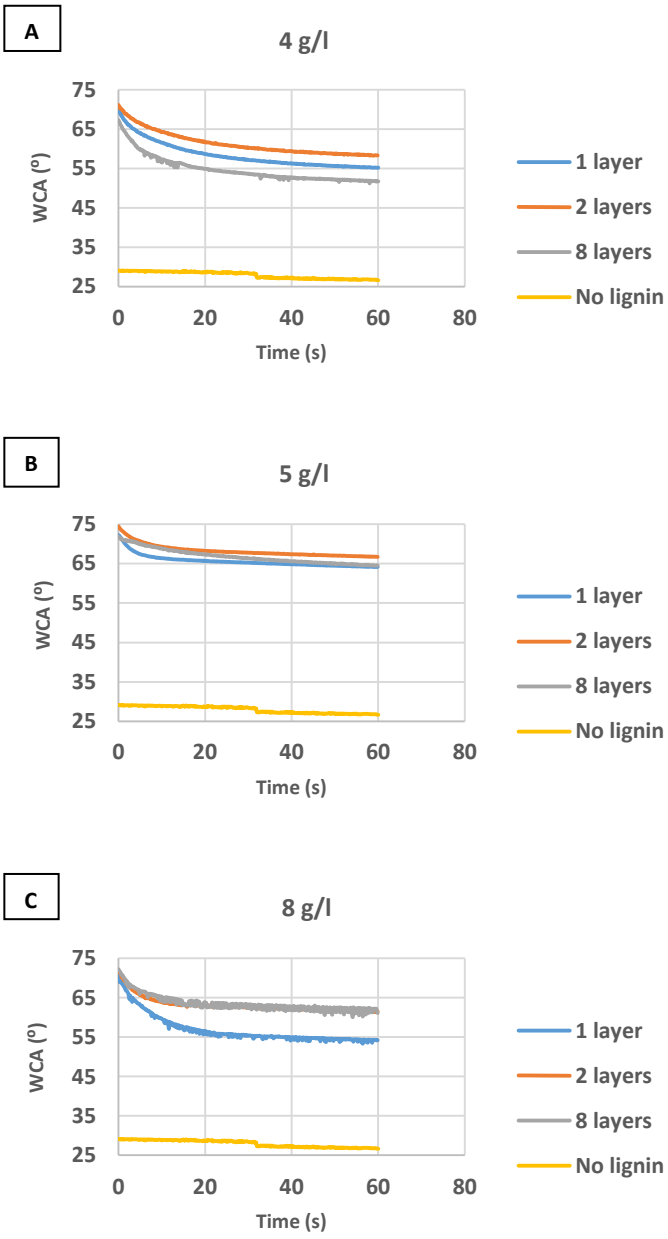


Figure 22. WCA as a function of time for lignin films with the concentrations of A) 4 g/l, B) 5 g/l and C) 8 g/l. The contact angle for pure silica is included as well.

According to the definition, a surface is hydrophilic when its WCA is under 90º and hydrophobic when its WCA is equal or above 90º (Yan and Lee, 2013, pp. 3-4). Thus, the original silica substrate was hydrophilic since its WCA was approximately 26-29$^0$ during the whole 60 seconds recording time. Adsorption of KL reduced its hydrophilicity by increasing the WCA, since KL is more hydrophobic than silica, mostly due to its aromatic structures and methoxyl

groups (Hatakeyama and Hatakeyama, 2010, pp. 1-20). On the other hand, the high amount of phenolic and aliphatic OH groups is the main reason that KL is still classified as hydrophilic. (Chakar and Ragauskas, 2004.) Moreover, the presence of carboxylic groups and carbohydrates contribute to the hydrophilicity as well (Tables 8 and 10, pages 37 and 38).

For all the concentrations, the contact angle drops during the 60 seconds recording time. The drop is only approximately 10-15$^0$, which indicates that water only partly wetted the film. Moreover, the drop is in similar range than what has been found in the literature: fully covering kraft lignin films by Norgren et al. (2006) observed a drop of approximately 8º in two minutes, while for coatings of modified lignin by Gordobil et al. (2017) the drop was approximately 10º in 120 seconds. In contrast, Indulin AT films by Lee and Luner (1972) were very porous, since their contact angle dropped rapidly from 60$^0$ to 0$^0$. Therefore, even though the films on silica contained cavities they did not have a significant effect on the wetting properties and all the produced films were relatively nonswelling (Lee and Luner, 1972; Norgren et al., 2006).

The drop in contact angle varies slightly between lignin concentrations and number of layers and it does not follow a clear trend. This is probably due to the different amounts and shapes of the cavities in the films. Also, presence of possible impurities or carbohydrates can affect the contact angle. In general, hydrophobicity can be improved by increasing the roughness (Wenzel, 1936). For example, Liu et al. (2009) created films with a roughness of 1.03 nm and a WCA of 30$^0$, while other films had a roughness of 5 nm and a WCA of 86$^0$. Figure 22C shows that for 8 g/l concentration films, the lower drop in the contact angle of eight layered film (RMS = 3.33) compared to one layered film (RMS = 1.31 nm) supports the assumption that increase in roughness increases the contact angle as well. However, the differences in the roughnesses cannot explain the WCAs comprehensively, which might be due to them being still relatively small between the different films.

It is also worth mentioning that the obtained WCAs are relative high compared to many studies in literature. Norgren et al. (2006) and Notley and Norgren (2010) both had stable, 46$^0$ contact angles for smooth kraft lignin films spin-coated on silica. In addition, Lee and Luner (1972) reported a WCA of 58º and Maximova et al. (2004) 55º, both for kraft lignin films. Since the extraction method is in

principle the same, the differences can be due to the high roughness of the films prepared here. On the other hand, small differences could be caused by the use of different wood species, like in the study by Pereira et al. (2017), who had $66^0$ WCA for spruce and $69^0$ for eucalyptus.

The impact of PS on the film wettability was studied, too. In Figure 23A, the contact angle as a function of time for 4 g/l films spin-coated on polystyrene pre-coated silica, is presented. Pure polystyrene is included as well. To facilitate the evaluation of the effect of polystyrene, the contact angle for 4 g/l films without polystyrene is shown here, too (Figure 23B). The curve for pure polystyrene shows that polystyrene made the silica more hydrophobic (contact angle of approximately 85º). It can also be seen that like for lignin films on silica, the WCA decreased only slightly during 60 seconds. For lignin films, the difference in the contact angles between the films containing and not containing a polystyrene layer is not significant. Thus, the substrate below the lignin film does not affect the WCA remarkably. Another major conclusion that can be drawn from Figure 23 is that with polystyrene there is less variance in the contact angles between different number of layers. This means that already one single layer covers the surface fully, like it was shown also in Figure 20 (page 46). Therefore, spin-coating lignin on polystyrene pre-coated silica could be used as method to measure the hydrophilicity of lignins.

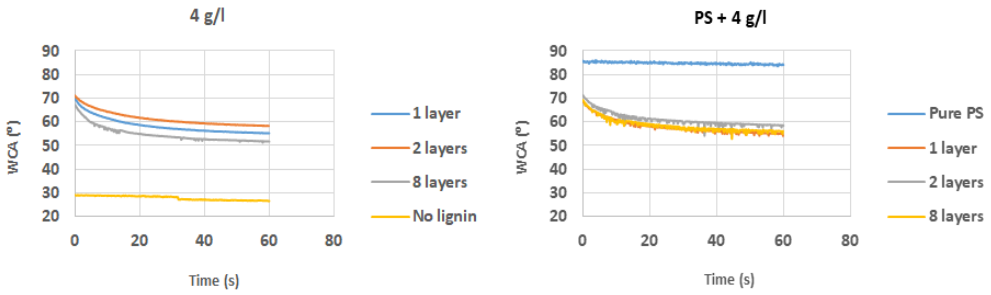


Figure 23. WCA as a function of time for A) 4 g/l lignin films spin-coated on polystyrene pre-coated silica (pure polystyrene is included as well) and B) 4 g/l lignin films spin-coated on silica.

## 7.2 Film preparation from kraft lignin fractions

From the solvent fractionation process (illustrated in Figure 16, page 37), five fractions, INS, PREC1, PREC2, PREC3 and PREC4, were obtained. In the fractionation process, the formation of fractions is based on the different solubility of the lignin molecules. Molecules with high OH group content dissolve more easily and thus, they precipitate only when the amount of anti-solvent is very

high. Hence, the PREC4 fraction was consisted of these molecules. (Jääskeläinen et al., 2017; Antonsson et al., 2008.) The properties of all the fractions are listed in Tables 7, 8, 9 and 10 (pages 37 and 38). Based on the results of film formation optimization introduced in chapter 7.1, the films of the kraft lignin fractions PREC2, PREC3 and PREC4 were prepared by spin-coating one layer of lignin (4 g/l concentration) on polystyrene pre-coated silica substrate. Films from the PREC1 and INS fractions were not produced successfully because of their poor solubility in $NH_4OH$ and poor film forming property when dissolved in 1,4-dioxane/water solution. In this section, the results of the film preparation of the kraft lignin fractions PREC2, PREC3 and PREC4 are discussed and compared to KL films. Film evaluation is based on AFM images and WCA.

### 7.2.1 Atomic force microscopy

In Figure 24, AFM height and phase images (5x5 $\mu m^2$) of the kraft lignin fraction films (PREC2, PREC3, and PREC4) are shown. In Figure 25, 1x1 $\mu m^2$ AFM height and phase images of these same fractions are presented. The KL used for the fractionation process is included as well.

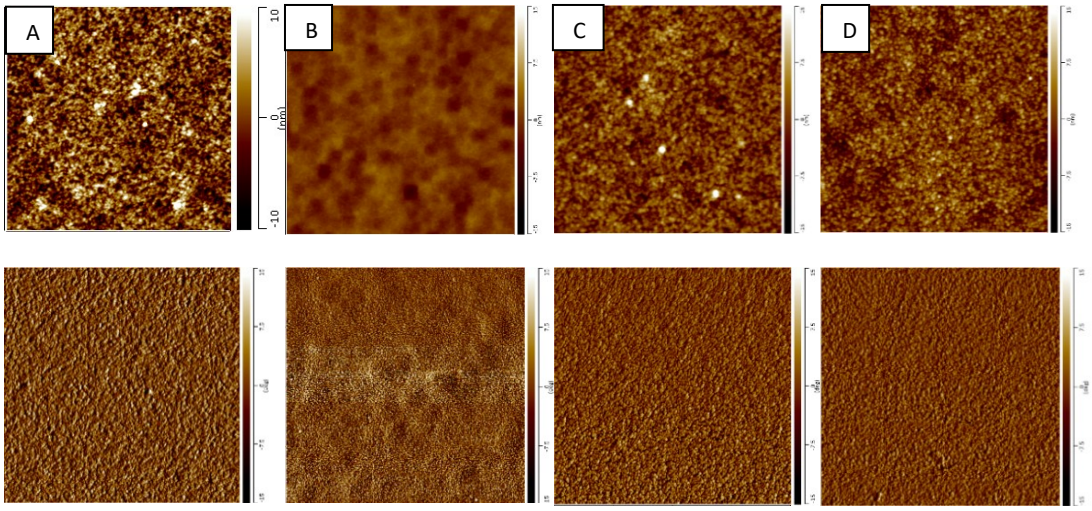


Figure 24. AFM height (upper row) and phase (lower row) images (5x5 $\mu m^2$) of lignin films prepared from the kraft lignin fractions. A) KL, B) PREC2, C) PREC3, D) PREC4.

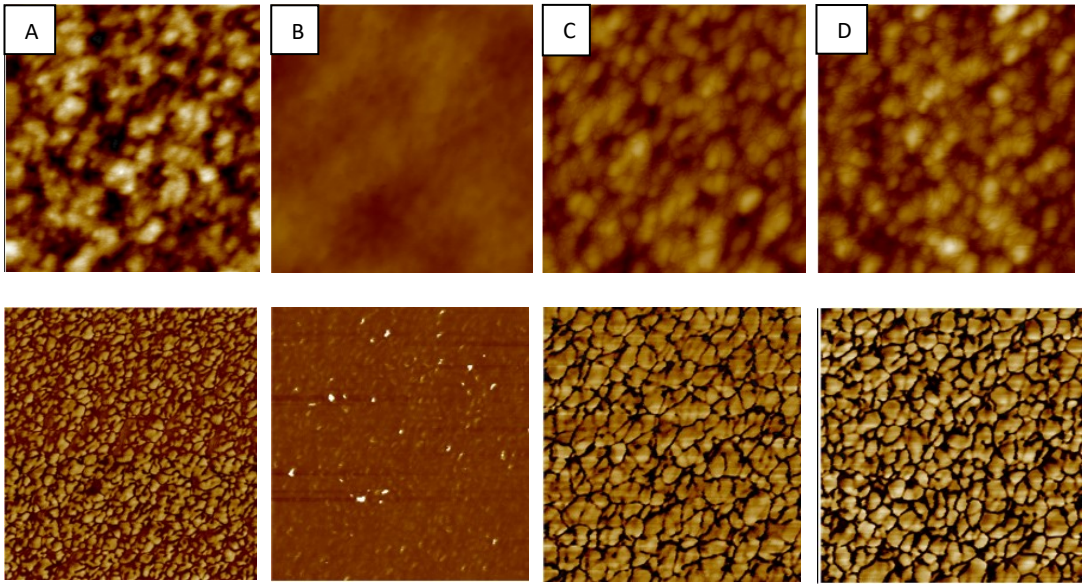


Figure 25. AFM height images (1x1 $\mu m^2$) of lignin films prepared from the kraft lignin fractions. A) KL, B) PREC2, C) PREC3, D) PREC4.

Based on Figures 24 and 25, PREC4 and PREC3 fractions formed similar globular structured films than KL in the optimization phase (Figure 20, page 46). On the other hand, films from PREC2 did not have a clear aggregated structure but contained slightly similar shapes of cavities as films formed on polystyrene-free silica substrate (Figures 17 and 18, pages 42 and 43). However, some cavities are detected in PREC4 and PREC3 films too. PREC1 and INS fractions did not form a film at all and hence AFM images of those are not included here.

Based on the AFM images, PREC4 and PREC3 fractions formed the best films. One reason for this is the complete dissolving of lignin. In many studies, the formation of smooth films has been related to good solubility of the lignin. Notley and Norgren (2010) noticed that kraft lignin formed smoother films and smaller aggregates compared to milled wood lignins because of the better solubility. Thus, it is crucial to be able to dissolve the lignin completely. In Figure 26, solutions of PREC4 and PREC1 in $NH_4OH$ are compared. By studying the solutions, it could be seen that while the PREC4 solution was clear and did not contain any undissolved particles, PREC1 looked more like a suspension and had small particles detectable by naked eye. Thus, the better solubility of PREC4 can partly explain the better film formation. Solution from the INS fraction was similar to PREC1, whereas PREC2, PREC3 were similar to PREC4.

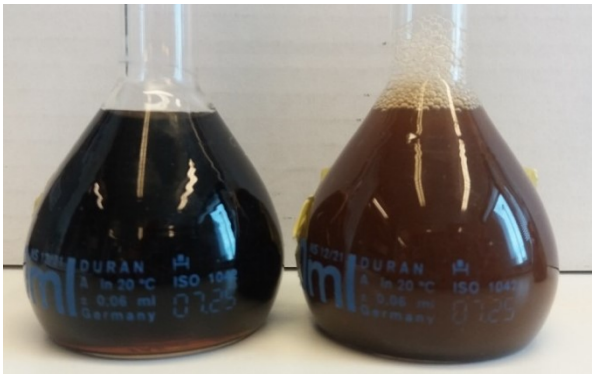

Figure 26. PREC4 (left) and PREC1 (right) lignin fractions dissolved in $NH_4OH$. PREC1 formed a suspension containing particles visible to the naked eye, indicating that $NH_4OH$ did

However, even though PREC2 fraction in $NH_4OH$ formed a clear solution, the respective film contained some cavities (Figure 24B). This suggests that either PREC2 was not completely soluble and the solution contained particles not visible for eye, or that solubility cannot alone explain the formation of cavities. Dallmeyer et al. (2013), who made films from kraft lignin fractions by combining electrospinning and heating, noticed that high molecular weight fractions formed less smooth films because of their lower mobility. Already Yoshida et al. (1987) claimed that the main chain of the high molecular weight fraction is very stiff. These perceptions could suggest that cavities were created in PREC2 film structure because this fraction did not spread as effectively as PREC4 and PREC3 fractions, because of its higher molecular weight and thus lower mobility. It has also been shown with LB films that lignin fractions with higher molecular weights formed films with less ordered structure (Gundersen et al., 2001). The molecular weights of all the fractions are collected in Table 7 (page 37).

Nonetheless, it is interesting that PREC2 had the lowest roughness, as it can be seen in Table 13 where all the RMS values are listed. At the same time, all the films had similar thicknesses, varying in the range of 12-15 nm (Table 13). Hence, PREC2 adsorbed on PS in the same amount as the other fractions but did not form the expected globular structure. The reason for this is not completely clear since a lot of studies on the surface properties of different lignin fractions has not been done.

Table 13. RMS roughnesses and thicknesses of KL, PREC2, PREC3 and PREC4 films on polystyrene.

| | RMS (nm) | Thickness (nm) |
|---|---|---|
| KL | 3.52 | 12-15 |
| PREC2 | 1.38 | |
| PREC3 | 3.1 | |
| PREC4 | 3.03 | |

### 7.2.2 X-ray photoelectron spectroscopy

XPS measurement was conducted for KL, PREC2 and PREC4 films in order to gain information of the chemical composition of the films. The results, more specifically the O/C ratio and nitrogen content of the films, were compared with the elemental analysis results conducted for the bulk lignin (data in Table 9, page 38). In Figure 27, the O/C ratios obtained both by XPS for the films and by elemental analysis for the bulk powder lignin, are presented.

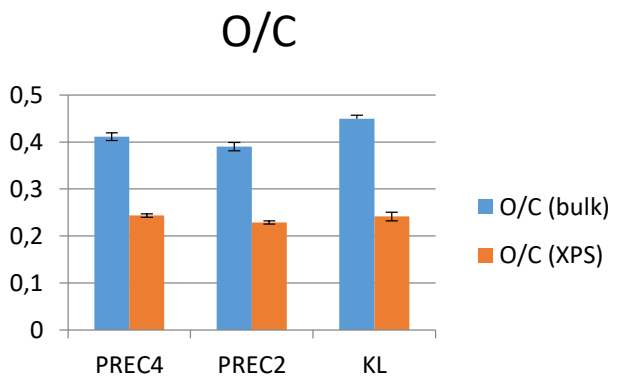


Figure 27. O/C ratio of KL, PREC2 and PREC4 obtained by XPS (film) and elemental analysis (bulk).

Figure 27 shows that the O/C ratio for the films is much lower than for bulk lignins. Partly the lower oxygen content of the films could result from the organization of lignin on the silica substrate. Since silica is hydrophilic, the hydrophilic groups and moieties of lignin turn easier towards silica, leaving the more hydrophobic parts sticking out of the surface. Since oxygen is hydrophilic, the surface would contain less oxygen (Drelich et al., 2011). However, since the difference in Figure 27 is large, the organization alone cannot be the cause of it. The lower oxygen content also explains the slightly higher WCA of the films

compared to literature, as discussed in chapter 7.1.2. To be able to explain this, further studies are needed.

The O/C ratio detected here with XPS is low also when compared to a theoretical value of 0.33 accepted in literature (Freudenberg and Neish, 1968), as well as to another study performed for kraft lignin (0.32, Laine et al., 1994). This can be seen in Figure 28, where the C-C content of the films is plotted as a function of the O/C ratio. This further shows the low oxygen content of the films.

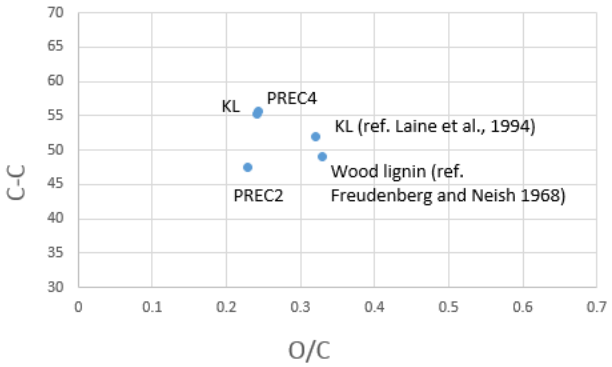


Figure 28. C-C as a function of O/C ratio for the KL, PREC2 and PREC4 films, as well as for a reference kraft lignin.

Comparison of nitrogen in film and bulk samples is also of interest, since the lignin solvent $NH_4OH$ contains nitrogen. In Figure 29, N/C ratios of films, obtained by XPS, and bulk lignins, obtained by elemental analysis, are shown.

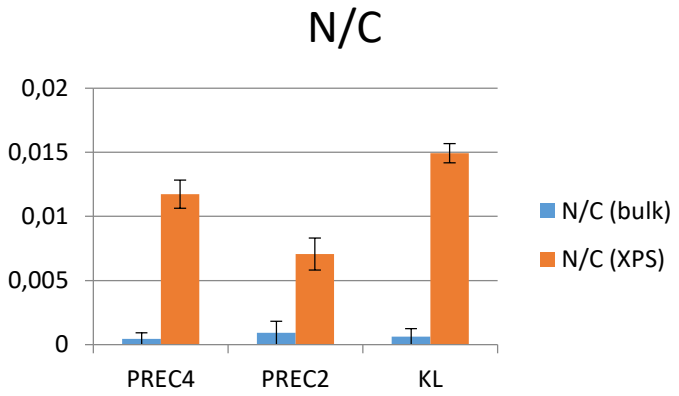


Figure 29. N/C ratio of KL, PREC2 and PREC4 obtained by XPS (film) and elemental analysis (bulk).

Clear rise in nitrogen content can be detected when the lignins are in the form of films (Figure 29). It seems that the $NH_4^+$ ion stays in the film when the solvent

evaporates during the spin-coating. The ion can stay, for example, as a counter ion in the carboxyl groups (Harland, 1994, pp. 1-2; Rahikainen et al., 2013).

### 7.2.3 Water contact angle

The WCA was measured for KL, as well as for the lignin fractions PREC2, PREC3 and PREC4, which managed to form homogeneous films according to the AFM images. For each lignin, two parallel measurements were performed and the results are presented in Figure 30.

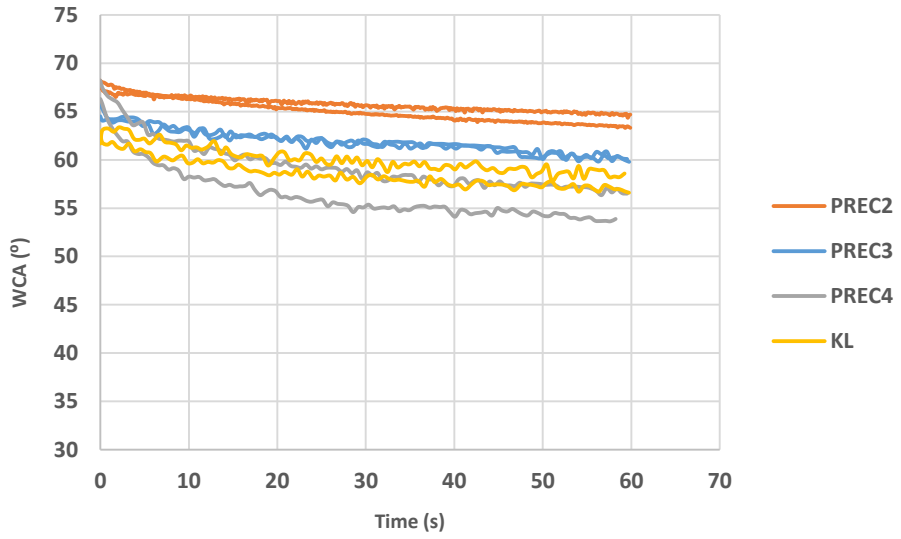


Figure 30. WCA as a function of time for KL and its fractions PREC2, PREC3 and PREC4. Two parallel measurements for each lignin are included.

According to Figure 30, PREC2 fraction had the highest WCA, approximately 64º, followed by the PREC3 fraction with a contact angle of approximately 60º. PREC4 and KL had more variation in the contact angle between the parallel measurements than PREC2 and PREC3. However, it can be said that PREC4 and KL had an average contact angle of approximately 55º and 57º, respectively. The results can be explained based on structural characteristics of lignin. According to Table 8 (page 37), out of the lignin fractions (PREC2, PREC3 and PREC4), the PREC2 fraction had the lowest amount of carboxylic acids, phenolic OH groups, as well as lowest total amount of OH groups. Moreover, the carbohydrate content was the lowest (Table 10, page 38). This explains the higher contact angle and thus higher hydrophobicity of the PREC2 fraction, since OH groups and carbohydrates are hydrophilic. On the other hand, PREC4 had

the highest total and phenolic OH group amount, as well as highest carbohydrate content, which correlates with the lowest WCA of this fraction. (Chakar and Ragauskas, 2004; Hatakeyama and Hatakeyama, 2010, pp. 1-20) The amount of aliphatic OH groups does not follow a clear trend, not even when also the highest molecular weight fractions (INS and PREC1) that did not manage to form films are taken into account (Table 8). This has been the case also elsewhere (Jääskeläinen et al., 2017) but in some other studies, the aliphatic OH content has increased with increasing molecular weight (Cui et al., 2014; Sadeghifar et al., 2017). However, in these studies the fractionation process has been different, which explains the differences.

It is interesting that KL had the lowest content of total and phenolic OH groups (Table 8), even though its WCA was very close to that of PREC4. On the other hand, both KL and PREC4 had similar, high carbohydrate contents (Table 10). Thus, it seems that the carbohydrates have a stronger effect on the wetting than the different OH groups. This also further explains the overlapping of KL and PREC4 curves in Figure 30. The high carbohydrate content of especially KL could also be deduced from the results of elemental analysis performed for the lignins (Table 9, page 38). It can be noticed that KL had the highest percentage of oxygen, which correlates with the high carbohydrate content. Furthermore, the fact that KL contained the lowest percentage of carbon supports the assumption that KL contains carbohydrates, since carbohydrates have significantly lower carbon content than lignin (Jääskeläinen et al., 2017).

## 7.3 Critical surface tension

The estimates of surface energies, the critical surface tensions, of the lignin films prepared (KL, PREC2, PREC3 and PREC4) were determined by measuring contact angles of solvents with different surface tensions. Based on the contact angles, Zisman plots were drawn and hence, the critical surface tensions were obtained. In this part, the Zisman plots and the critical surface tensions are presented and discussed.

In addition to water, the used solvents were acetic acid in water in three different mole percentages: 1.6, 3.2 and 5. The contact angles of these acetic acid in water solutions for the different fractions are shown in Figure 31. Two parallel measurements were performed for each lignin fraction.

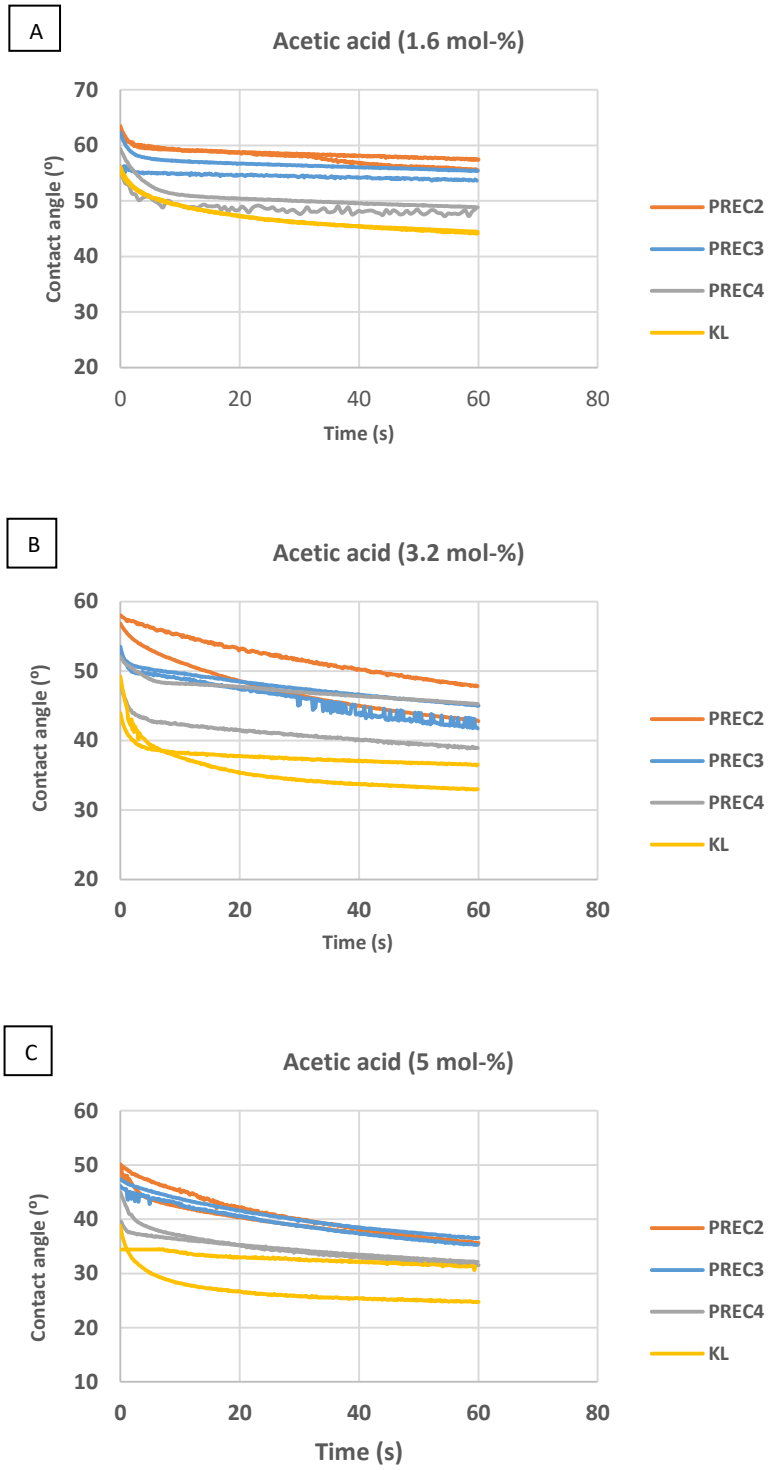


Figure 31. Contact angles of acetic acid in water solutions as a function of time for KL and its fractions PREC2, PREC3 and PREC4. A) Contact angle of 1.6 mol-% acetic acid (aq), B) Contact angle of 3.2 mol-% acetic acid (aq), C) Contact angle of 5 mol-% acetic acid (aq).

Figure 31A demonstrates that with 1.6 mol-% acetic acid, the different lignins follow quite nicely the same trend as with water in Figure 30 (page 56): PREC2 had the highest contact angle and KL the lowest. Thus, the behavior can be explained with $^{31}$P NMR, elemental analysis and carbohydrate content results similarly than the behavior in Figure 30. However, with 3.2 and 5 mol-% acetic acids the lignin fractions did not follow the same trend and overlapping occurred. For example, Figure 31B shows that in one measurement PREC4 (green curve) had a higher contact angle than PREC2 (orange curve). Moreover, in Figure 31C, PREC2 and PREC3, as well as PREC4 and KL, had among themselves basically the same final contact angles. Both of these examples show very different behavior compared to the behavior detected in Figure 30. This implies that even though there were differences in the OH group contents and oxygen content between the lignin fractions (based on Tables 8 and 9, pages 37 and 38), they are still so small that with several parallel measurements, the differences in contact angles become minor. However, also the slightly different roughnesses of the films (Table 13, page 54) could have had some effect on the contact angles, especially with the 5 mol % acetic acid where the angles were smaller than with the more dilute acetic acids (Zisman, 1964, pp. 1-51).

The wetting behavior seen in Figure 31 could further be explained by plotting the Zisman plots. Zisman (1964) noticed that when measuring contact angles of different liquids on a surface, the cosine of the contact angle increases linearly when the surface tension of the liquid is decreased. Thus, there is a linear relation between the surface tension and 1-cos θ (where θ is the contact angle), too. This relation is called Zisman plot. (Zisman 1964, pp- 1-51.)

Zisman plots are useful because they provide an easy tool to obtain the critical surface tension of a surface. Critical surface tension is defined as the maximum surface tension that leads to complete wetting (contact angle θ = 0) of the surface. In other words, liquids containing the same or lower surface tension than the critical surface tension, always wet the surface completely and the contact angle goes to zero. The critical surface tension can be obtained from the Zisman plots by extrapolating the curve to the point where it intersects the x-axis. At this point, both 1-cos θ and the contact angle θ equal to zero and thus, total wetting follows. (Zisman 1964, pp- 1-51.)

It is important to notice that critical surface tension does not equal to free surface energy but can rather be used as an estimate of it. It has been accepted that critical surface tension values obtained with Zisman plot are always lower than surface tension obtained with other methods. Thus, critical surface tension can be used to compare the wettabilities of different surfaces. (Zisman, 1964, pp. 1-51; Wu et al., 1979; Gindl et al., 2001; Hubbe et al., 2015.)

The surface tensions for water and the different acetic acid solutions were obtained from the literature (Álvarez et al., 1997) and they are listed in Table 14. In Figure 32, the Zisman plots for KL and PREC2, PREC3 and PREC4 fractions can be seen.

Table 14. Surface tensions of the liquids used for the contact angle measurements (Álvarez et al., 1997).

| | Surface tension (mN/m) |
|---|---|
| Water | 72.8 |
| 1.6 mol-% acetic acid | 62.4 |
| 3.2 mol-% acetic acid | 56.3 |
| 5 mol-% acetic acid | 51.8 |

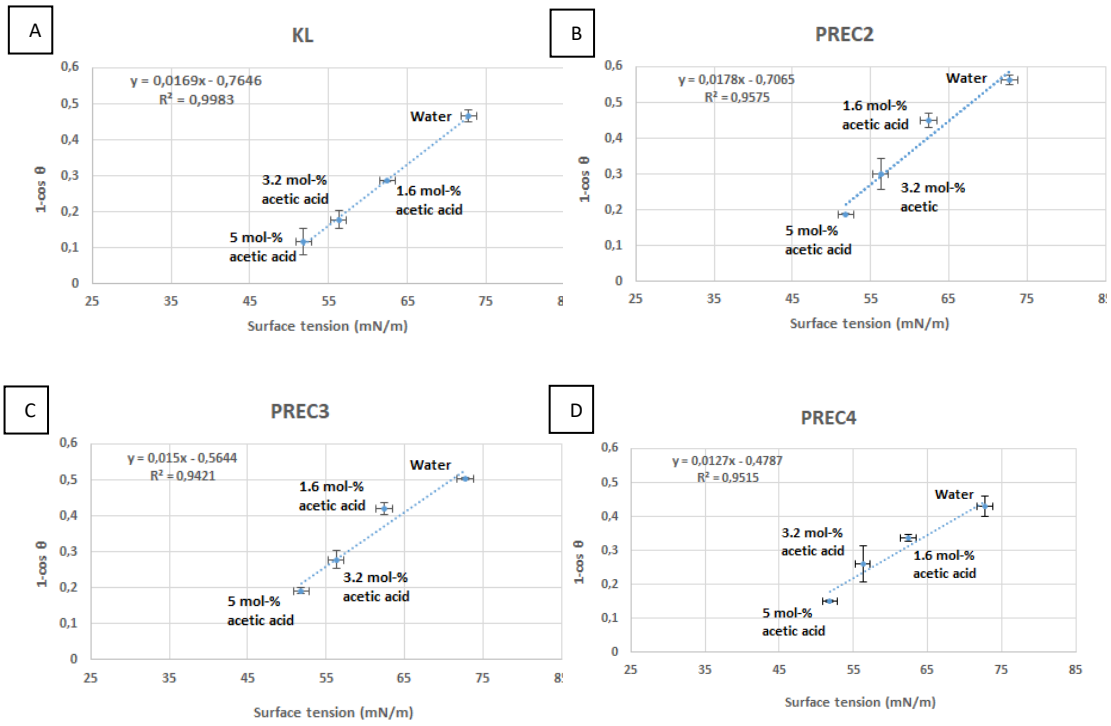


Figure 32. Zisman plots for A) KL, B) PREC2, C) PREC3 and D) PREC4 films.

A linear curve could be plotted for all the fractions (Figure 32). The critical surface tensions extrapolated from the curves for KL and the fractions PREC2, PREC3 and PREC4 are listed in Table 15.

Table 15. Critical surface tensions of KL and the PREC2, PREC3 and PREC4 fractions obtained from the Zisman plots.

| | Critical surface tension ($mJ/m^2$) |
|---|---|
| KL | 45.24 |
| PREC2 | 39.69 |
| PREC3 | 37.63 |
| PREC4 | 37.69 |

The lignin fractions PREC2, PREC3 and PREC4 all had a critical surface tension of similar magnitude (Table 15). This means that also the wetting properties of the different fractions are quite similar (Zisman, 1964, pp. 1-51) as it could already be deduced from the overlapping of the contact angles in Figure 31. Before, Lee and Luner (1972) also found critical surface tensions of similar magnitude for dioxane, soft wood and hard wood lignins. On the other hand, KL has a slightly higher critical surface tension than its fractions. Compared to PREC2 and PREC3, KL had a higher carbohydrate content, which implies that the carbohydrates in KL (as discussed in chapter 7.2, page 57) strongly affect the wettability and hydrophilicity. However, PREC4 had a similar amount of carbohydrates as KL and yet its critical surface tension was lower. It is possible that different carbohydrates affect the wettability in different ways and magnitudes. However, this result is interesting and slightly unexpected and in order to fully understand it, more studies are needed. Based on the contact angles (Figure 31) and the critical surface tension values obtained from the Zisman plots (Table 15) it can be concluded that the unfractionated KL had higher critical surface tension, and thus also higher surface energy (Zisman, 1964, pp. 1-51; Wu et al., 1979; Gindl et al., 2001; Hubbe et al., 2015.) than its fractions.

Lee and Luner (1972) utilized the Zisman plot and obtained a critical surface tension of approximately 37 $mJ/m^2$ for softwood kraft lignin. This is quite close to the values obtained for the fractions PREC2, PREC3 and PREC4, but the actual unfractionated KL had a slightly higher critical surface tension. Notley and Norgren (2010) and Jiang et al. (2017) measured the surface tension for kraft

lignin with Owens and Wendt- method (Owens and Wendt, 1969), obtaining values of 57.1 and 56 mJ/m$^2$, respectively. These results confirm that the actual surface energy is always higher than the critical surface tension. Thus, the latter can be utilized as a fast and easy tool to get the first prospect of the surface energy.

Surface energy influences adhesion, adsorption and wetting of a surface (Collett, 1972, pp. 1-42). Thus, it is important when considering the use of lignin in many applications. For example, in food applications, if lignin films are wanted to be used in protecting food, it is crucial to know how the film interacts with its surroundings, such as moisture, as well as with the food itself (Han et al., 2005, pp. 45-49). As a comparison, for polyethylene, which is widely used in food packaging (Ebnesajjad, 2013, pp. 1-2), surface energy values of 33, 36 and 37 mJ/m$^2$ have been measured (Mangipudi et al., 1995; Aliev, 2001; O`Kell et al., 1995). These are much lower than the over 50 mJ/m$^2$ measured for lignin before (Notley and Norgren, 2010; Jiang et al., 2017). This is one reason for polyethylene`s popularity in food packaging, because its full wetting requires a liquid with low surface tension.

## 7.4 Heat treatment

Slow heat treatments in air are known to modify lignin characteristics. Changes in lignin structure and chemical composition due to heating at different conditions have been studied extensively for lignin in the form of fiber and powder (Braun et al., 2005; Brodin et al., 2012; Foston et al., 2013; Norberg et al., 2013). In the presence of air and at lower temperatures, the oxidation reactions dominate. The amount of carbonyl and carboxyl structures is reported to increase via autooxidation. According to Braun et al. (2005) at temperatures close to 250 ºC, these structures further cross-link to anhydrides and esters. Thus, condensation of the aromatic rings takes place, which could also be detected as a rise in average molecular weight. At temperatures above 250 ºC (Braun et al., 2005), oxygen content starts to decrease due to elimination of for example water, $CO_2$ and CO. (Braun et al., 2005; Brodin et al., 2012; Foston et al., 2013; Norberg et al., 2013.) In this part, the effect of the heat treatment on morphology, hydrophilicity and elemental composition of the KL, PREC2 and PREC4 films is evaluated.

### 7.4.1 Atomic force microscopy

In Figure 33, the AFM height images (5x5 $\mu m^2$ and 1x1 $\mu m^2$) of KL, PREC2 and PREC4 films after the heat treatment are presented. When compared to the films before heat treatment (Figure 24, page 51), it can be noticed that the globular structure of KL and PREC4, as well as the cavities in the structure of PREC2, disappeared. Consequently, the films became much smoother: the RMS roughness decreased from approximately 3 nm to below 1 nm for KL and PREC4 and from 1.38 nm to 0.48 nm for PREC2 (Table 13, page 54, and Table 16). The increased smoothness might have been due to fusion of the lignin during heating. In several studies where lignin carbon fibers have been produced by combining thermostabilization and carbonization, it has been stated that heating rate has an essential effect on the morphology of the fibers. When the heating rate is kept low enough, the glass transition temperature of lignin increases faster than the temperature and thus lignin stays in its glassy state. Hence, the lignin fibers do not fuse together but rather stay as individual fibers. (Wisanrakkit and Gillham, 1991; Braun et al., 2005.) Dallmeyer et al. (2013) exploited this property by making smooth films of kraft lignin fractions by heating and fusing together electrospun lignin fibers. They also noticed that low molecular weight fractions formed smooth films more easily, even when the heating rates were very low (0.5 ºC/min). Hence, the low roughnesses of the films in Figure 33 could be explained by lignin fusing together, which further causes the loss of the globular structure. However, it is also likely that the PS layer had an effect on the morphology, which will be discussed next.

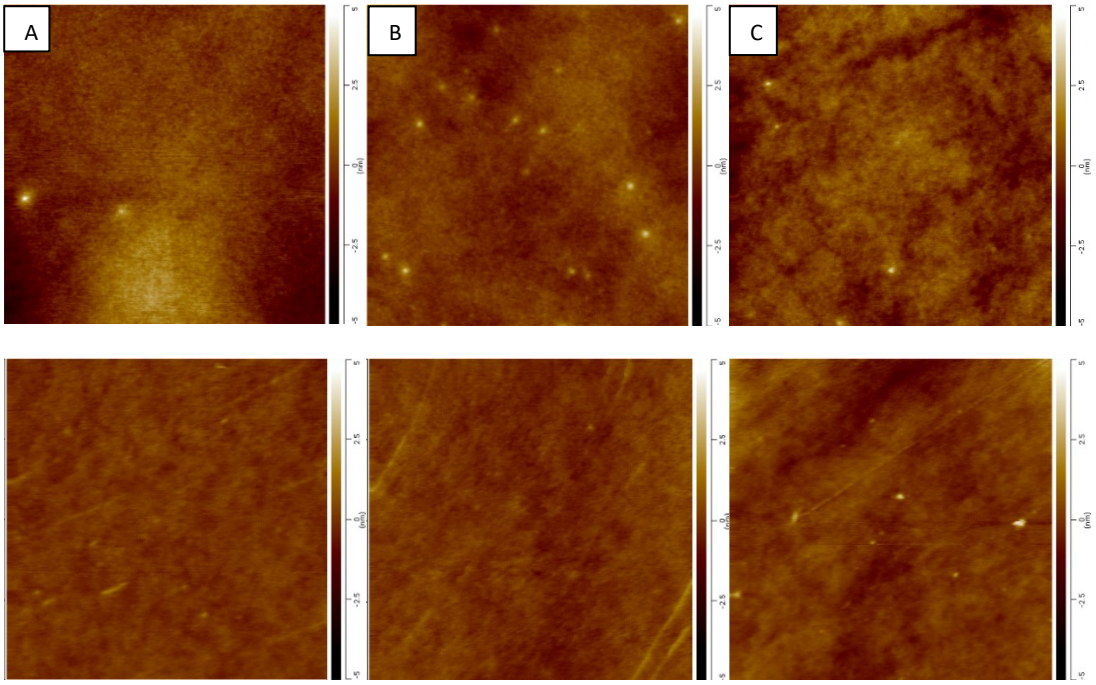


Figure 33. AFM height images (5x5 μm$^2$ the upper row and 1x1 μm$^2$ the lower row) of lignin films after heat treatment. A) KL, B) PREC2, C) PREC4. Corresponding images of films before heating are shown in Figure 24, page 51).

Table 16. RMS roughnesses and thicknesses of KL, PREC2 and PREC4 films on polystyrene and silica, after heat treatment.

| | RMS (nm, on PS) | RMS (nm, on silica) | Thickness (nm, on PS) |
|---|---|---|---|
| KL | 0.83 | 3.97 | 12-15 |
| PREC2 | 0.48 | 2.55 | |
| PREC4 | 0.6 | 2.8 | |

The heat treatment was also applied on films spin-coated on silica, without the PS layer to anchor lignin on silica. This was done in order to see if PS has an effect in the heating, especially on the WCA, which will be discussed in chapter 7.4.2. The AFM height images (5x5 μm$^2$) of KL, PREC2 and PREC4 films on silica are shown in Figure 34. Here, without PS layer, the produced films contained similar cavities as the films in the film preparation optimization chapter 7.1 (Figures 17 and 18, pages 42 and 43). The heat treatment did not manage to make the films smoother, the RMS roughness being around 3 nm both before (Table 13, page 54) and after (Table 16) the heat treatment. It is possible that some lignin fusion occurred also when no PS was present. Nevertheless, the cavities could not be evened out and the structure made more uniform in a similar manner than for the films containing a PS layer. Thus, it seems that when PS is

present, it softens and the lignin simply “sinks” in or mixes with its structure. This is explained more next in chapter 7.4.2.

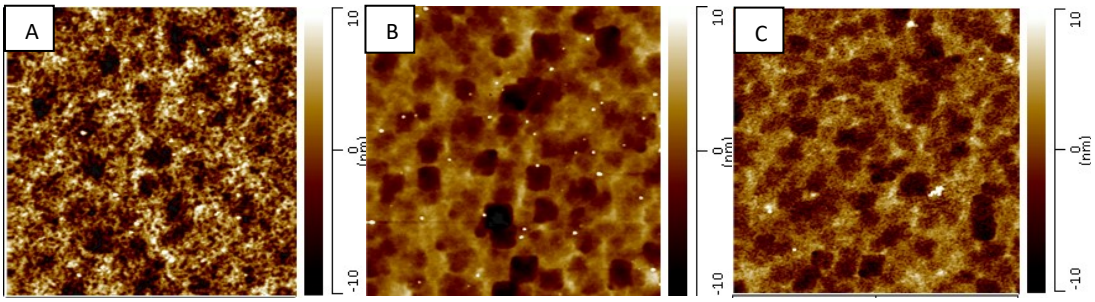


Figure 34. AFM height images (5x5 μm$^2$) of lignin films on silica after heat treatment. A) KL, B) PREC2, C) PREC4.

### 7.4.2 Water contact angle

In Figure 35, the WCA of KL, PREC2 and PREC4 films before and after the heat treatment are plotted as a function of time. From Figure 35A it can be noticed that all the films became more hydrophobic because of the heat treatment. However, the contact angle of all the different lignin fractions after the heating was very close to the one of pure polystyrene, approximately 84°. Thus, it seems that the PS layer somehow affects the contact angle of the lignin. Polystyrene has a glass transition temperature of 100 ºC (Klein, 2009, p. 15). Since the films were heated to 250º C, polystyrene entered its rubbery state. Moreover, Kubo and Kadla (2005) studied lignin/synthetic polymer blend carbon fibers and noticed that lignin formed a miscible blend with PET (polyethylene terephthalate). The miscibility was related to similar aromatic structures, thus enabling π-type interactions between PET and lignin. Since PS also has an aromatic ring, these similar interactions could occur between lignin and PS, as well. Hence, combined with PS`s rubbery state, it is likely that PS and lignin fused together and reorganized during heating, rather than stayed as separate layers. Therefore, the WCA close to that of PS could be explained, too. Moreover, the smoothness of the films (Figure 33, page 64) could also further be explained with this mixing rather than with lignin fusion: PS melts and is mixed with lignin, resulting in a homogeneous, smooth film.

To evaluate more the possible effect of PS on the WCA, the heat treatment was done for the same lignin fractions spin-coated on silica substrate free from PS. The WCA against time for these films are plotted in Figure 35B.

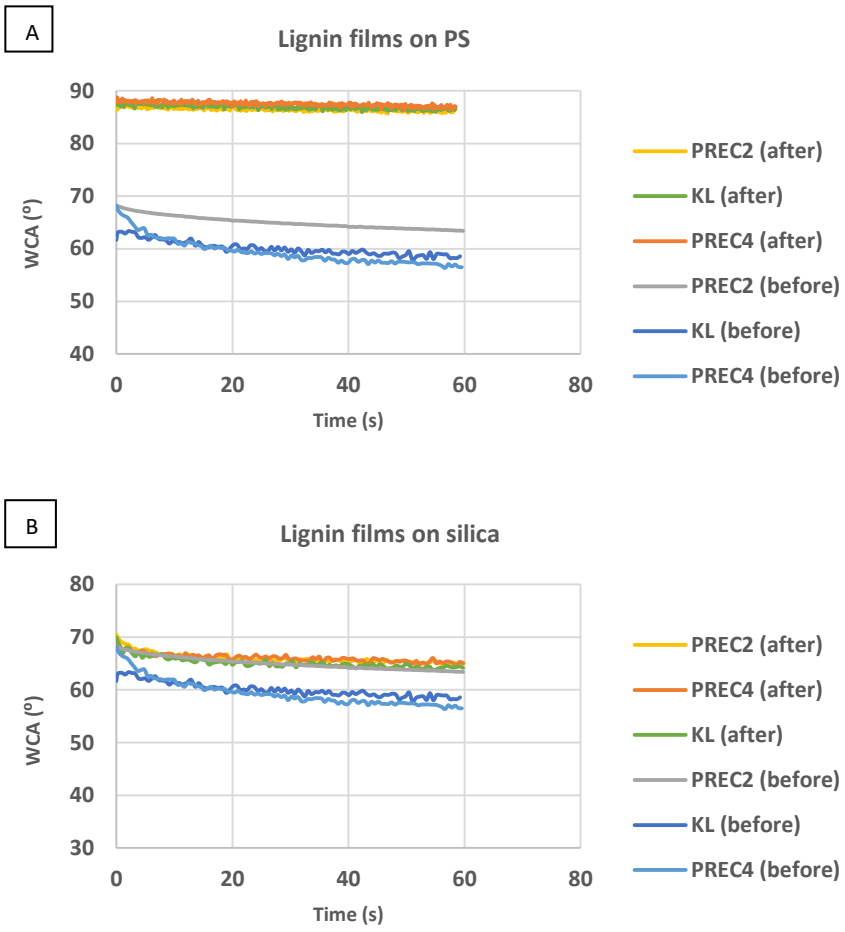


Figure 35. WCA as a function of time for the KL, PREC2 and PREC4 films before and after the heat treatment. A) Lignin films on polystyrene substrate, B) lignin films on silica substrate.

Figure 35B shows that without the PS layer, the WCA increased due to the heating but not all the way to the level of pure PS. In fact, without PS, the WCA increased to approximately 65°, being almost 20° lower than with the presence of PS. Hence, it was confirmed that PS indeed interacts with lignin during the heating and thus interferes with the WCA of lignin. Regardless, heat treatments have potential to be used in making lignin more hydrophobic. Further, increased hydrophobicity could be utilized in food applications where protecting food from for example water is of interest. Moreover, more hydrophobic films could also protect food from bacteria, which prefer and grow better in moist environments (Petersen et al., 1999). In addition, lignin composite films containing only a small amount of PS could also be considered as a material for these purposes.

Since the lignin films here were heated to 250 ºC, oxygen content, and further also hydrophilicity should increase, as it was discussed on page 62. The

increased hydrophobicity noted here is explained more based on the XPS results in chapter 7.5. Foston et al. (2013) showed that upon heating, the relative amount of aryl ethers decreased with respect to aryl and condensed aryl structures. Also Braun et al. (2005) detected modest decrease in aromatic C-O content, which was attributed to the degradation of β-aryl ethers. In addition, Nakamura et al. (2007) reported that with some lignin model compounds, the phenolic β-ethers could be transformed to carbon-carbon bonds. Thus, the rise in hydrophobicity detected here could at least partly be explained with formation of new carbon-carbon bonds. The possible formation of new carbon-carbon bonds is discussed more in chapter 7.5 where the XPS results are presented. Moreover, it is well known that hydrolysis of carbohydrates takes place approximately at 160-220 ºC (Domansky and Rendos, 1962; Kocaefe et al., 2008; Kudo and Yoshida, 1957), which could also contribute to the increased hydrophobicity.

### 7.4.3 X-ray photoelectron spectroscopy

The X-ray photoelectron spectroscopy (XPS) measurement was also done for the heat-treated films in order to further evaluate their effect. The low resolution (wide scan) and high resolution scan data were obtained both before and after the heat treatment for KL, PREC2 and PREC4 films spin-coated on silica. The spectra is shown in Appendix 1. The elemental compositions and chemical state of carbon atoms of these films can be seen in Appendix 2 and 3, respectively. Next, the most important ones are presented here in graphs.

In Figure 36, the effect of the heating on the oxygen, sulfur and nitrogen contents in the films is presented. It can be seen that the amount of oxygen increased, while sulfur and nitrogen contents decreased. As it was already stated in chapter 7.4.2 (page 62), the oxidation reactions dominate in the presence of air and at lower temperatures (Braun et al., 2005; Brodin et al., 2012; Foston et al., 2013; Norberg et al., 2013). In fact, in the study by Braun et al. (2005), at temperatures below 250 °C the oxygen content increased. This is in line with the oxygen gain shown in Figure 36A. It has also been observed that lower heating rates favor more dramatic oxygen gain (Braun et al., 2005; Norberg et al., 2013). Thus, by lowering the heating rate from the 10 °C/min used here, the oxygen gain could probably be increased even further.

Due to the reduction of the sulfur content (Figure 36B), heat treatment could possible provide a method to reduce the odor of lignin, which is partly caused by

sulfur compounds. Before, laccase-catalyzed oxidation has been tested to decrease the volatile organic compounds, such as sulfur compounds. (Kalliola et al., 2012.) The nitrogen content of the films was very low and it was reduced further during the heating (Figure 36C).

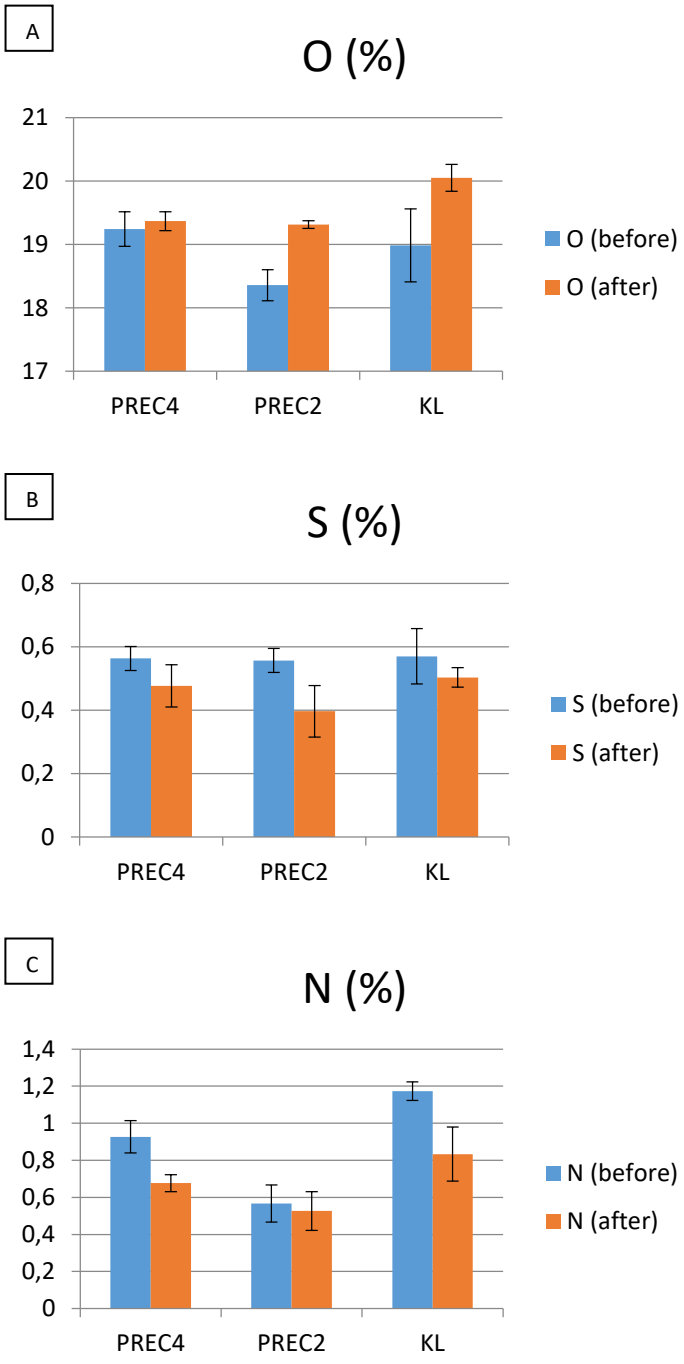


Figure 36. A) Oxygen, B) sulfur and C) nitrogen contents of the KL, PREC2 and PREC4 films before and after the heat treatment.

The effect of the heating on the chemical state of the carbon atoms in the films is illustrated in Figure 37. The content of COO, consisting of carboxyl groups, esters and anhydrides, increased which is in accordance with the literature (Braun et al., 2005; Brodin et al., 2012; Foston et al., 2013; Norberg et al., 2013). Moreover, modest decrease of CO and OCO has been detected earlier due to degradation of β-aryl ethers and carbonyls cross-linking to anhydrides and esters, respectively (Braun et al., 2005). Similar decrease is detected in Figure 37B and 37C. In addition, slight increase of CC is shown as well. Nakamura et al. (2007) showed with some lignin model compounds that phenolic β-ethers could be transformed to carbon-carbon bonds. However, lignin contains very few β-ethers, and thus their contribution is expected to be negligible. Overall, based on the XPS results it can be concluded that the most probable reason for the increased hydrophobicity due to the heating detected in Figure 35B (page 66), is the hydrolysis of the carbohydrates. As it was already discussed, carbohydrates have a strong effect on wetting and thus also their degrading is the main source for the increased hydrophobicity.

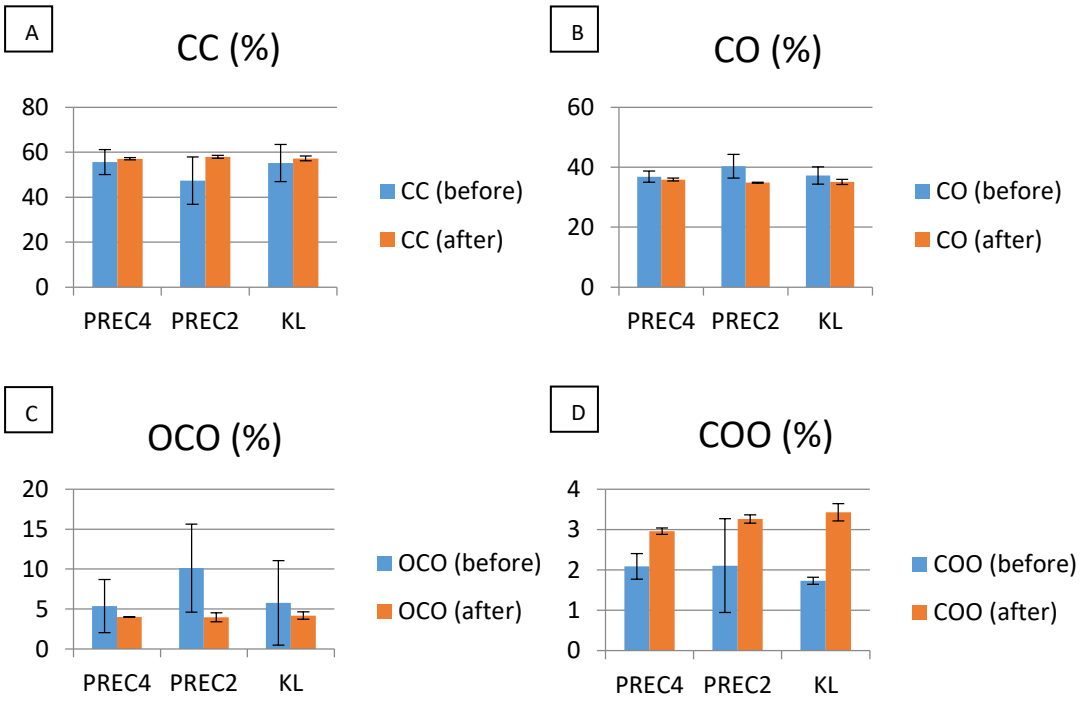


Figure 37. Chemical state of carbon in KL, PREC2 and PREC4 films before and after the heat treatment. A) CC, B) CO, C) OCO and D) COO.

# 8 Conclusions

In this thesis, thin films were produced from kraft lignin and its fractions, obtained by solvent fractionation. Since the fractions have different structures and functional group composition, the aim was to use these films to study the relationship between structure and properties of the lignins. Further, the goal was that with the enhanced understanding, ideas about application areas suitable for specific lignin fractions could be achieved. Particularly, knowing lignin properties, food applications could be realized, such as in packaging and edible films, including preservation and protection of food stuff. Other properties include barrier, antioxidant, UV-blocking and water stability.

The films were produced by spin-coating. AFM images showed that adhesion between lignin and the substrate is crucial when smooth and fully covering films are desired. While films containing cavities were created on silica substrate, a polystyrene pre-layer enabled the formation of uniform, globular structured films that fully covered the substrate. The water contact angle of films both on silica and PS were similar magnitude, indicating that neither the cavities nor the substrate below affected the measurement.

Wetting and critical surface tension were studied by measuring contact angles of several solutions and by developing Zisman plots. Different compositions of functional OH groups of the fractions were confirmed by $^{31}$P NMR but the calculated critical surface tensions were very close to each other. Since critical surface tension can be used as a quick tool to estimate the surface free energy, all the fractions had similar surface energies and thus would work equally well for example as food packaging films to protect the food from wetting. On the other hand, the unfractionated KL had a slightly higher critical surface tension, which was partly attributed to the higher carbohydrate content. Thus, it was concluded that compared to OH groups, the carbohydrates have a stronger effect on increasing the critical surface tension. However, since PREC4 had almost equal amount of carbohydrates as KL, they alone cannot explain the differences.

Heat treatments applied on the films increased their hydrophobicity more extensively when films were spin-coated on PS instead of silica. Moreover, the films containing the PS pre-layer became smoother and the globular structure disappeared. It was concluded that during heating, PS softens and is mixed with lignin. This was supported by the WCA rising to the level of pure PS, due to the

heating. Again, there were no significant differences in the hydrophobicity between the fractions indicating that all the films are equally suitable to be heat-treated when increased hydrophobicity is targeted. In addition, the XPS measurement performed for films on silica substrate showed that the oxygen content increased during the heating. Hence, the increased hydrophobicity was attributed mainly to the degradation of carbohydrates.

Overall, lignin films of KL and three of its fractions were successfully produced by spin-coating. Even though the fractions had different structures, they performed similarly in the terms of critical surface tension and hydrophobicity after heat treatment. In order to realize lignin products from solvent fractionation, it is important to find applications for the given fractions. However, since the unfractionated KL had a higher critical surface tension than its fractions, films from the fractions could be more suitable and effective in shielding food than films from KL.

In the future, there is still plenty of room for basic research like the one carried out in this thesis. Zisman plots and critical surface tensions for heat treated films would provide more information about the effects of this kind of slow thermal processing. QCM could be used to study the water-lignin interactions, such as water stability, and the viscoelastic behavior. Moreover, the possibility of chemical modifications and their impact on film properties could be considered as well. Particularly, to find a simply, environmentally friendly chemical modification that would enhance a property of a specific fraction would be interesting. Considering food applications, more applied research could be performed by forming lignin films on for example nanocellulose or by preparing even self-standing films. Hence, also features such as barrier properties could be examined.

A few questions were left unanswered from the results obtained in this thesis. For example, the low oxygen content detected with XPS and a comprehensive understanding of the film wetting require more work. The ultimate goal is to have an understanding of the structure-property relationship of lignin and thus find applications were given lignin fractions function better than the others. In this way the originally heterogeneous lignin could possibly be utilized more effectively and in a larger scale.

# 9 References


Aadil, K.R., Prajapati, D. and Jha, H., Improvement of physcio-chemical and functional properties of alginate film by Acacia lignin, *Food Packaging and Shelf Life* **10** (2016) 25-33.

Aguié-Béghin, V., Foulon, L., Soto, P., Croînier, D., Corti, E., Legée, F., Cézard, L., Chabbert, B., Maillard, M., Huijgen, W.J.J. and Baumberger, S., Use of Food and Packaging Model Matrices to Investigate the Antioxidant Properties of Biorefinery Grass Lignins, *Journal of Agricultural and Food Chemistry* **63**(45) (2015) 10022-10031.

Aguié-Béghin, V., Baumberger, S., Monties, B. and Douillard, R., Formation and characterization of spread lignin layers at the air/water interface, *Langmuir* **18**(13) (2002) 5190-5196.

Aliev, R., Hydrophilicity and surface energy of polyethylene modified by radiation grafting of acrylamide, *Polymer Bulletin* **47**(1) (2001) 99-104.

Álvarez, E., Vázquez, G., Sánchez-Vilas, M., Sanjurjo, B. and Navaza, J.M., Surface Tension of Organic Acids + Water Binary Mixtures from 20 °C to 50 °C, *Journal of Chemical & Engineering Data* **42**(5) (1997) 957-960.

Anonymous A, Food and Agriculture Organization of the United Nations, Save Food: Global Initiative on Food Loss and Waste Reduction, http://www.fao.org/save-food/resources/keyfindings/en/, 1.2.2018.

Anonymous B, Asumi Giken, Limited, http://www.dip-coater.com/english/about_dip_coating.html, 9.1.2018.

Anonymous C, Major chemical components of cereal grains, http://www.fao.org/docrep/x2184e/x2184e04.htm, 21.5.2018.

Antonsson, S., Henriksson, G., Johansson, M., Lindström, M.E., Low Mw-lignin fractions together with vegetable oils as available oligomers for novel paper-coating applications as hydrophobic barrier, *Industrial Crops and Products* **27**(1) (2008) 98-103.

Barros, A.M., Dhanabalan, A., Constantino, C.J.L., Balogh, D.T. and Oliveira Jr., O.N., Langmuir monolayers of lignins obtained with different isolation methods, *Thin Solid Films* **354**(1) (1999).

Bhat, R., Abdullah, N., Din, R.H. and Tay, G.-S., Producing novel sago starch based food packaging films by incorporating lignin isolated from oil palm black liquor waste, *Journal of Food Engineering* **119**(4) (2013).

Birnie, D.P., “Spin-coating technique” in *Sol-Gel Technologies for Glass Producers and Users,* Aegerter, M.A. and Mennig, M. (eds.), Springer, Boston 2004, pp. 49-55.

Bodirlau, R., Teaca, C.-A. and Spiridon, I., Influence of natural fillers on the properties of starch-based biocomposite films, *Composites Part B: Engineering* **44**(1) (2013) 575-583.

Bornside, D.E., Brown, R. A., Ackmann, P. W., Frank, J. R. F., Tryba, A. A. and Geyling, F. T., The effects of gas phase convection on mass transfer in spincoating, *Journal of Applied Physics* **73** (1993) 585.

Braun, J.L., Holtman, K.M. and Kadla, J.F., Lignin-based carbon fibers: Oxidative thermostabilization of kraft lignin, *Carbon* **43**(2) (2005) 385-394.

Brodin, I, Ernstsson, M., Gellerstedt, G., Sjöholm, E., Oxidative stabilisation of kraft lignin for carbon fibre production, *Holzforschung* **66**(2) (2012) 141-147.

Brunow, K., Lundquist, K., Gellerstedt, G., *Analytical methods in wood chemistry, pulping and paper-making*, Sjöström, J. and Alen, R. (eds.), Springer-Verlag, Berlin 1999, pp. 77–124.

Chakar, F.S. and Ragauskas, A.J., Review of current and future softwood kraft lignin process chemistry, *Industrial Crops and Products* **20**(2) (2004) 131-141.

Collett, B.M., A review of surface and interfacial adhesion in wood science and related fields, *Wood Science and Technology* **6**(1) (1972) 1-42.

Constantino, C.J.L., Juliani, L.P., Botaro, V.R., Balogh, D.T., Pereira, M.R., Ticianelli, E.A., Curvelo, A.A.S. and Oliveira Jr., O.N., Langmuir-Blodgett films from lignins, *Thin Solid Films* **284-285** (1996) 191-194.

Crouvisier-Urion, K., Borart, P.R., Winckler, P., Raya, J., Gougeon, R.D., Cayot, P., Domenek, S., Debeaufort, F. and Karbowiak, T., Biobased Composite Films from Chitosan and Lignin: Antioxidant Activity Related to Structure and Moisture, *ACS Sustainable Chemistry and Engineering* **4**(12) (2016) 6371-6381.

Cui, C., Sun, R. and Argyropoulos, D.S., Fractional Precipitation of Softwood Kraft Lignin: Isolation of Narrow Fractions Common to a Variety of Lignins, *ACS Sustainable Chemistry & Engineering* **2**(4) (2014) 959-968.

Dallmeyer, I., Chowdhury, S. and Kadla, J.F., Preparation and characterization of kraft lignin-based moisture-responsive films with reversible shape-change capability, *Biomacromolecules* **14**(7) (2013) 2354-2363.

Dawson, P., Cooksey, K. and Mangalassary, S., “Environmentally friendly packaging of muscle food” in *Environmentally Compatible Food Packaging,* Chiellini, E. (ed.), CRC; Woodhead, Cambridge 2008, pp. 504-507.

De Miranda, C.S., Fereira, M.S., Magalhães, M.T., Goncalves, A.P.B., De Oliveira, J.C., Guimarães, D.H. and José, N.M., Effect of the glycerol and lignin extracted from piassava fiber in cassava and corn starch films, *Materials Research* **18**(2015) 260-264.

De Vlieger, J.J., “Green plastics for food packaging” in *Novel Food Packaging Techniques,* Ahvenainen, R. (ed.), CRC Press; Woodhead Pub, Cambridge 2003, pp. 519-520.

Doherty, W.O.S., Mousavioun, P. and Fellows, C.M., Value-adding to cellulosic ethanol: Lignin polymers, *Industrial Crops and Products* **33**(2) (2011) 259-276.

Domansky, G. and Rendos, F., On the pyrolysis of wood and its components, *Holz- als Roh- und Werkstoff: European Journal of Wood and Wood Industries* **20**(12) (1962) 473-476.

Drelich, J., Chibowski, E., Desheng Meng, D. and Terpilowski, K., Hydrophilic and Superhydrophilic Surfaces and Materials, *Soft Matter* **7**(21) (2011) 9804-9828.

Duval, A. and Lawoko, M., A review on lignin-based polymeric, micro- and nano-structured materials, *Reactive & Functional Polymers* **85** (2014) 78-96.

Eastwood, M.A. and Girdwood, R.H., Lignin: A bile-salt sequestrating agent, *The Lancet* **292**(7579) (1968) 1170-1172.

Ebnesajjad, S., *Plastic films in food packaging: materials, technology, and applications*, William Andrew, Oxford 2013, pp. 1-2.

Espinoza-Acosta, J.L., Torres-Chávez, P.I., Ramírez-Wong, B., López-Saiz, C.M. and Montaño-Leyva, B. Antioxidant, Antimicrobial, and Antimutagenic Properties of Technical Lignins and Their Applications, *BioResources* **11**(2) (2016) 5452-5482.

Espinoza-Acosta, J.L., Torres Chávez, P.I., Ramírez-Wong, B., Bello-Pérez, L.A., Vega Ríos, A., Carvajal Millán, E., Plascencia Jatomea, M. and Ledesma Osuna, A.I., Mechanical, thermal, and antioxidant properties of composite films prepared from durum wheat starch and lignin, *Starch/Staerke* **67**(5-6) (2015) 502-511.

Figueiredo, P., Lintinen, K., Hirvonen, J.T., Kostiainen, M.A. and Santos, H.A., Properties and chemical modifications of lignin: Towards lignin-based nanomaterials for biomedical applications, *Progress in Materials Science* **93** (2018) 233-269.

Foston, M., Nunnery, G.A., Meng, X., Sun, Q., Baker, F.S. and Ragauskas, A., NMR a critical tool to study the production of carbon fiber from lignin, *Carbon* **52** (2013) 65-73.

Freudenberg, K. and Neish, A.C., *Constitution and biosynthesis of lignin*, Springer-Verlag, Berlin 1968, pp. 129.

Fritz, C., Salas, C., Jameel, H. and Rojas, O.J., Self-association and aggregation of kraft lignins via electrolyte and nonionic surfactant regulation: stabilization of lignin particles and effects on filtration, *Nordic Pulp & Paper Research Journal* **32**(4) (2017) 572-585.

Garcia-Caurel, E., Ossikovski, R., Foldyna, M., Pierangelo, A., Drévillon, B. and De Martino, A., “Advanced Mueller Ellipsometry Instrumentation and Data Analysis ” in *Ellipsometry at the nanoscale,* Losurdo, M. and Hingerl, K. (eds.), Springer cop., Berlin; New York 2013, pp. 32-62.

George, J., *Preparation of Thin Films*, Marcel Dekker Inc., New York 1992, pp. 335-338.

Gindl, M., Sinn, G., Gindl, W., Reiterer, A. and Tschegg, S., A comparison of different methods to calculate the surface free energy of wood using contact angle measurements, *Colloids and Surfaces A: Physicochemical and Engineering Aspects* **181**(1-3) (2001) 279-287.

Gordobil, O., Herrera, R., Llano-Ponte, R. and Labidi, J., Esterified organosolv lignin as hydrophobic agent for use on wood products, *Progress in Organic Coatings* **103** (2017)143-151.

Gordobil, O., Egüés, I. and Labidi, J., Modification of Eucalyptus and Spruce organosolv lignins with fatty acids to use as filler in PLA, *Reactive and Functional Polymers* **104** (2016) 45-52.

Granata, A. and Argyropoulos, D.S., 2-Chloro-4,4,5,5-tetramethyl-1,3,2-dioxaphospholane, a reagent for the accurate determination of the uncondensed and condensed phenolic moieties in lignins, *Journal of Agricultural and Food Chemistry* **43** (1995) 1538-1544.

Gundersen, S.A., Ese, M.-H. and Sjöblom, J., Langmuir surface and interface films of lignosulfonates and Kraft lignins in the presence of electrolyte and asphaltenes: correlation to emulsion stability, *Colloids and Surfaces A: Physicochemical and Engineering Aspects* **182**(1-3) (2001) 199-218.

Hambardzumyan, A., Molinari, M., Dumelie, N., Fuolon, L., Habrant, A., Chabbert, B. and Aguié-Béghin, V., Structure and optical properties of plant cell wall bio-inspired materials: Cellulose-lignin multilayer nanocomposites, *Comptes Rendus - Biologies* **334**(11) (2011) 839-850.

Han, J.H., Zhang, Y. and Buffo, B., "Surface chemistry of food, packaging and biopolymer materials" in *Innovations in Food Packaging*, Han, J.H. (ed.), Elsevier Academic; Elsevier Science, San Diego; Oxford 2005, pp. 45-49.

Harland, C.E., *Ion-exchange: theory and practice,* 2nd edn, Royal Society of Chemistry, London 1994, pp. 1-2.

Hatakeyama, H. and Hatakeyama, T., "Lignin Structure, Properties, and Applications" in *Biopolymers: lignin, proteins, bioactive nanocomposites,* Abe, A., Dušek, K. and Kobayashi, S. (eds.), Springer, Berlin 2010, pp. 1-20.

Hoeger, I.C., Filpponen, I., Martin-Sampedro, R., Johansson, L.-S., Österberg, M., Laine, J., Kelley, S. and Rojas, O.J., Bicomponent Lignocellulose Thin Films to Study the Role of Surface Lignin in Cellulolytic Reactions, *Biomacromolecules* **13**(10) (2012) 3228-3240.

Hubbe, M.A., Gardner, D.J. and Shen, W., Contact Angles and Wettability of Cellulosic Surfaces: A Review of Proposed Mechanism and Test Strategies, *BioResources* **10**(4) (2015) 8657-8749.

Hult, E.-L., Koivu, K., Asikkala, J., Ropponen, J., Wrigstedt, P., Sipilä, J. and Ropponen, K., Esterified lignin coating as water vapor and oxygen barrier for fiber-based packaging, *Holzforschung* **67**(8) (2013) 899-905.

Hult, E.-L., Ropponen, J., Ropponen, K., Ohra-Aho, T. and Tamminen, T., Enhancing the barrier properties of paper board by a novel lignin coating, *Industrial Crops and Products* **50** (2013) 694-700.

Humlíček, J., "Polarized Light and Ellipsometry" in *Handbook of Ellipsometry*, Tompkins, H.G. and Irene E.A. (eds.), William Andrew, Inc., New York 2005, pp. 9-10.

Jiang, F., Qian, C., Esker, A.R. and Roman, M., Effect of Nonionic Surfactants on Dispersion and Polar Interactions in the Adsorption of Cellulases onto Lignin, *The Journal of Physical Chemistry* **121**(41) (2017) 9607-9620.

Johansson, K., Gillgren, T., Winestrand, S., Järnström, L. and Jönsson, L.J., Comparison of lignin derivatives as substrates for laccase-catalyzed scavenging of oxygen in coatings and films, *Journal of Biological Engineering* **8**(1) (2014).

Johansson, K., Winestrand, S., Johansson, C., Järnström, L. and Jönsson, L.J., Oxygen-scavenging coatings and films based on lignosulfonates and laccase, *Journal of Biotechnology* **161**(1) (2012) 14-18.

Johansson, L.-S. and Campbell, J.M., Reproducible XPS on biopolymers: cellulose studies, *Surface and Interface Analysis* **36**(8) (2004) 1018-1022.

Jääskeläinen, A.-S., Liitiä, T., Mikkelson, A., Tamminen, T., Aqueous organic solvent fractionation as means to improve lignin homogeneity and purity, *Industrial Crops and Products* **103**(2017) 51-58.

Kalliola, A., Savolainen, A., Ohra-aho, T., Faccio, G. and Tamminen, T., Reducing the content of VOCs of softwood kraft lignins for material applications, *BioResources* **7**(3) (2012) 2871-2882.

Kent, M.S., Avina, I.C., Rader, N., Busse, M.L., George, A., Sathitsuksanoh, N., Baidoo, E., Timlin, J., Giron, N.H., Celina, M.C., Martin, L.E., Polsky, R., Chavez, V.H., Huber, D.L., Keasling, J.D., Singh, S., Simmons, B.A. and Sale, K.L., Assay for lignin breakdown based on lignin films: insights into the Fenton reaction with insoluble lignin, *Green Chemistry* **17**(10) (2015) 4830-4845.

Kivioja, A.O., Jääskeläinen, A.-S., Ahtee, V. and Vuorinen, T., Thickness measurement of thin polymer films by total internal reflection Raman and attenuated total reflection infrared spectroscopy, *Vibrational Spectroscopy* **61** (2012) 1-9.

Klein, P.W., *Fundamentals of plastics thermoforming,* Morgan & Claypool Publishers, California 2009, p. 15.

Klein, L.C., “Sol-Gel Coatings” in *Thin Film Processes* II, Vossen, J.L. and Kern, W. (eds.), Academic Press cop., Boston 1991, pp. 511-512.

Kocaefe, D., Poncsak, S. and Boluk, Y., Effect of thermal treatment on the chemical composition and mechanical properties of birch and aspen, *BioResources* **3**(2) (2008) 517-537.

Kontturi, E., Tammelin, T., and Österberg, M., Cellulose—model films and the fundamental approach, *Chemical Society Reviews* **35**(12) (2006) 1287-1304.

Kontturi, E., Thüne, P.C. and (Hans) Niemantsverdriet, J.W., Cellulose Model Surfaces- Simplified Preparation by Spin Coating and Characterization by X-ray Photoelectron Spectroscopy, Infrared Spectroscopy, and Atomic Force Microscopy, *Langmuir* **19**(14) (2003) 5735-5741.

Korbag, I. and Mohamed Saleh, S., Studies on mechanical and biodegradability properties of PVA/lignin blend films, *International Journal of Environmental Studies* **73**(1) (2016) 18-24.

Kubo, S. and Kadla, J.F., Lignin-based Carbon Fibers: Effect of Synthetic Polymer Blending on Fiber Properties, *Journal of Polymers and the Environment* **13**(2) (2005) 97-105.

Kudo, K. and Yoshida, E., On the decomposition process of wood constituents in the course of carbonization. I. The decomposition of carbohydrate and lignin in mizunara (Quercus crispula Blume) wood, *The Japan Wood Research Society* **3**(4) (1957) 125-127.

Laine, J., Stenius, P., Carlsson, G. and Ström, G., Surface characterization of unbleached kraft pulps by means of ESCA, *Cellulose* **1** (1994) 145-160.

Laurichesse, S. and Avérous, L.**,** "Towards biobased aromatic polymers from lignins" in *Biodegradable and biobased polymers for environmental and biomedical applications*, Kali, S. and Avérous, L. (eds.), John Wiley & Sons, Inc., New York 2016, pp. 385-436.

Lee, S.-S., Lee, K.-B. and Hong, J.-D., Evidence for Spin Coating Electrostatic Self-Assembly of Polyelectrolytes, *Langmuir* **19**(18) (2003) 7992-7596.

Lee, S.-S., Hong, J.-D., Kim, C.H., Kim, K., Koo, J.P. and Lee, K.-B., Layer-by-Layer Deposited Multilayer Assemblies of Ionene-Type Polyelectrolytes Based on the Spin-Coating Method, *Macromolecules* **34**(16) (2001) 5358-5360.

Lee, S.B. and Luner, P., The wetting and interfacial properties of lignin, *Tappi* **55**(1) (1972) 116-121.

Li, J., Wang, M., She, D. and Zhao, Y., Structural functionalization of industrial softwood kraft lignin for simple dip-coating of urea as highly efficient nitrogen fertilizer, *Industrial Crops and Products* **109** (2017) 255-265.

Liu, H., Fu, S., Li, H. and Zhan, H., Layer-by-layer assembly of lignosulfonates for hydrophilic surface modification, *Industrial Crops and Products* **30**(2) (2009) 287-291.

Lovell, E.L. and Hibbert, H., Studies on Lignin and Related Compounds. LII. New Method for the Fractionation of Lignin and Other Polymers, *Journal of the American Chemical Society* **63**(8) (1941) 2070-2073.

Lu, F. J., Chu, L. H., and Gau, R. J., Free radical-scavenging properties of lignin, *Nutrition and Cancer* **30**(1) (1998) 31-38.

Mangipudi, V., Tirrell, M. and Pocius, A.V., Direct Measurement of the Surface Energy of Corona-Treated Polyethylene Using the Surface Forces Apparatus, *Langmuir* **11**(1) (1995) 19-23.

Mattox, D.M. *Handbook of Physical Vapor Deposition (PVD) Processing*, Noyes Publications, Westwood, NJ 1998, pp. 288-295.

Mattox, D.M. *Handbook of Physical Vapor Deposition (PVD) Processing*, Noyes Publications, Westwood, NJ 1998, pp. 32.

Maximova, N., Österberg, M., Laine, J. and Stenius, P., The wetting properties and morphology of lignin adsorbed on cellulose fibres and mica, *Colloids and Surfaces A: Physicochemical and Engineering Aspects* **239**(1-3) (2004) 65-75.

Meincken, M. and Evans, P.D., Use of atomic force microscopy to detect wavelength dependent changes in wood veneers, and spin coated lignin and cellulose films exposed to solar radiation, *International Wood Products Journal* **1**(2) (2010) 75-80.

Meyerhofer, D., Characteristics of resist films produced by spinning, *Jounal of Applied Physics* **49**(7) (1978) 3993.

Mörck, R., Reimann, A. and Kringstad, K.P., Fractionation of kraft lignin by successive extraction with organic solvents. III. Fractionation of Kraft Lignin from Birch, *Holzforschung* **42**(2) (1988) 111–116.

Nakamura, T., Kawamoto, H. and Saka, S., Condensation Reactions of Some Lignin Related Compounds at Relatively Low Pyrolysis Temperature, *Journal of Wood Chemistry and Technology* **27**(2) (2007) 121-133.

Nakasone, K. and Kobayashi, T., Cytocompatible cellulose hydrogels containing trace lignin, *Materials Science and Engineering C* **64** (2016) 269-277.

Niepel, M.S., Kirchhof, K., Menzel, M., Heilmann, A. and Groth, T., "Controlling Cell Adhesion Using pH-Modified Polyelectrolyte Multilayered Films" in *Layer-by-Layer Films for Biomedical Applications,* Picart, C., Caruso, F. and Voegel, J.C. (eds.), Wiley-VCH Verlag & Co. KGaA, Weinheim 2015, pp. 3-5.

Norberg, I., Nordström, Y., Drougge, R., Gellerstedt, G. and Sjöholm, E., A New Method for Stabilizing Softwood Kraft Lignin Fibers for Carbon Fiber Production, *Journal of Applied Polymer Science* **128**(6) (2013) 3824-3830.

Norgren, M., Notley, S.M., Majtnerova, A. and Gellerstedt, G., Smooth model surfaces from lignin derivatives. I. Preparation and characterization, *Langmuir* **22**(3) (2006) 1209-1214.

Notley, S.M. and Norgren, M., Surface energy and wettability of spin-coated thin films of lignin isolated from wood, *Langmuir* **26**(8) (2010) 5484-5490.

Notley, S.M. and Norgren, M., Adsorption of a strong polyelectrolyte to model lignin surfaces, *Biomacromolecules* **9**(7) (2008) 2081-2086.

Notley, S.M. and Norgren, M., Measurement of interaction forces between lignin and cellulose as a function of aqueous electrolyte solution conditions, *Langmuir* **22**(26) (2006) 11199-11204.

Ohring, M., *Materials science of thin films: deposition and structure,* 2nd edn, Academic Press, San Diego 2002, pp. 711-716.

O`Kell, S., Henshaw, T., Farrow, G., Aindow, M. and Jones, C., Effects of low-power plasma treatment on polyethylene surfaces, *Surface and Interface Analysis* **23**(5) (1995) 319-327.

Owens, D.K. and Wendt, R.C., Estimation of the surface free energy of polymers, *Journal of Applied Polymer Science* **13**(8) (1969).

Pasquini, D., Balogh, D.T., Oliveira JR., O.N. and Curvelo, A.A.S., Lignin molecular arrangements in Langmuir and Langmuir-Blodgett films: The influence of extraction processes, *Colloids and Surfaces A: Physicochemical and Engineering Aspects* **252**(2-3) (2005) 193-200.

Pereira, A., Hoeger, I.C., Ferrer, A., Rencoret, J., Del Ril, J.C., Kruus, K., Rahikainen, J., Kellock, M., Gutiérrez, A. and Rojas, O.J., Lignin Films from Spruce, Eucalyptus, and Wheat Straw Studied with Electroacoustic and Optical Sensors: Effect of Composition and Electrostatic Screening on Enzyme Binding, *Biomacromolecules* **18**(4) (2017) 1322-1332.

Pereira, A.A., Martins, G.F., Antunes, P.A., Conrrado, R., Pasquini, D., Job, A.E., Curvelo, A.A.S., Ferreira, M., Riul JR., A. and Constantino, C.J.L., Lignin from sugar cane bagasse: Extraction, fabrication of nanostructured films, and application, *Langmuir* **23**(12) (2007) 6652-6659.

Petersen, K., Vñggemose Nielsen, P., Bertelsen, G., Lawther, M., Olsen, M.B., Nilsson, N.H. and Mortensen, G., Potential of biobased materials for food packaging, *Trends in Food Science & Technology* **10**(2) (1999) 52-68.

Pike, L., "Current Practices in the Measurement of Oxygen Transmission Rates of Packaging Films under Humid Conditions" in *Food Packaging Technology,* Henyon, D.K. (ed.), ASTM Committee F-2 on Flexible Barrier Materials, Philadelphia 1991, p. 37.

Pillai, K., Arzate, F.N., Zhang, W. and Renneckar, S., Towards biomimicking wood: Fabricated free-standing films of nanocellulose, lignin, and a synthetic polycation, *Journal of Visualized Experiments* **88** (2014).

Rahikainen, J.L., Martin-Sampedro, R., Heikkinen, H., Rovio, S., Marjamaa, K., Tamminen, T., Rojas, O.J. and Kruus, K., Inhibitory effect of lignin during cellulose bioconversion: The effect of lignin chemistry on non-productive enzyme adsorption, *Bioresource Technology* **133** (2013) 270-278.

Ramakrishna, S., *An introduction to electrospinning and nanofibers*, World Scientific, Hackensack 2005, pp. 90-96.

Rojo, E., Peresin, M.S., Sampson, W.W., Hoeger, I.C., Vartiainen, J., Laine, J. and Rojas, O.J., Comprehensive elucidation of the effect of residual lignin on the physical, barrier, mechanical and surface properties of nanocellulose films, *Green Chemistry* **17**(3) (2015) 1853-1866.

Rooney, M.L., "Oxygen-Scavenging Packaging*" in Innovations in Food Packaging,* Han, J.H. (ed.), Elsevier Academic; Elsevier Science, San Diego; Oxford 2005, pp. 123-135.

Roy, S. and Ranjan Singha, N., Polymeric Nanocomposite Membranes for Next Generation Pervaporation Process: Strategies, Challenges and Future Prospects, *Membranes* **7**(3) (2017).

Sadeghifar, H., Wells, T., Khuu Le, R., Sadeghifar, F., Yuan, J.S. and Ragauskas, A.J., Fractionation of Organosolv Lignin Using Acetone: Water and Properties of the Obtained Fractions, *ACS Sustainable Chemistry & Engineering* **5**(1) (2017) 580-587.

Sadeghifar, H., Venditti, R., Jur, J., Gorga, R.E. and Pawlak, J.J., Cellulose-Lignin Biodegradable and Flexible UV Protection Film, *ACS Sustainable Chemistry and Engineering* **5**(1) (2016) 625-631.

Sarkanen, S., Teller, D.C., Stevens, C.R. and McCarthy, J.L., Lignin. 20. Associative Interactions between Kraft Lignin Components, *Macromolecules* **17**(12) (1984) 2588-2597.

Sarkanen, K.V., *Lignins - Occurence, formation: structure and reactions,* Wiley-Interscience, 1971, pp. 95.

Schubert, D.W., Spin coating as a method for polymer molecular weight determination, *Polymer Bulletin* **38**(2) (1997) 177-184.

Shankar, S., Reddy, J.P. and Rhim, J.-W., Effect of lignin on water vapor barrier, mechanical, and structural properties of agar/lignin composite films, *International journal of biological macromolecules* **81**(2015) 267-273.

Stewart, D., Lignin as a base material for materials applications: Chemistry, application and economics, *Industrial Crops and Products*, **27**(2) (2008) 202-207.

Sukanek, P.C., Dependence of film thickness on speed in spin coating, *Journal of The Electrochemical Society* **138**(6) (1991) 1712.

Sun Lee, D., "Antioxidative Packaging System" in *Innovations in Food Packaging,* 2nd edn, Han, J.H. (ed.), Academic Press, London 2014, pp. 111-112.

Szindler, M., Sol gel TiO 2 antireflection coatings for silicon solar cells, *Journal of Achievements in Materials and Manufacturing Engineering* **52**(1) (2012) 7-12.

Tammelin, T., Österberg, M., Johansson, L.-S. and Laine, J., Preparation of lignin and extractive model surfaces by using spincoating technique - Application for QCM-D studies, *Nordic Pulp and Paper Research Journal* **21**(4) (2006) 444-450.

Thiebaud, S., Borredon, M.E., Baziard, G. and Senocq, F., Properties of wood esterified by fatty-acid chlorides, *Bioresource Technology* **59**(1-2) (1997) 103-107.

Tsukruk, V.V. and Singamaneni, S., *Scanning Probe Microscopy of Soft Matter: Fundamentals and Practices,* Wiley-VCH, Weinheim 2012, pp. 3-28.

Volpati, D., Machado, A.D., Olivati, C.A., Alves, N., Curvelo, A.A.S., Pasquini, D. and Constantino, C.J.L., Physical vapor deposited thin films of lignins extracted from sugar cane bagasse: Morphology, electrical properties, and sensing applications, *Biomacromolecules* **12**(9) (2011) 3223-3231.

Wagner, T., LOT-QuantumDesign GmbH, Langmuir and Langmuir-Blodgett troughs and deposition troughs, https://lot-qd.de/en/products/materials-science/langmuir-blodgett-systems/product/langmuir-and-langmuir-blodgett-troughs-and-deposition-troughs/, 9.1.2018.

Wang, Y.-Y., Chen, Y.-R. and Sarkanen, S., Path to plastics composed of ligninsulphonates (lignosulfonates), *Green Chemistry* **17**(11) (2015) 5069-5078.

Wenzel, R., Resistance of solid surfaces to wetting by water, *Industrial and Engineering Chemistry* **28**(8) (1936) 988-994.

Wisanrakkit, G. and Gillham, J.K., Continuous heating transformation (CHT) cure diagram of an aromatic amine epoxy system at constant heating rates, *Journal of Applied Polymer Science* **42**(9) (1991) 2453-2463.

Wu, S., Surface tension of solids: An equation of state analysis, *Journal of Colloid and Interface Science* **71**(3) (1979) 605-609.

Xie, J., Hse, C.-.Y, Shupe, T.F. and Hu, T., Physicochemical characterization of lignin recovered from microwave-assisted delignified lignocellulosic biomass for use in biobased materials, *Journal of Applied Polymer Science* **132**(40) (2015) 42635-42635.

Xue, B.-L., Wen, J.-L., Zhu, M.-Q. and Sun, R.-C., Lignin-based polyurethane film reinforced with cellulose nanocrystals, *RSC Advances* **4**(68) (2014) 36089-36096.

Yan, Y. and Lee, T.R., "Contact Angle and Wetting Properties" in *Surface Science Techniques,* Bracco, G. and Holst, B. (eds.), Springer, Berlin 2013, pp. 3-4.

Yoshida, H., Mörck, R., Kringstad, K.P. and Hatakeyama, H., Fractionation of Kraft Lignin by Successive Extraction with Organic Solvents. II. Thermal Properties of Kraft Lignin Fractions, *Holzforschung* **41**(3) (1987) 171-176.

Zhu, N. and Chen, X., "Biofabrication of Tissue Scaffolds" in *Advances in Biomaterials Science and Biomedical Applications*, Pignatello, R. (ed.), InTech, 2013, p. 319.

Zisman, W.A., "Relation of the equilibrium contact angle to liquid and solid constitution" in *Contact Angle, Wettability and Adhesion,* Gould, R.F (ed.), American Chemical Society, Washington D.C. 1964, pp. 1-51.

# XPS wide and high resolution scans spectra

A

wide/30

XPS Spectrum Lens Mode:Hybrid Res:80 Iris(Aper):slot(Slot)
Acqn. Time(s): 599 Sweeps: 2 Anode:Mono(Al (Mono))(100 W) Step(meV): 1000.0
Dwell Time(ms): 272 Charge Neutraliser :On (Current 2.0 A: Balance 3.9 V: Bias 0.7 V) Acquired On :18/06/06 12:48:19
3 1

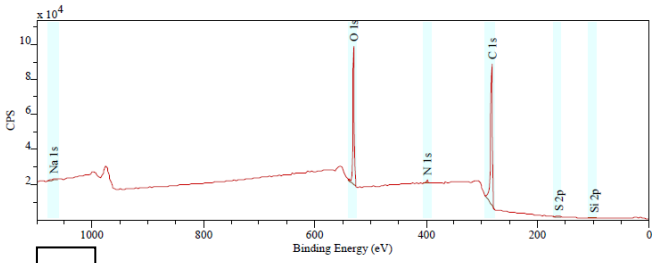


B

wide/46

XPS Spectrum Lens Mode:Hybrid Res:80 Iris(Aper):slot(Slot)
Acqn. Time(s): 599 Sweeps: 2 Anode:Mono(Al (Mono))(100 W) Step(meV): 1000.0
Dwell Time(ms): 272 Charge Neutraliser :On (Current 2.0 A: Balance 3.9 V: Bias 0.7 V) Acquired On :18/06/06 14:48:56
1 2

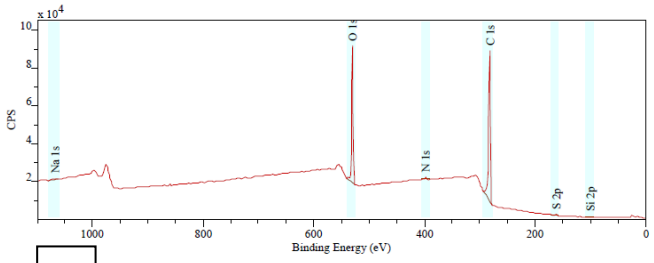


C

wide/34

XPS Spectrum Lens Mode:Hybrid Res:80 Iris(Aper):slot(Slot)
Acqn. Time(s): 599 Sweeps: 2 Anode:Mono(Al (Mono))(100 W) Step(meV): 1000.0
Dwell Time(ms): 272 Charge Neutraliser :On (Current 2.0 A: Balance 3.9 V: Bias 0.7 V) Acquired On :18/06/06 13:44:36
1 3

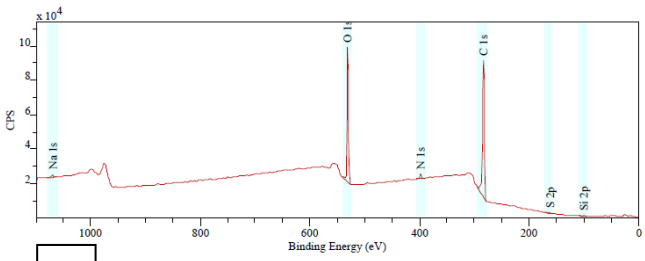


D

wide/62

XPS Spectrum Lens Mode:Hybrid Res:80 Iris(Aper):slot(Slot)
Acqn. Time(s): 599 Sweeps: 2 Anode:Mono(Al (Mono))(100 W) Step(meV): 1000.0
Dwell Time(ms): 272 Charge Neutraliser :On (Current 2.0 A: Balance 3.9 V: Bias 0.7 V) Acquired On :18/06/06 15:58:44
2 4

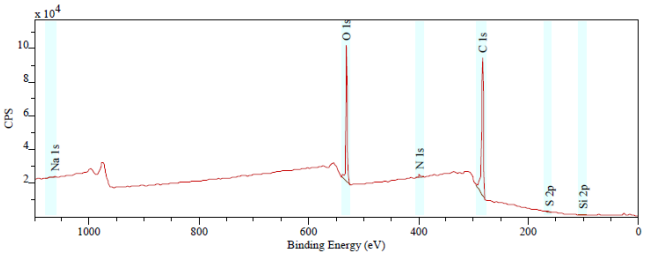

## XPS wide and high resolution scans spectra

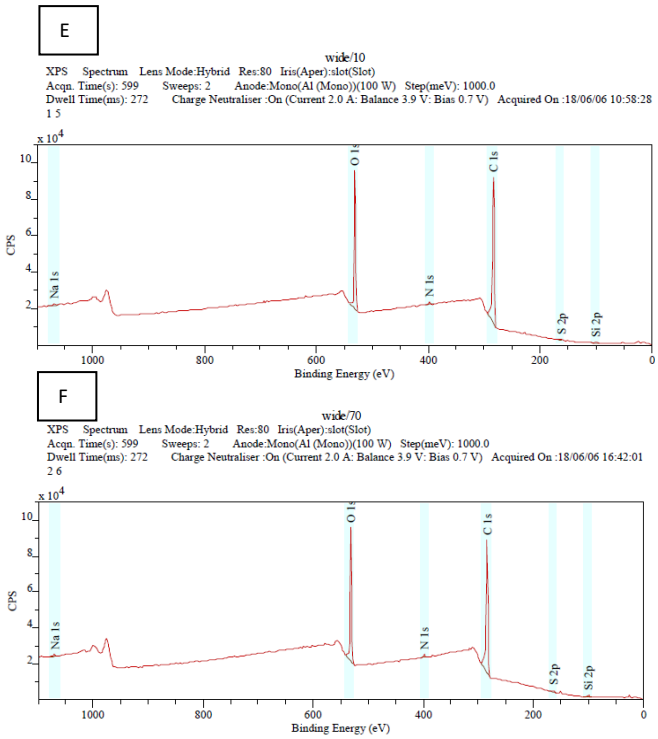


Figure 1. Wide scan spectra from XPS measurement for PREC4, PREC2 and KL films before (A, C, E) and after (B,D,F) heat treatment, respectively.

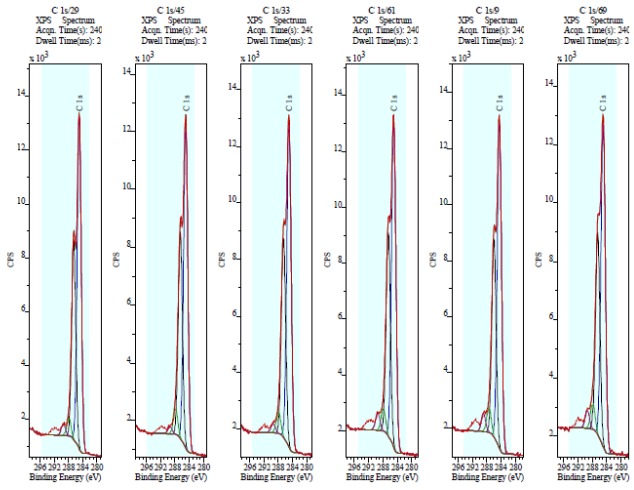


Figure 2. High resolution scan spectra from XPS measurement. From left to right: PREC4 before, PREC2 before, KL before, PREC4 after, PREC2 after and KL after the heat treatment.

APPENDIX 2

## Elemental composition (atomic %) by XPS

Table 1. Elemental composition (atomic %) of KL, PREC2 and PREC4 films before heat treatment, measured by XPS. Standard deviation is in the parenthesis.

| | O | C | N | S | Si | Na |
|---|---|---|---|---|---|---|
| KL | 18.98 (0.58) | 78.60 (0.63) | 1.17 (0.05) | 0.57 (0.09) | 0.43 (0.15) | 0.25 (0.10) |
| PREC2 | 18.36 (0.25) | 80.16 (0.12) | 0.57 (0.10) | 0.56 (0.04) | 0.31 (0.09) | 0.04 (0.04) |
| PREC4 | 19.24 (0.27) | 79.01 (0.15) | 0.93 (0.09) | 0.56 (0.04) | 0.15 (0.12) | 0.11 (0.02) |

Table 2. Elemental composition (atomic %) of KL, PREC2 and PREC4 films after heat treatment, measured by XPS. Standard deviation is in the parenthesis.

| | O | C | N | S | Si | Na |
|---|---|---|---|---|---|---|
| KL | 20.05 (0.21) | 76.8 (0.10) | 0.83 (0.15) | 0.50 (0.03) | 1.71 (0.26) | 0.1 (0.04) |
| PREC2 | 19.31 (0.06) | 79.04 (0.31) | 0.53 (0.10) | 0.40 (0.08) | 0.67 (0.16) | 0.05 (0.04) |
| PREC4 | 19.37 (0.15) | 78.84 (0.05) | 0.68 (0.05) | 0.48 (0.07) | 0.6 (0.14) | 0.04 (0.06) |

APPENDIX 3

## Chemical state of carbon atoms (atomic %) by XPS

Table 1. Chemical state of carbon atoms (atomic %) of KL, PREC2 and PREC4 films before heat treatment, measured by XPS. Standard deviation is in the parenthesis.

| | CC | CO | OCO | COO |
|---|---|---|---|---|
| KL | 55.27 (8.25) | 37.23 (2.89) | 5.77 (5.29) | 1.73 (0.09) |
| PREC2 | 47.42 (10.51) | 40.35 (3.91) | 10.13 (5.51) | 2.11 (1.16) |
| PREC4 | 55.66 (5.53) | 36.88 (1.91) | 5.37 (3.32) | 2.09 (0.32) |

Table 2. Chemical state of carbon atoms (atomic %) of KL, PREC2 and PREC4 films after heat treatment, measured by XPS. Standard deviation is in the parenthesis.

| | CC | CO | OCO | COO |
|---|---|---|---|---|
| KL | 57.29 (1.09) | 35.11 (0.83) | 4.17 (0.46) | 3.43 (0.21) |
| PREC2 | 57.94 (0.64) | 34.85 (0.17) | 3.95 (0.56) | 3.26 (0.10) |
| PREC4 | 57.12 (0.48) | 35.91 (0.45) | 4.01 (0.04) | 2.96 (0.08) |